Properties of $Sr_3Cr_2O_7$ synthesized under High Pressure and High Temperature

Justin Jeanneau
Institut Néel (Grenoble)
Supervisors : M. Nunez-Regueiro & P. Toulemonde

Common properties of high temperature superconductors

Layered (2D compounds)

AFM parent compound

High T_N

Low Magnetic Moment

↓

candidates based on :
V, Cr, Mn, Fe, Co, Ni, Cu

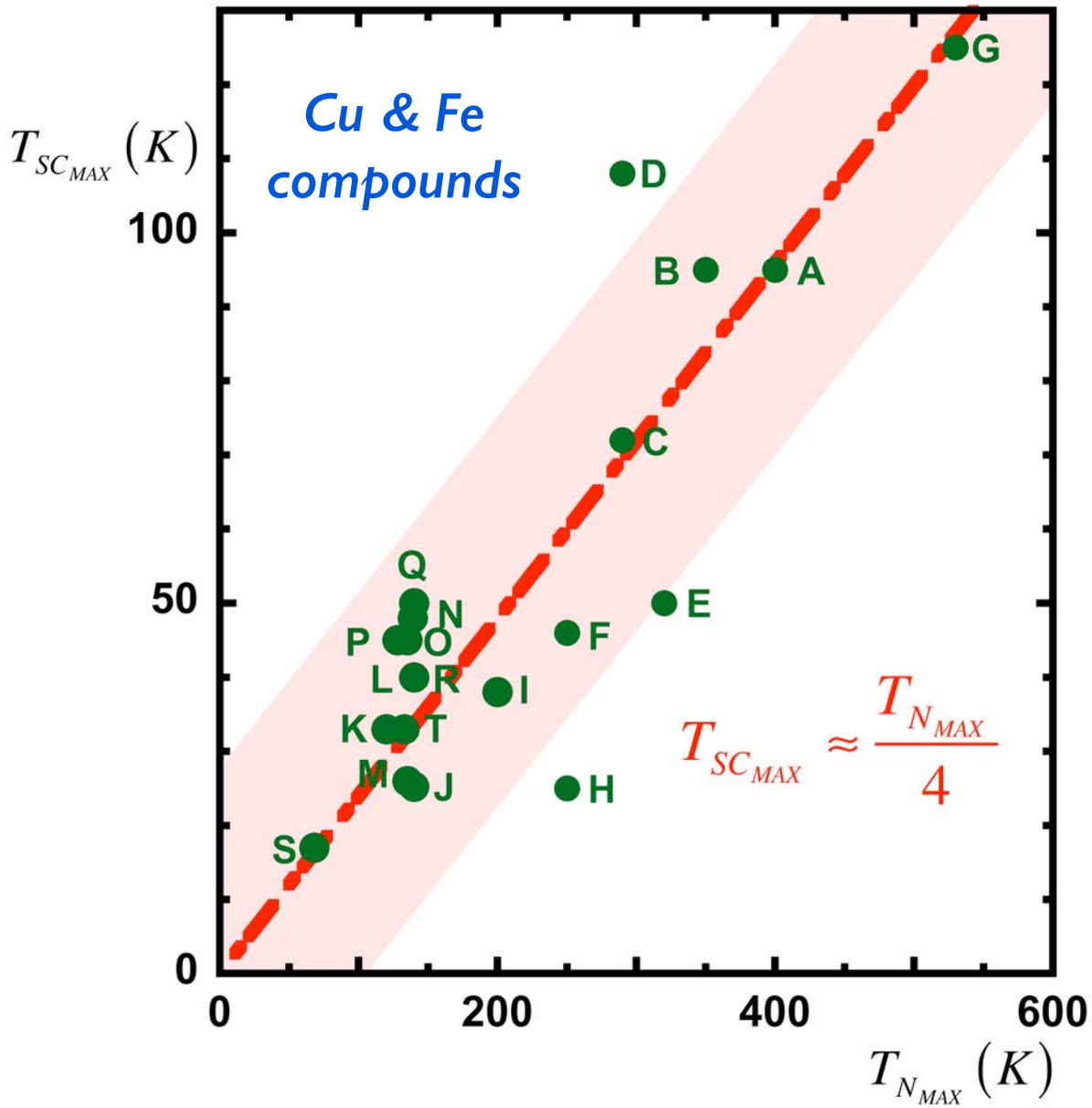

A) *YBa*2*Cu*3*Ox*; B) *Bi*2*Sr*2*MCu*2*O*8+*d* C) *Hg*-1245; D) *Hg*-1245 ; E) *La*2*CuO*4+ *y* ; F) $SSr2CuO2F2$; G)$CaxSr1\text{-}xCuO2$; H)$Nd1\text{-}xCexCuO4$;I) *Sr*1-*xKxFe*2*As*2 ; J) *BaFe*2- *xCoxAs*2; K) Ca1- xNaxFe2As2; L) Ba1-xKxFe2As2 ; M) LaFeAsO1- xFx; N) PrFeAsO1- xFx; O) SmFeAsO1- xFx ; P) GdFeAsO1- xFx ; Q) NdFeAsO1- xFx; R) CeFeAsO1-xFx; S) *Fe*1+ *x* (*Te*1-*xSex*) ; T) *KyFe*2-*xSe*2

Ruddlesden-Popper phases : $Sr_{n+1}Cr_nO_{3n+1}$

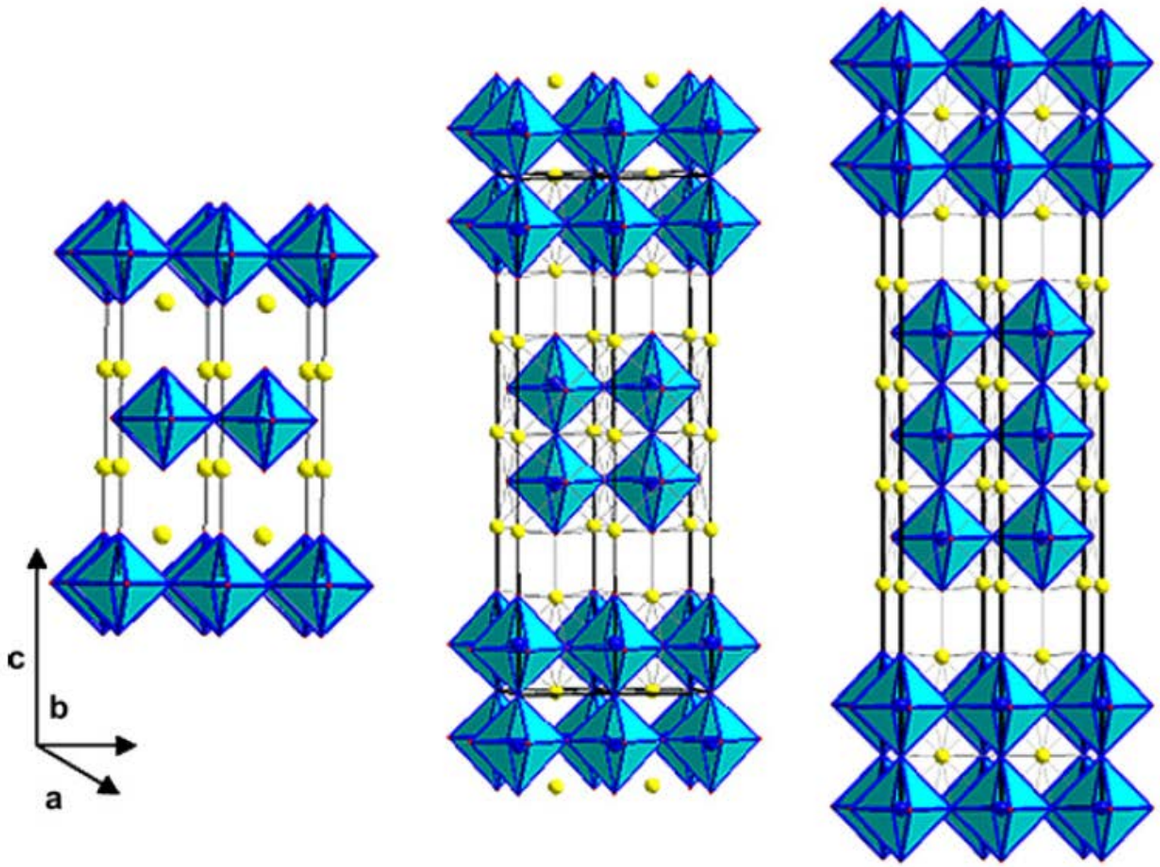

n= 1 n=2 n=3 n= ∞

Sr_2CrO_4 $Sr_3Cr_2O_7$ $Sr_4Cr_3O_{10}$ $SrCrO_3$

Cr^{IV}

e^- config. : $3d^2$

n : number of Perovskite layers

J.A. Kafalas and J.M. Longo, J. Sol. St. Chem. ***4****, 55 (1972).*

Ruddlesden-Popper phases : $Sr_{n+1}Cr_nO_{3n+1}$

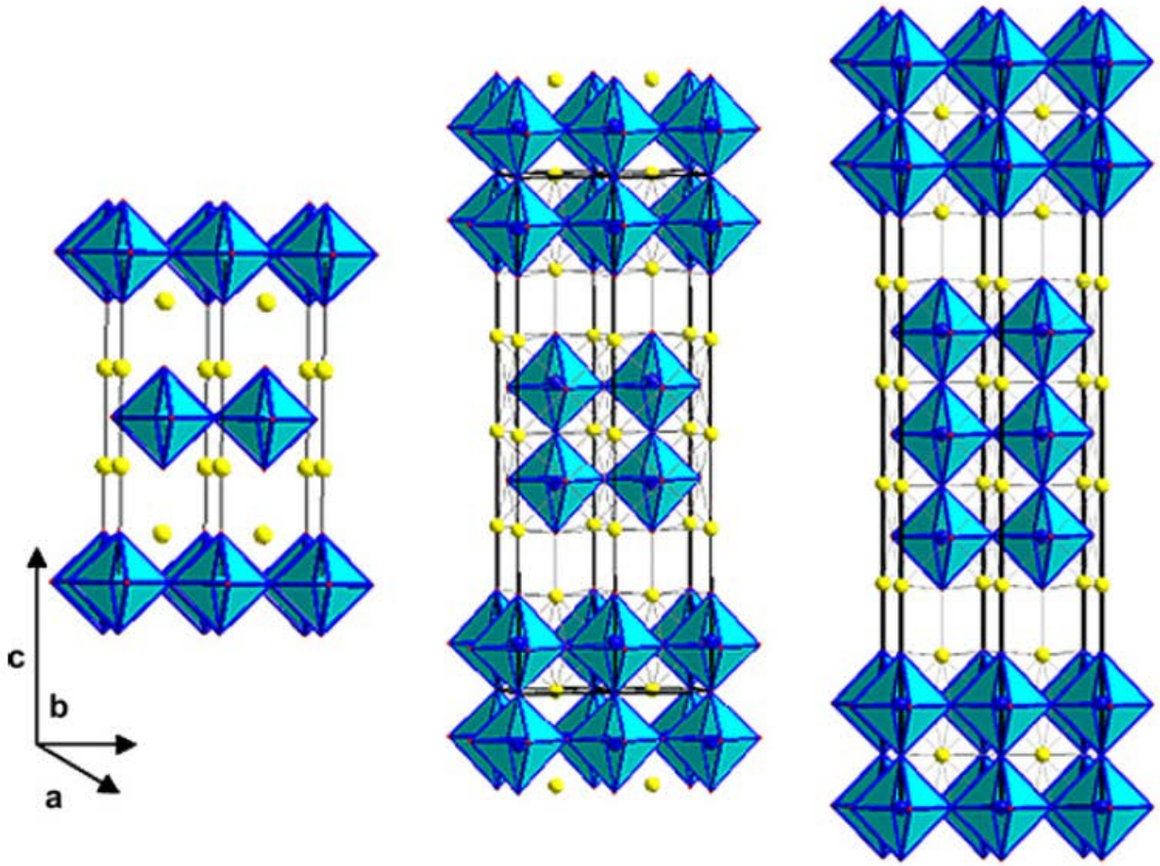

n= 1 n=2 n=3 n= ∞

Sr_2CrO_4 $Sr_3Cr_2O_7$ $Sr_4Cr_3O_{10}$ $SrCrO_3$

n : number of Perovskite layers

J.A. Kafalas and J.M. Longo, J. Sol. St. Chem. ***4****, 55 (1972).*

Cr^{IV}

e^- config. : $3d^2$

Difficult synthesis conditions : High Pressure/Temperature phases !

High Pressure & High Temperature Synthesis

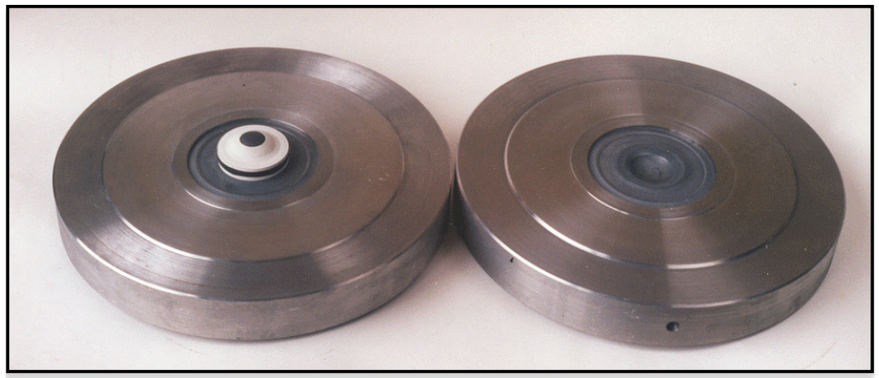

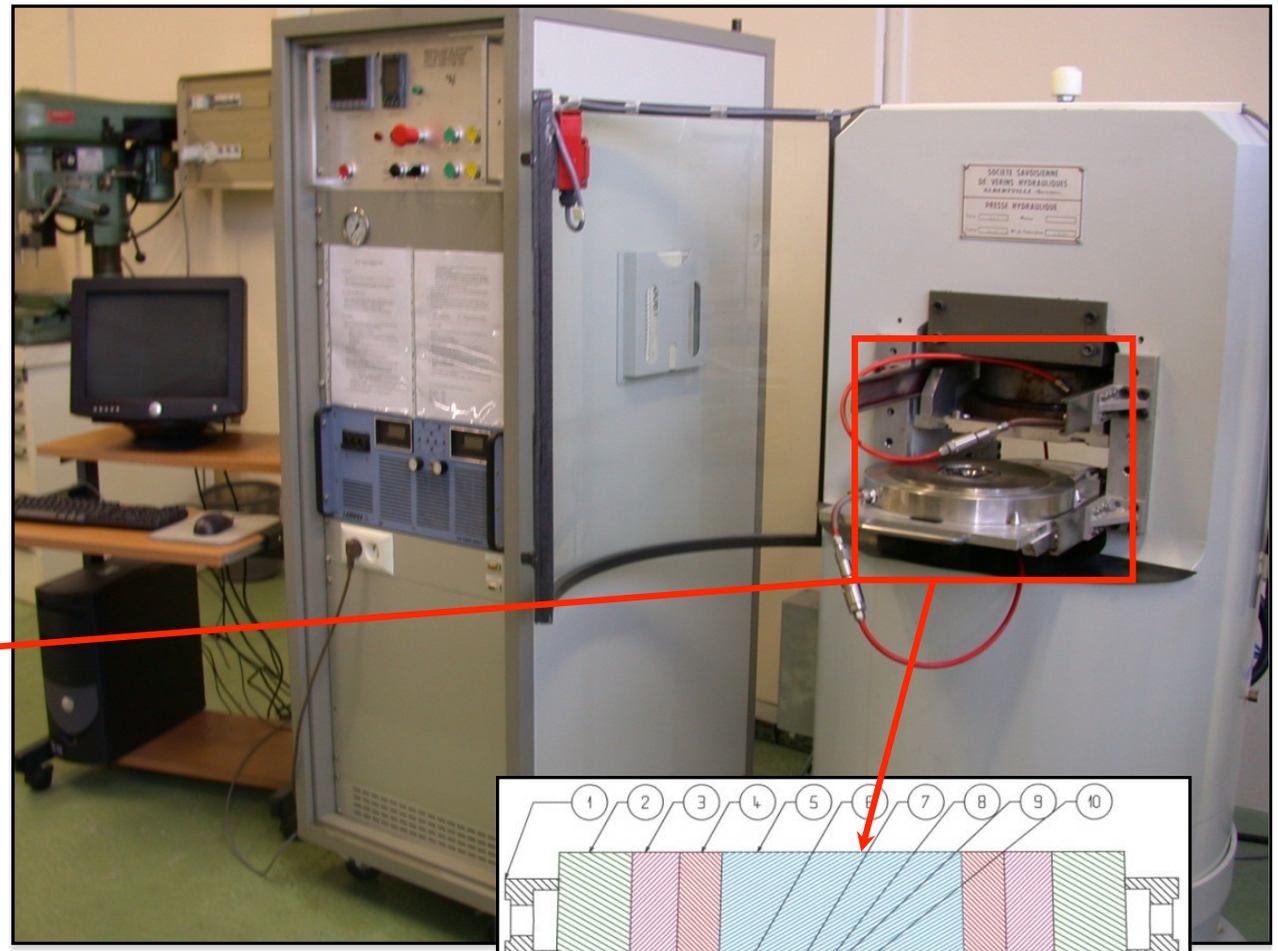

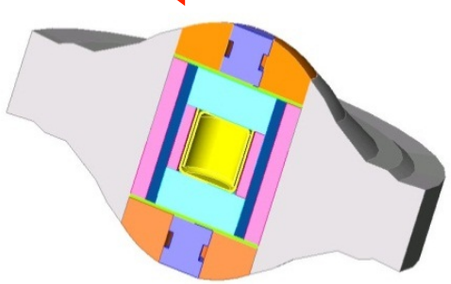

T_{max} ~ 1500°C.	Belt	Conac	
Cells diameter	12 mm	40mm	28mm
Capsule volume (Au,Pt,acier,CuBe,Ta,BN)	0.04 cm^3	0.8 cm^3	0.2 cm^3
Mass product	160 mg	2 g	0.5 g
Pressure range	0 - 8 GPa	0 - 5.5 GPa	0 - 7 GPa

High Pressure & High Temperature Synthesis

Some pressure orders of magnitude..

(source : Wikipédia)

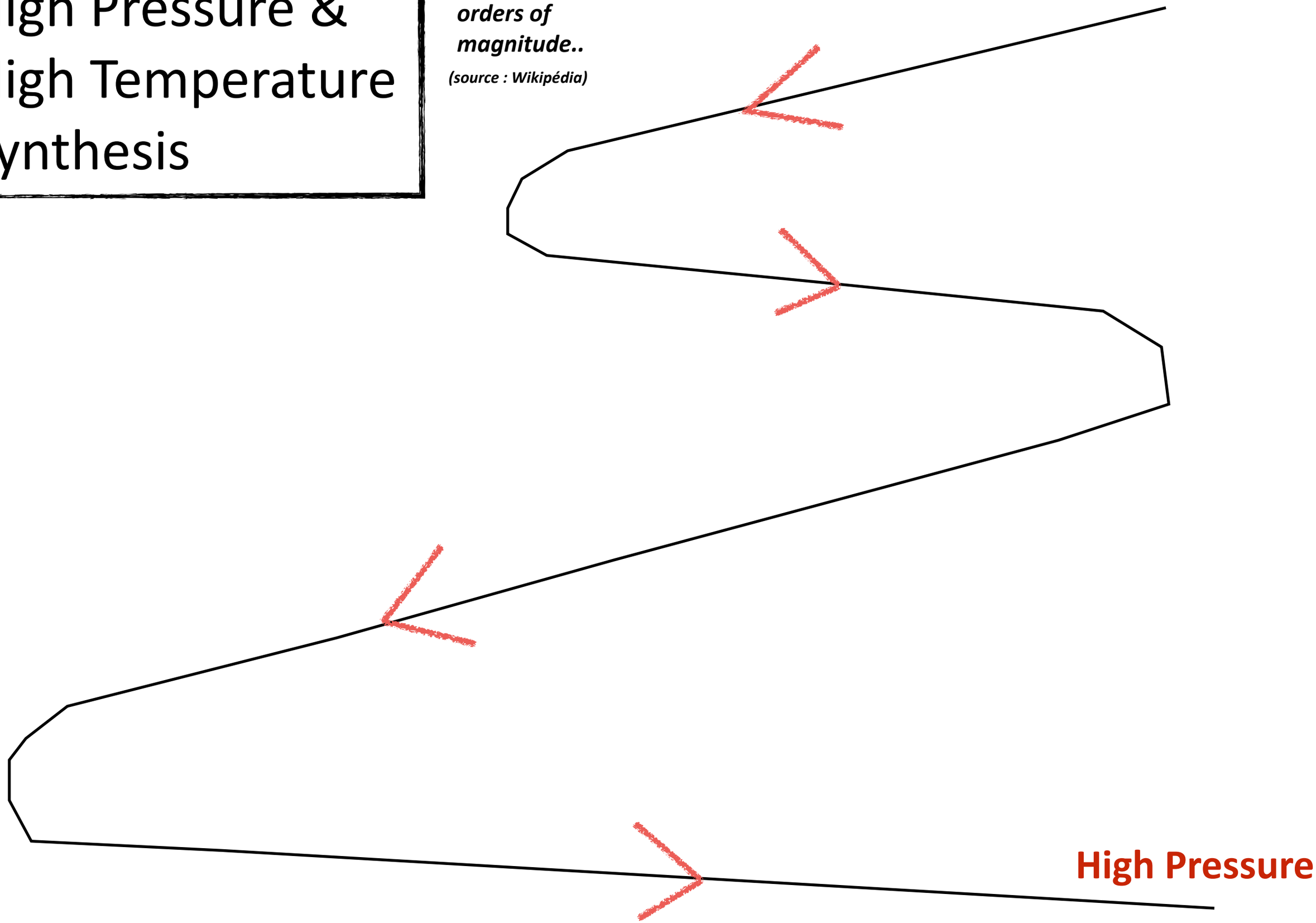

High Pressure & High Temperature Synthesis

Some pressure orders of magnitude..

(source : Wikipédia)

10^{2} Pa
threshold of pain
pressure level for
sound (~130dB)

10^{-5} Pa
threshold of human hearing

10^{-15} Pa

between stars in the Milky Way

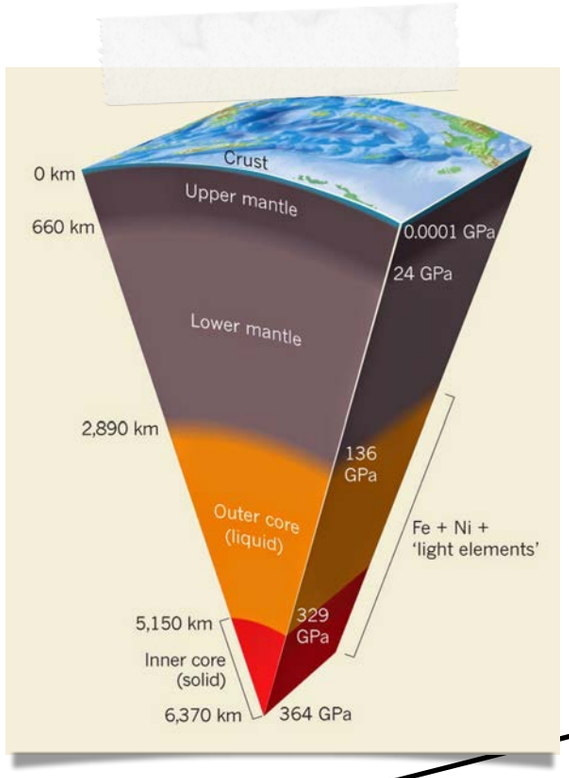

100 MPa
at bottom
of Mariana trench
(around 11km)

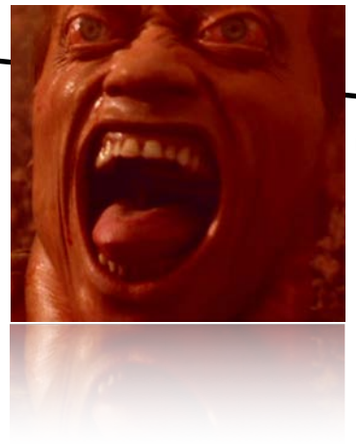

6.3 kPa
Pressure where water
boils at normal human
body temperature (37°C)

10^{5} Pa
pressure on hands of a (good) weightlifter

1 MPa
average human bite

69 GPa
highest water
jet pressure

10^{16} Pa
inside core of the Sun

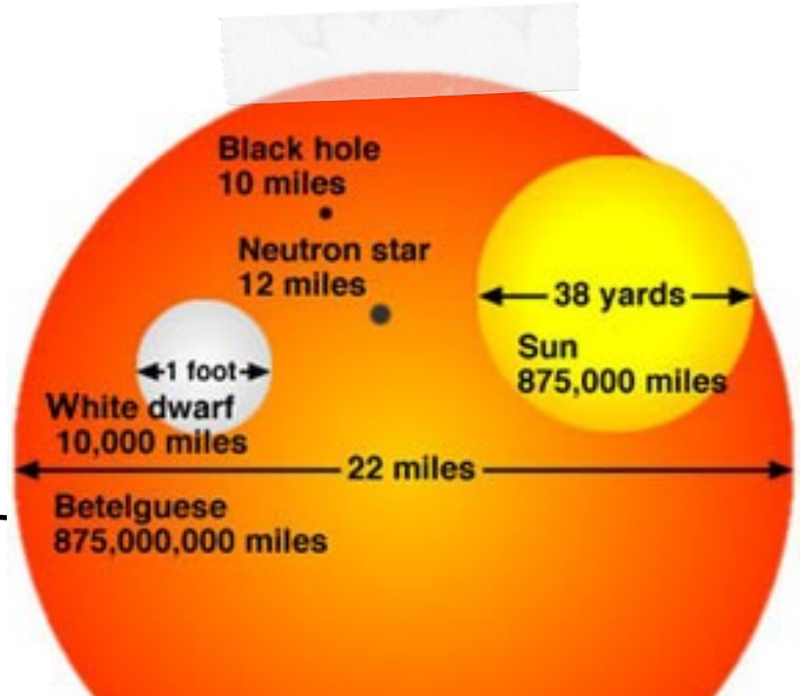

10^{34} Pa
inside a neutron star

High Pressure & High Temperature Synthesis

Some pressure orders of magnitude..

(source : Wikipédia)

10^{-15} Pa

between stars in the Milky Way

10^{2} Pa

threshold of pain
pressure level for sound (~130dB)

10^{-5} Pa

threshold of human hearing

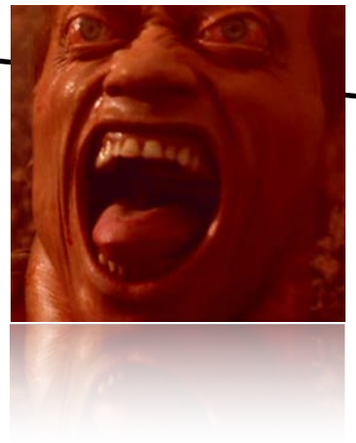

6.3 kPa

Pressure where water boils at normal human body temperature (37°C)

10^{5} Pa

pressure on hands of a (good) weightlifter

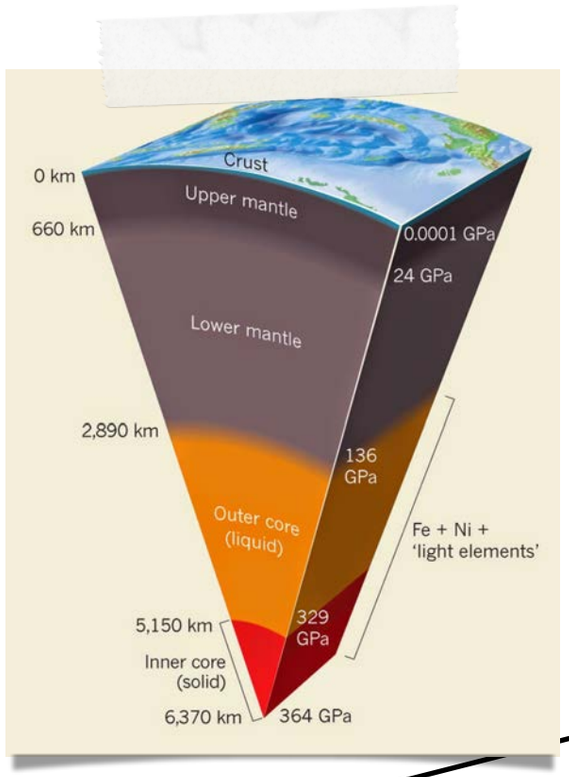

100 MPa

at bottom of Mariana trench (around 11km)

1 MPa

average human bite

Our samples

~6 GPa / 1100°C

25km depth (Middle Crust)

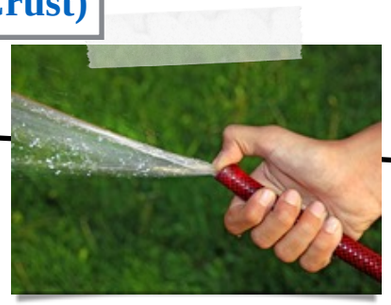

69 GPa

highest water jet pressure

10^{16} Pa

inside core of the Sun

10^{34} Pa

inside a neutron star

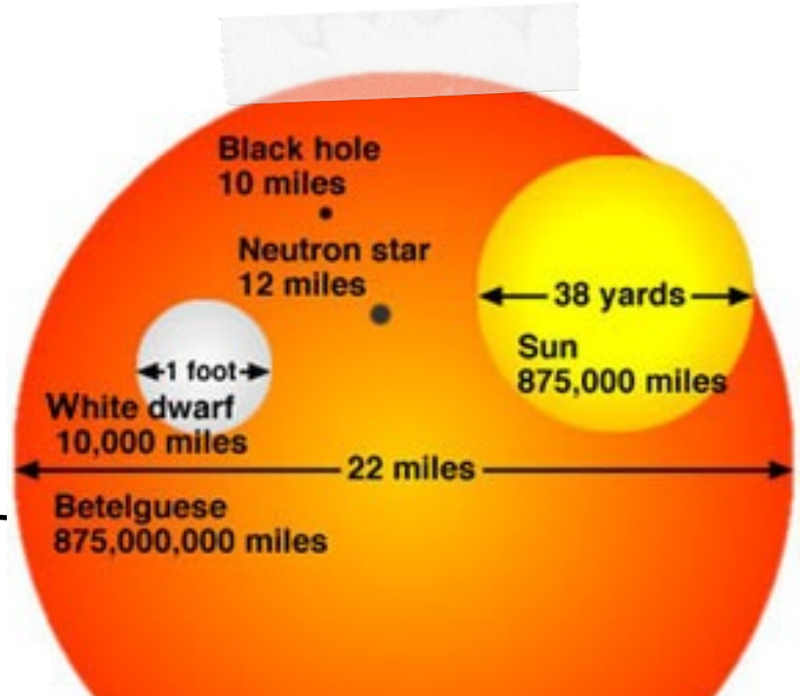

Introduction : Perovskite $SrCrO_3$

Introduction : Perovskite $SrCrO_3$

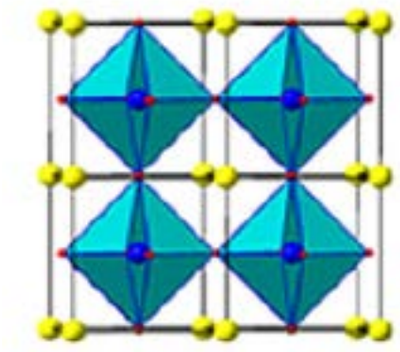

T>40K

cubic

paramagnetic

orbital degenerescence

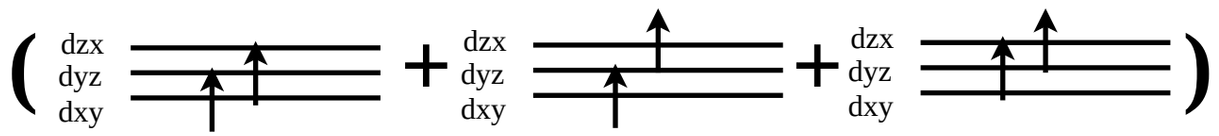

Introduction : Perovskite $SrCrO_3$

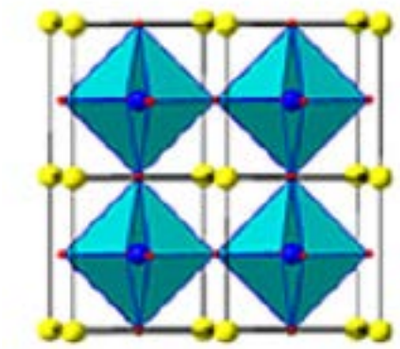

T>40K

cubic

paramagnetic

orbital degenerescence

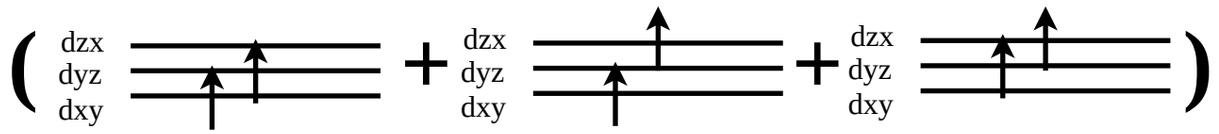

Neutron powder diffraction
Ortega *et al.*,
PRL **99** (2007)
255701

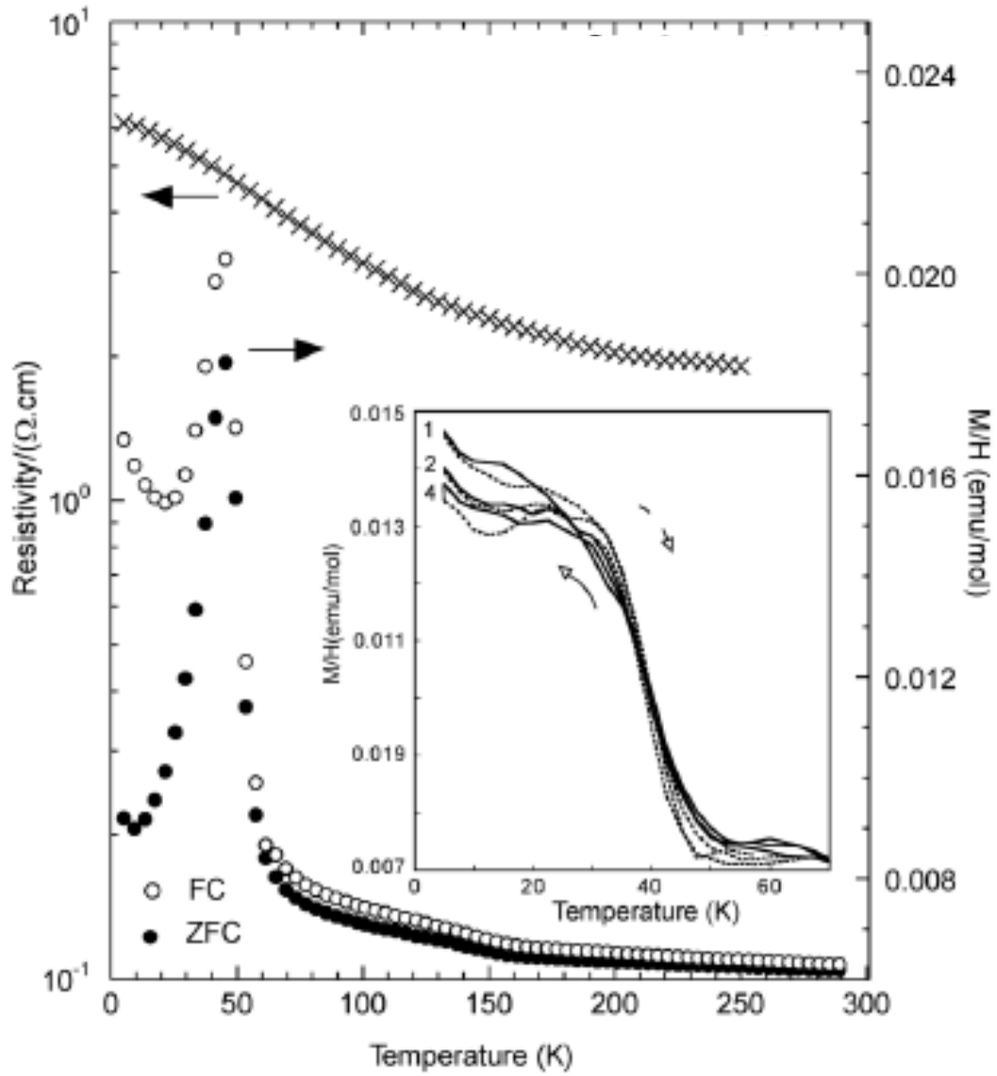

Introduction : Perovskite $SrCrO_3$

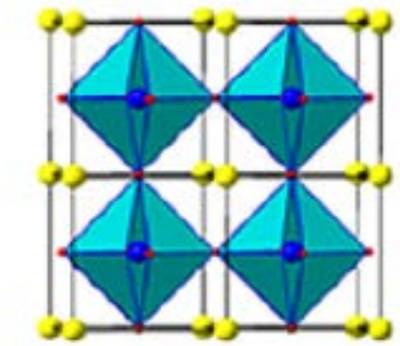

T>40K

cubic

paramagnetic

orbital degenerescence

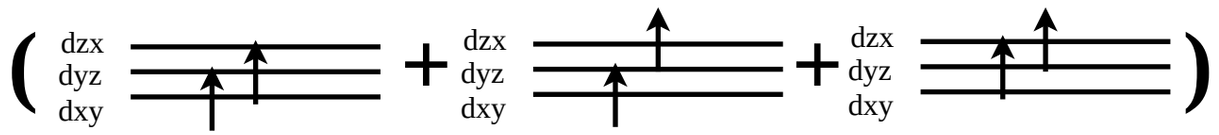

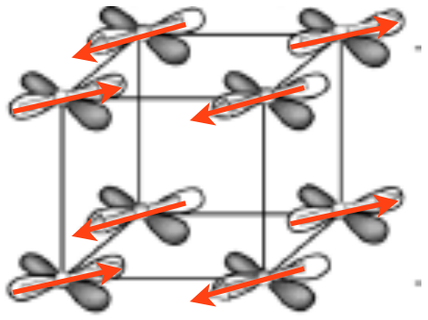

Neutron powder diffraction
Ortega *et al*., PRL **99** (2007) 255701

T<40K

tetragonal c/a=0.992

antiferromagnetic order

partial orbital order

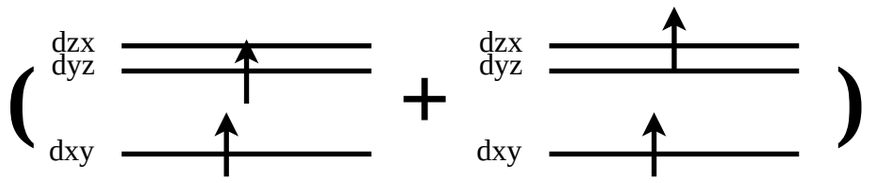

$Sr_3Cr_2O_7$

Sr327
I4/mmm

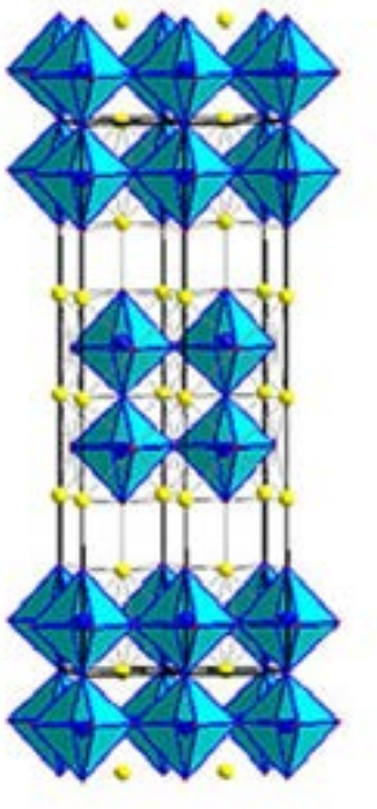

a ~ 3.82 Å

c ~ 20.14 Å

$Sr_3Cr_2O_7$

X-ray diffraction

Sr327
I4/mmm

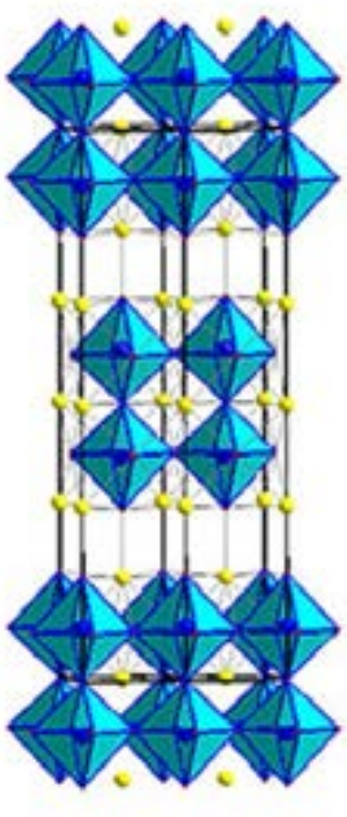

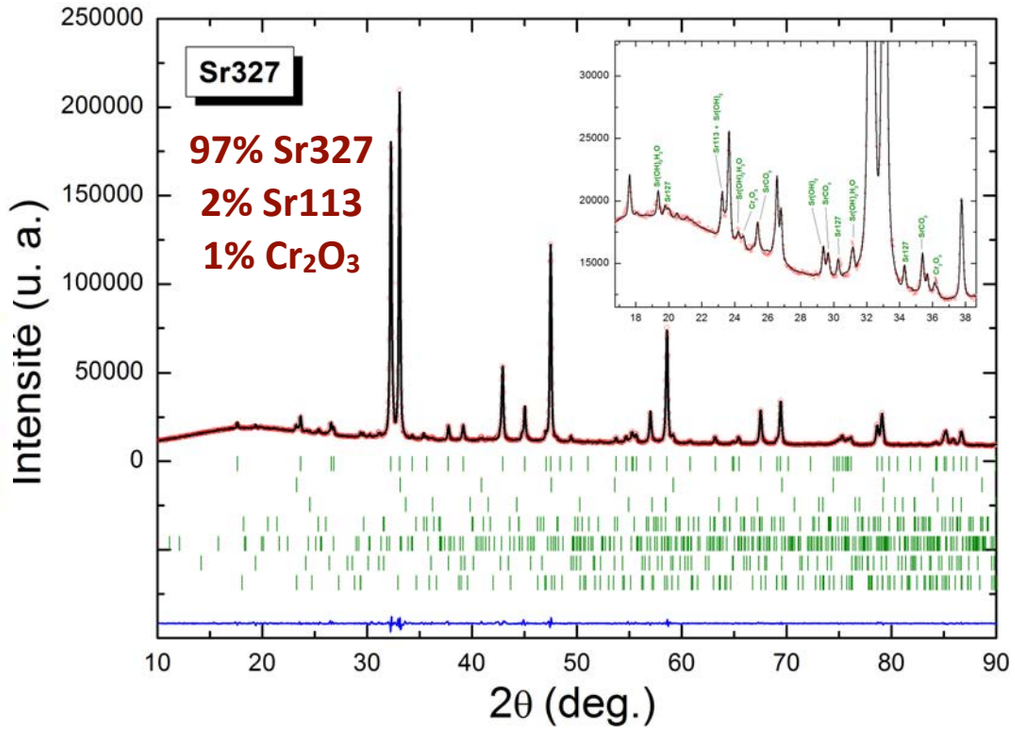

a ~ 3.82 Å

c ~ 20.14 Å

$Sr_3Cr_2O_7$

Sr327
I4/mmm

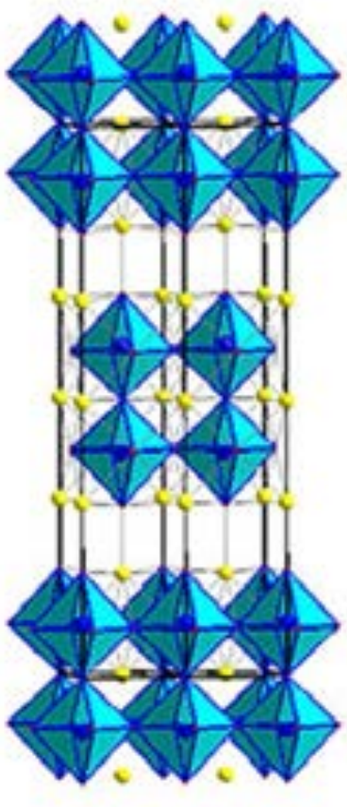

a ~ 3.82 Å

c ~ 20.14 Å

X-ray diffraction

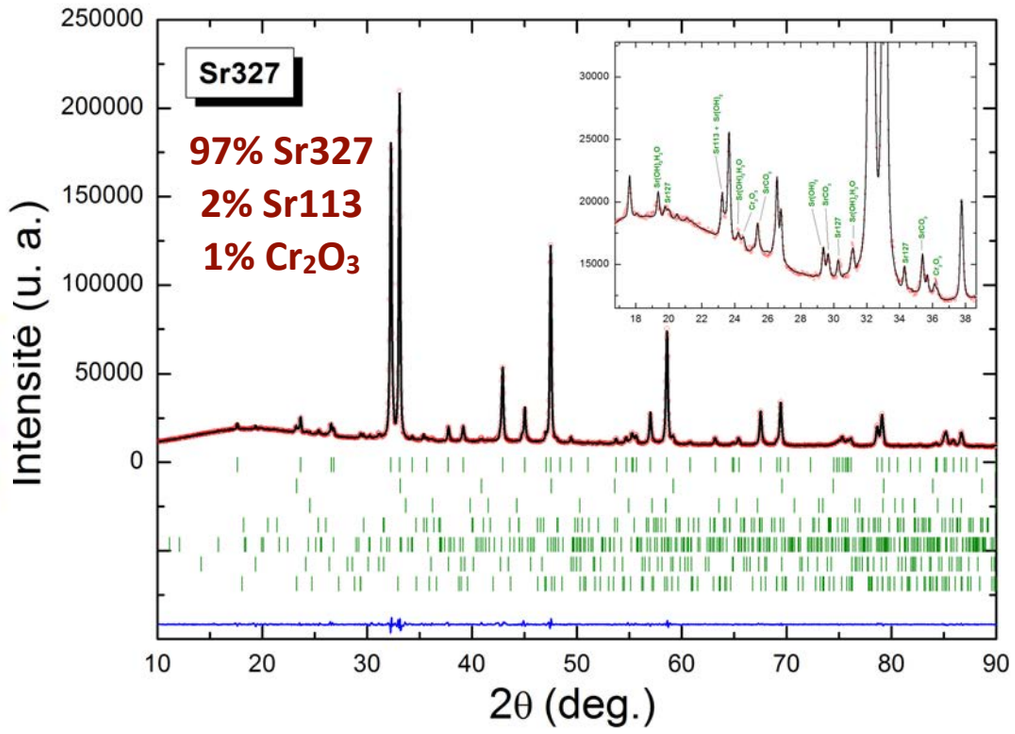

Transport measurement

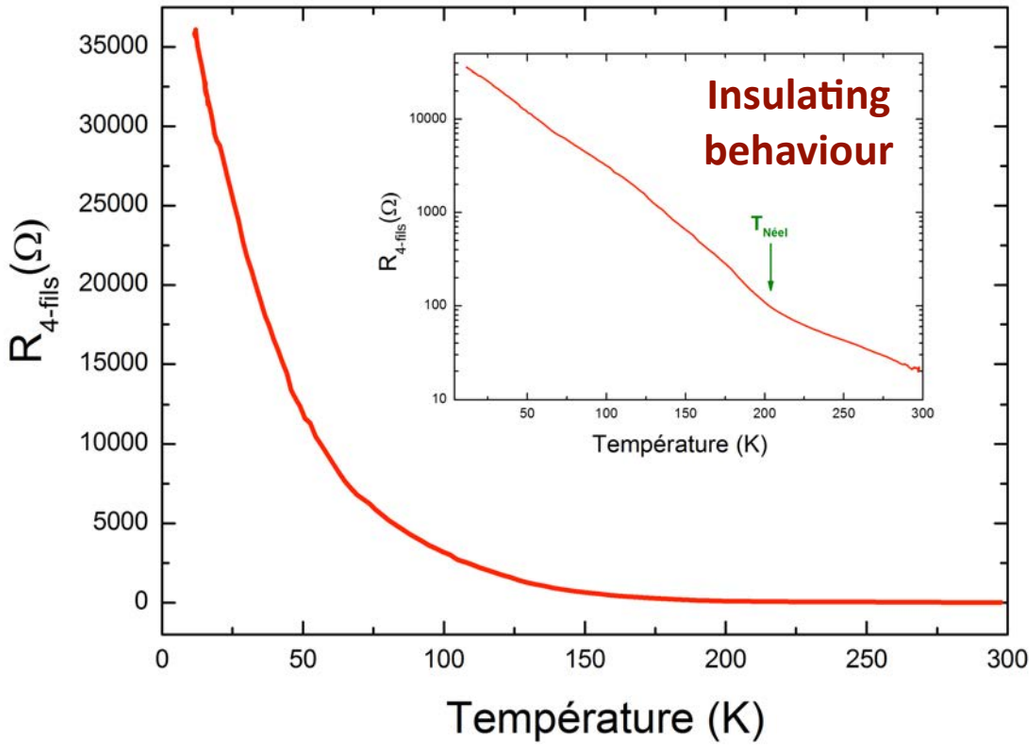

Calculations give metallic
(without magnetism & U)

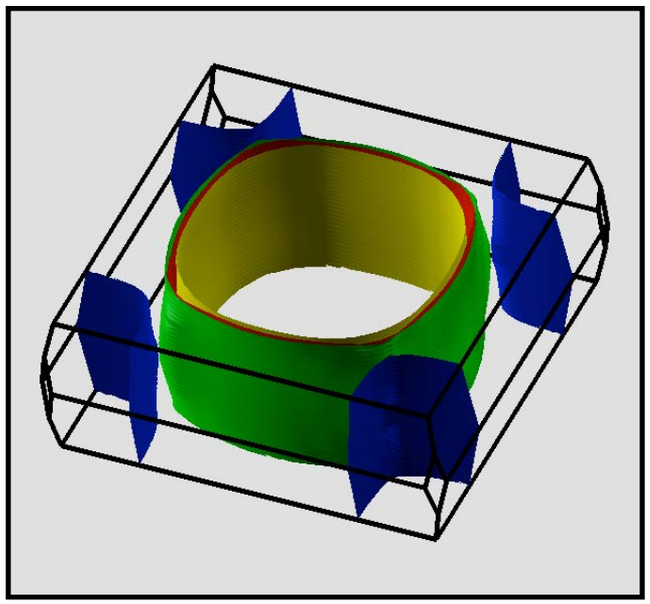

Ruben Weht

$Sr_3Cr_2O_7$

Sr327
I4/mmm

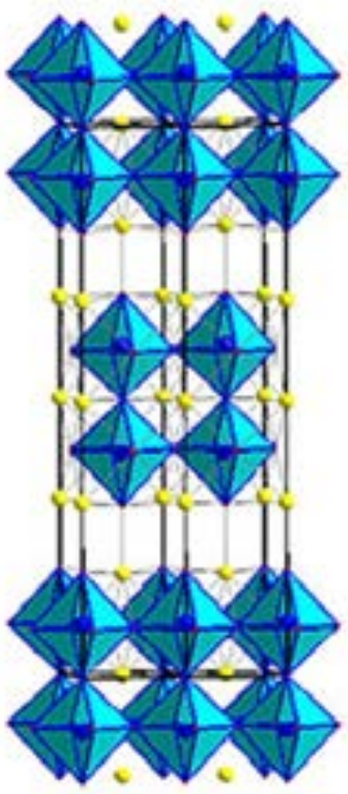

a ~ 3.82 Å

c ~ 20.14 Å

X-ray diffraction

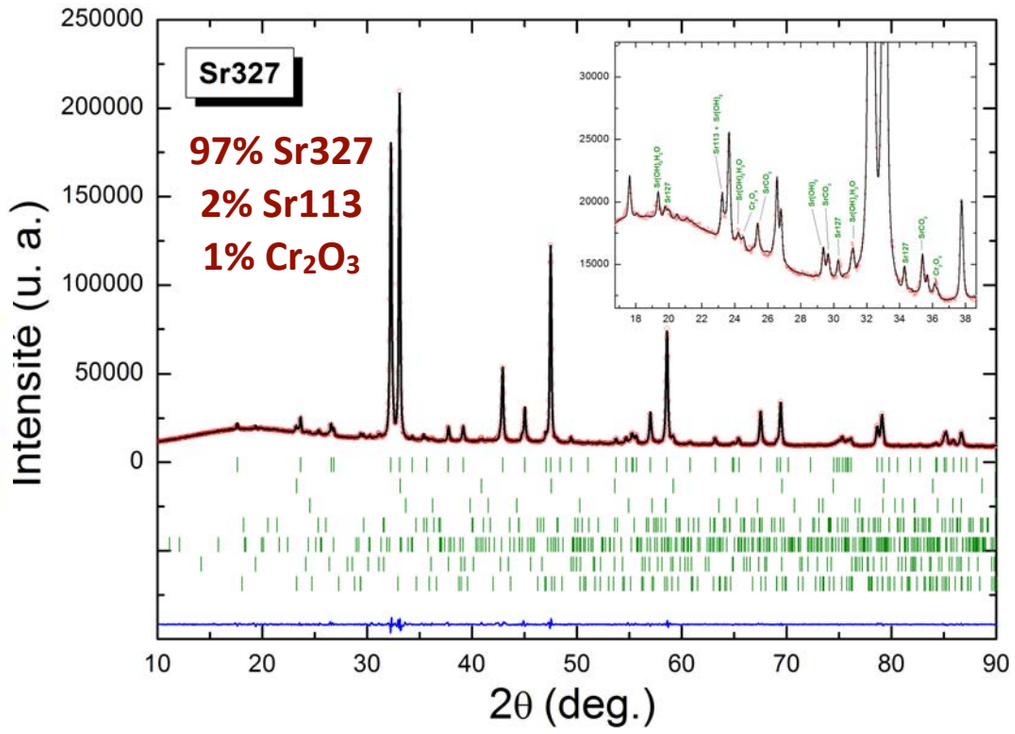

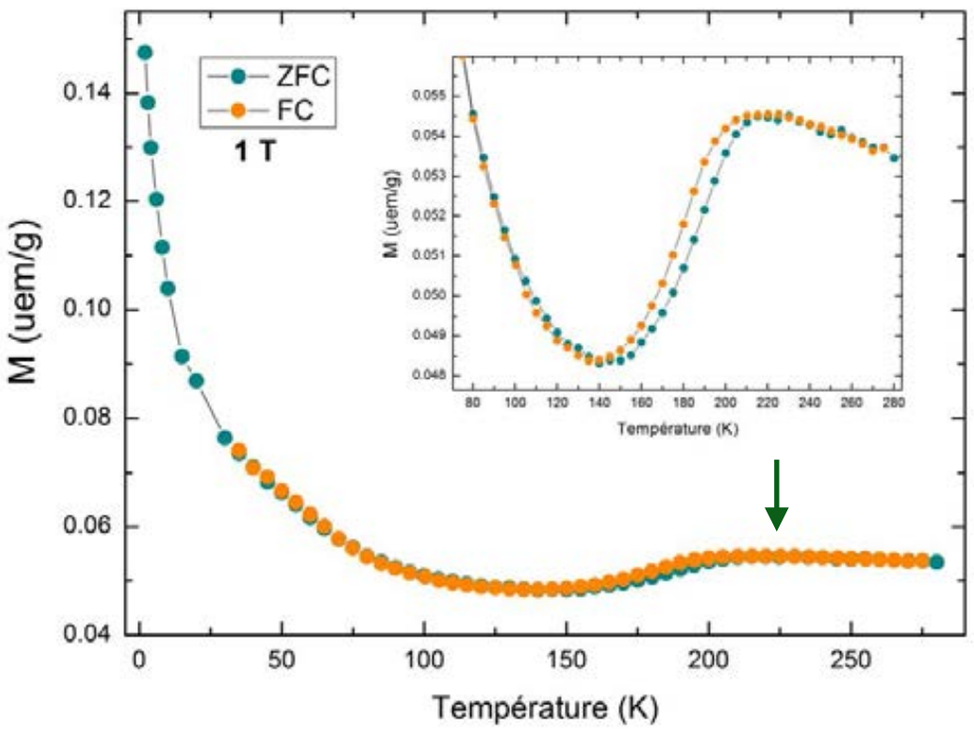

Transport measurement

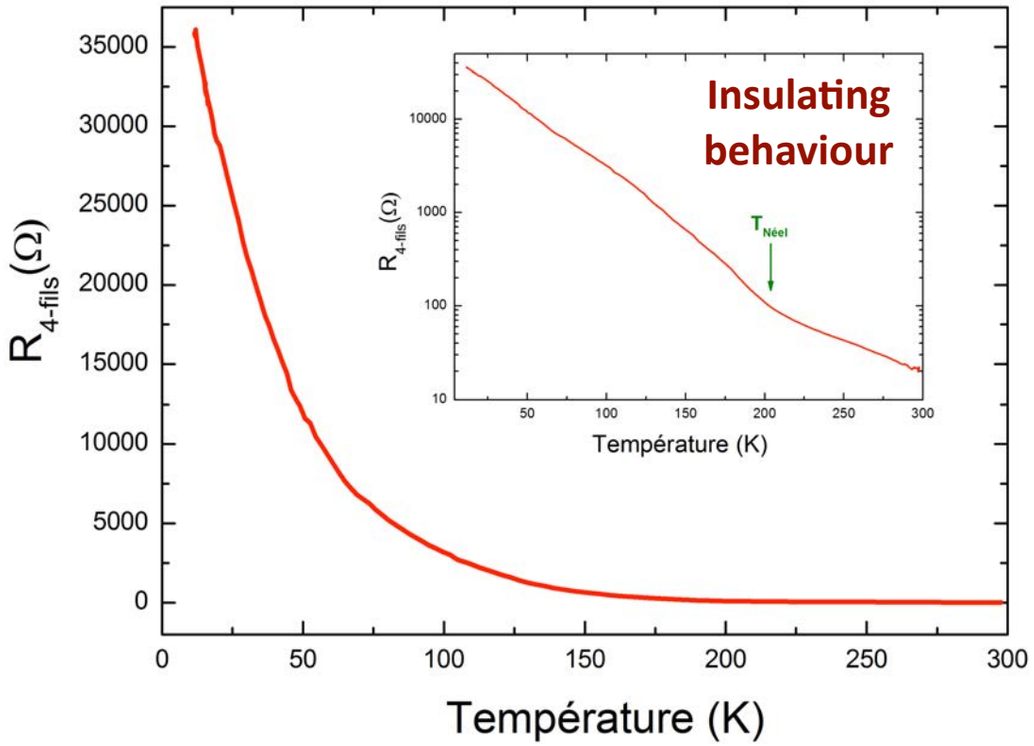

AFM

$T_{Néel}$ = 210K

$Sr_3Cr_2O_7$

Sr327
I4/mmm

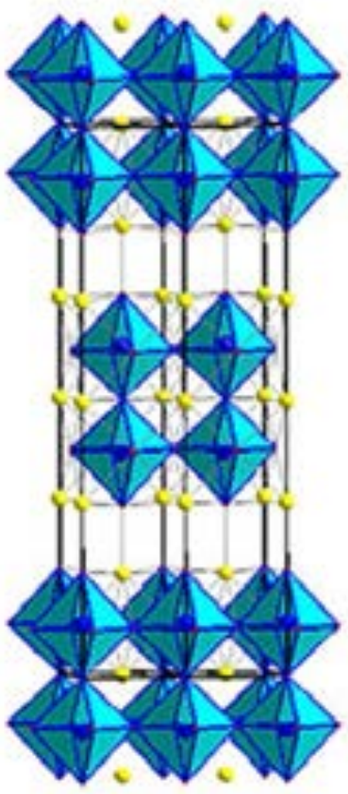

a ~ 3.82 Å

c ~ 20.14 Å

X-ray diffraction

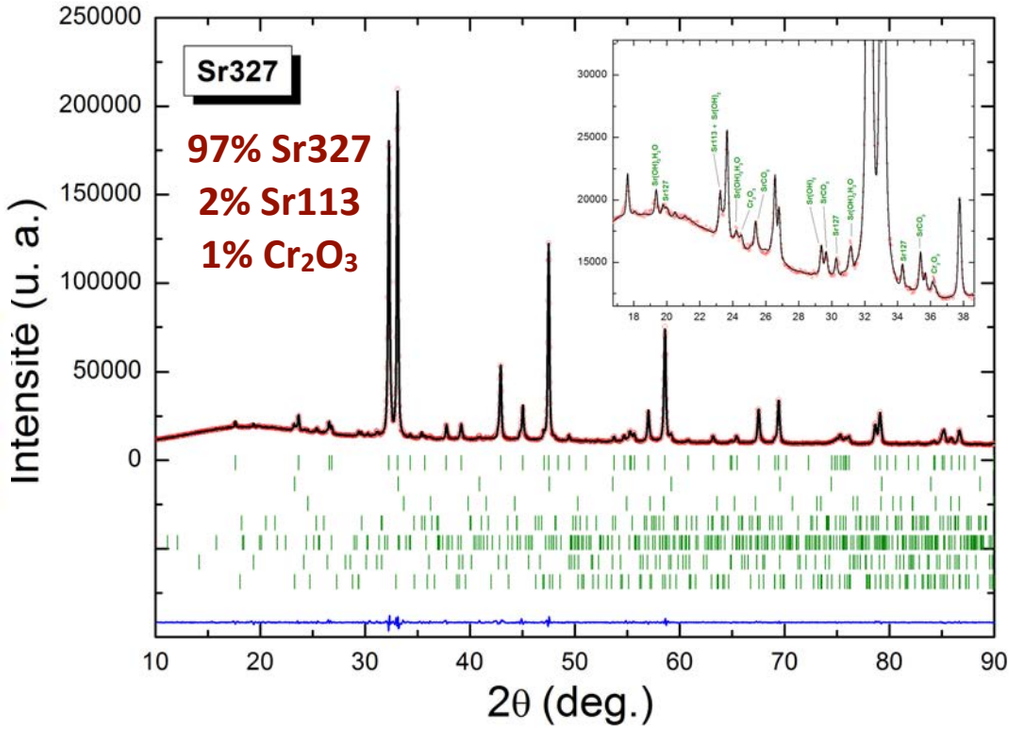

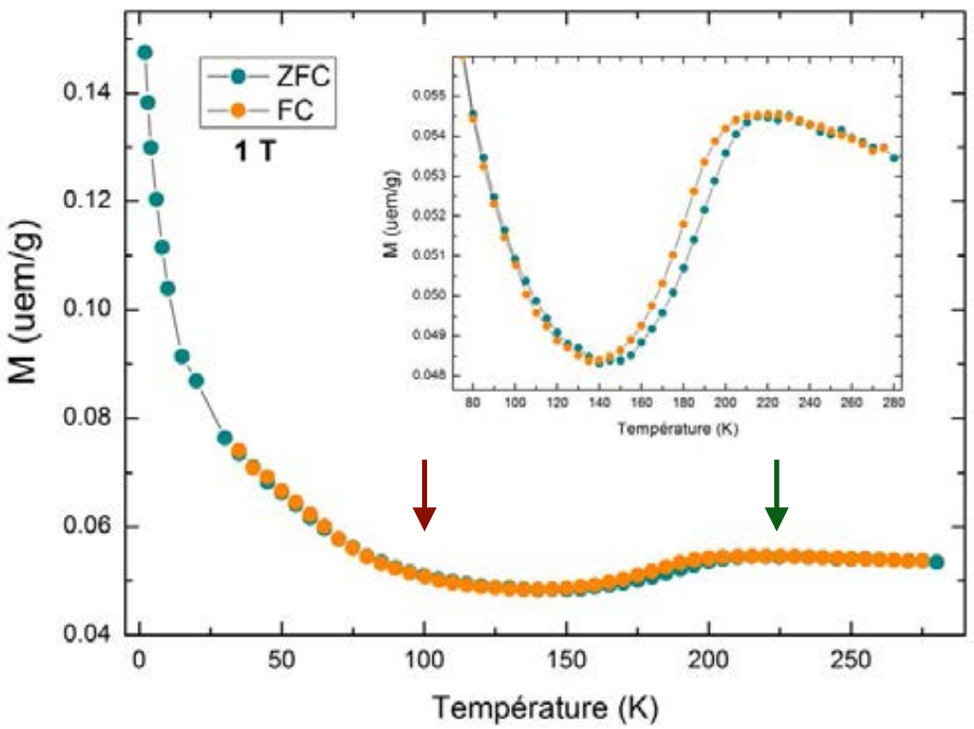

Transport measurement

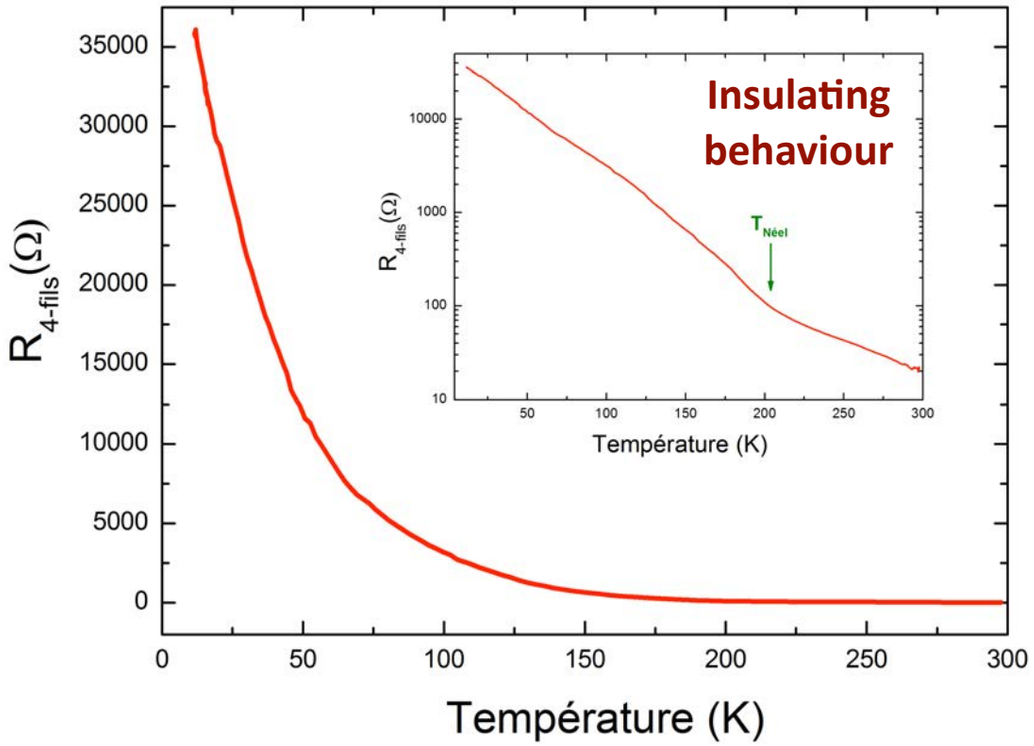

AFM

$T_{Néel}$ = 210K

anomaly
T = 100K ?

$Sr_3Cr_2O_7$

Neutron Powder diffraction

ILL, D1B & D2B instruments

$Sr_3Cr_2O_7$

Neutron Powder diffraction

ILL, D1B & D2B instruments

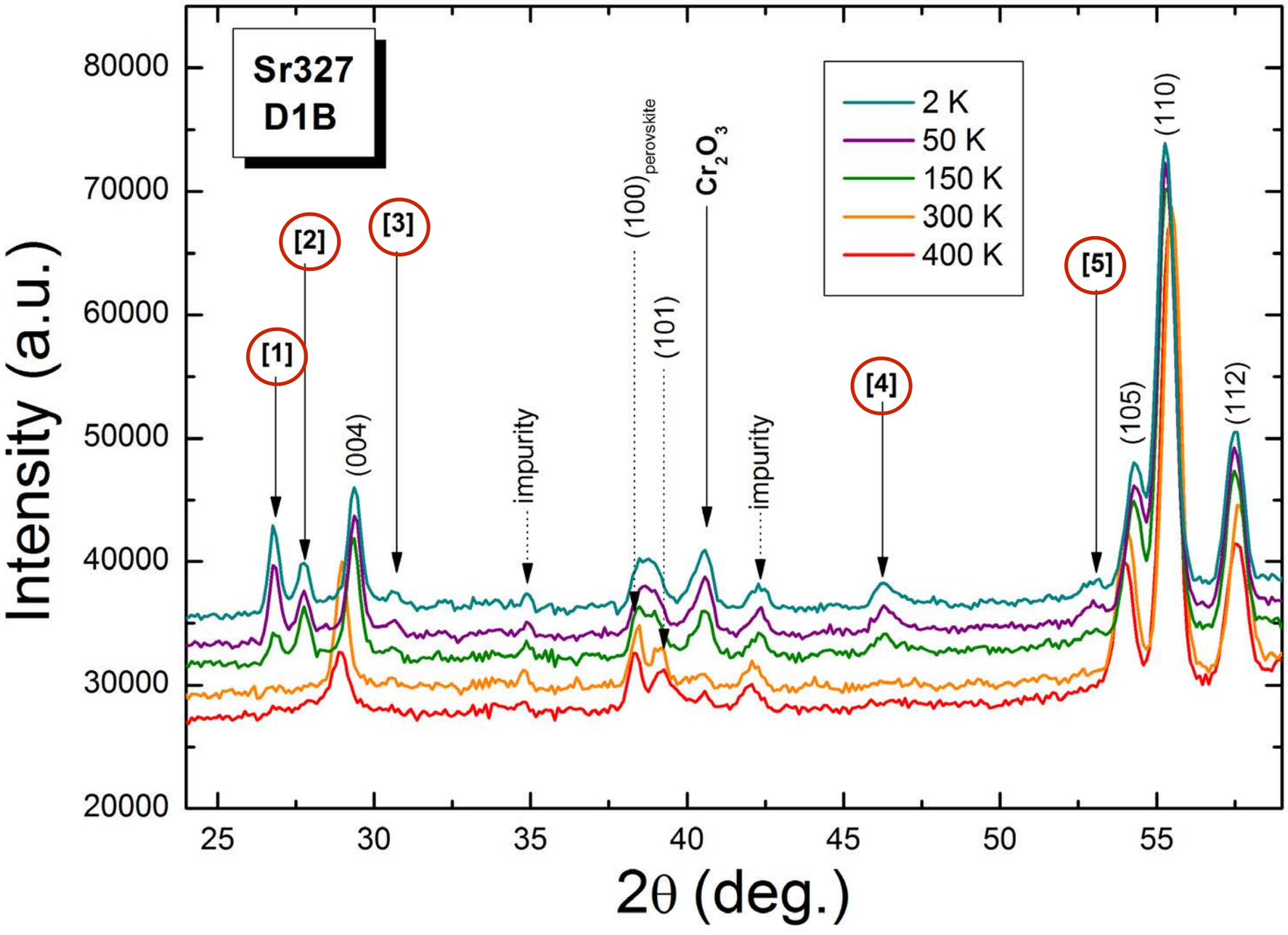

Magnetic peaks appearance between 300 & 150 K

$Sr_3Cr_2O_7$

Neutron Powder diffraction

ILL, D1B & D2B instruments

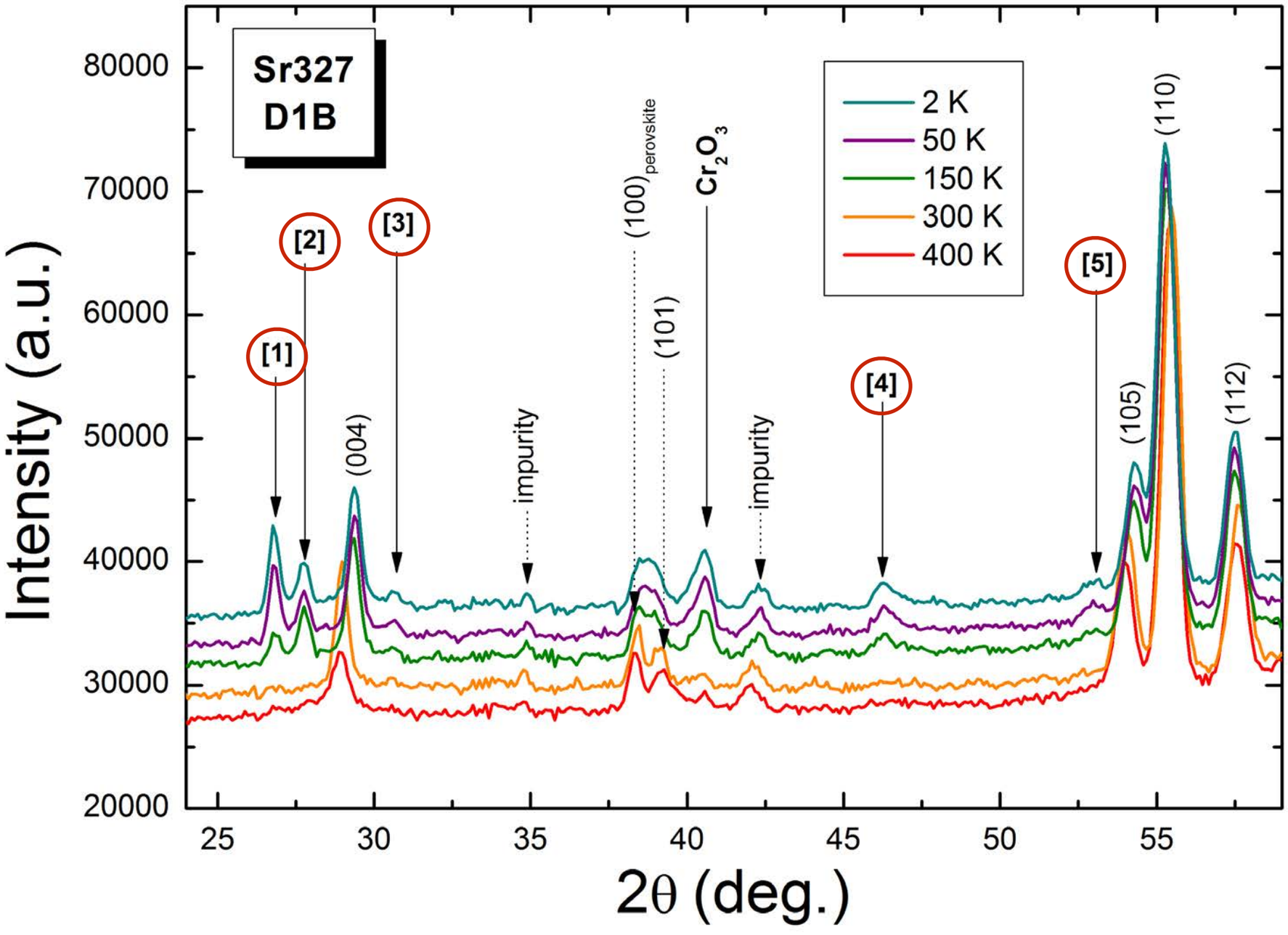

Magnetic peaks appearance between 300 & 150 K

OK with $T_{Néel}$ = 210 K

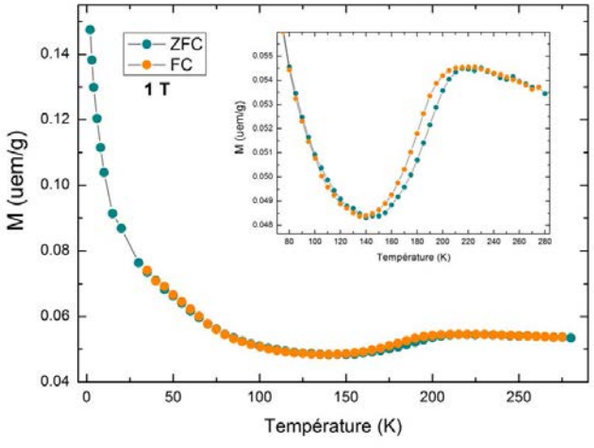

$Sr_3Cr_2O_7$

Neutron Powder diffraction

ILL, D1B & D2B instruments

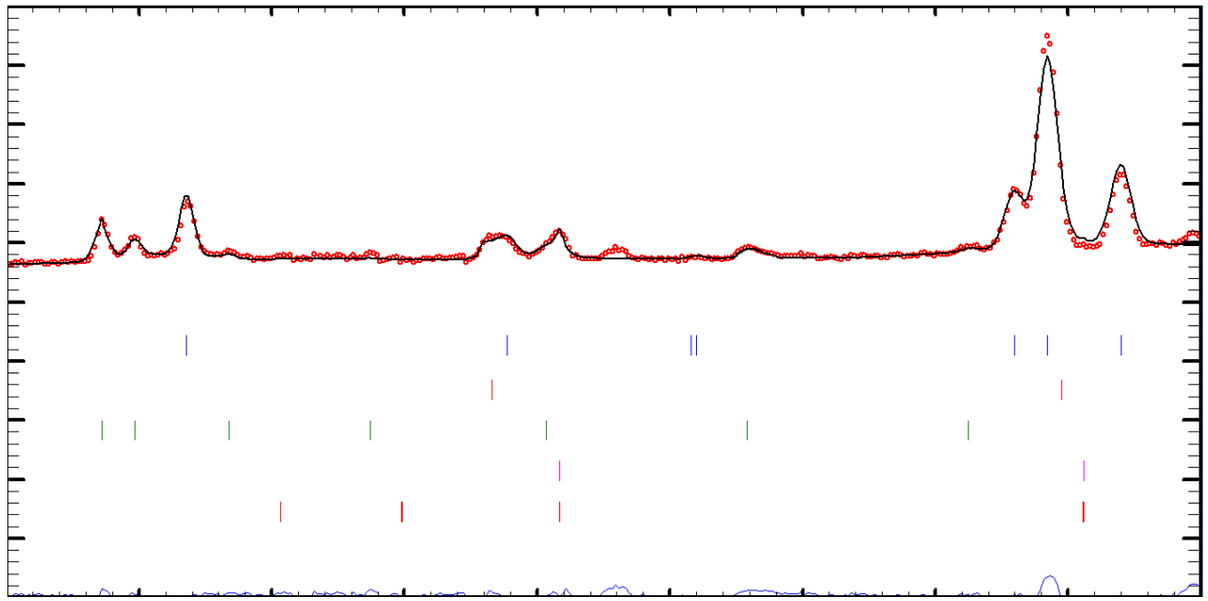

$Sr_3Cr_2O_7$

Neutron Powder diffraction

ILL, D1B & D2B instruments

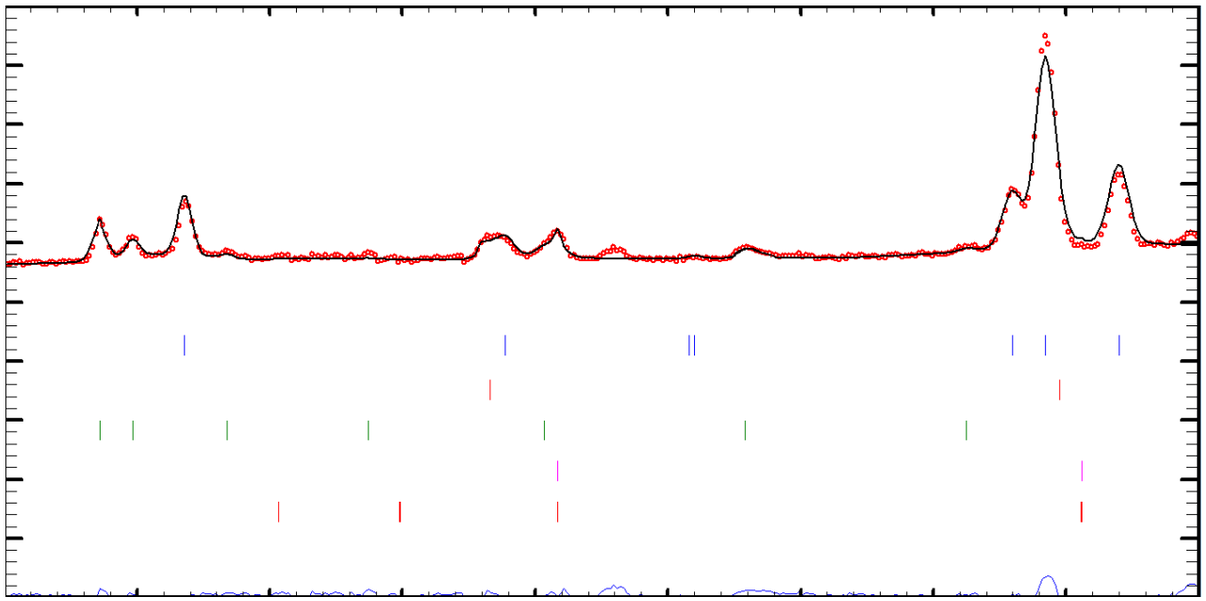

Magnetic phase refinement

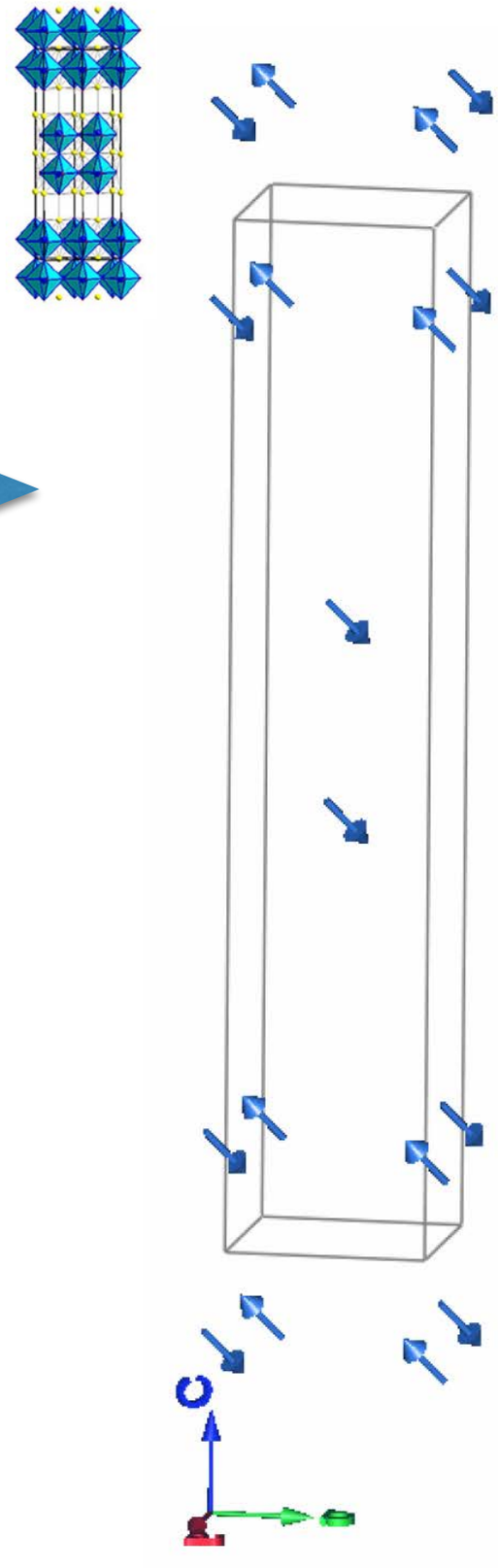

$Sr_3Cr_2O_7$

Neutron Powder diffraction

ILL, D1B & D2B instruments

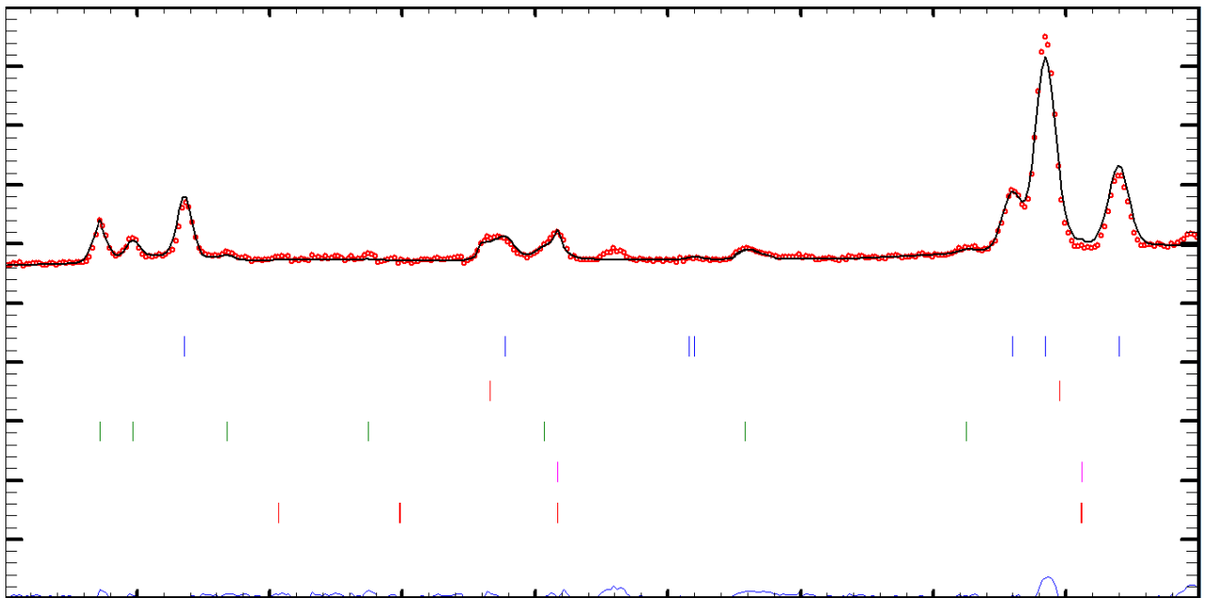

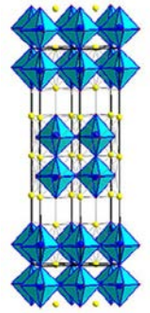

Magnetic phase refinement

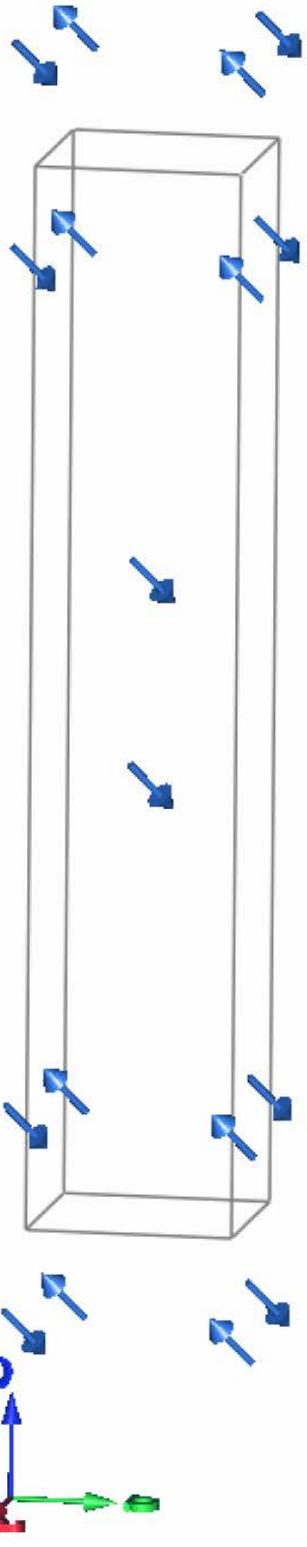

Calculated and measured magnetic structure coincide

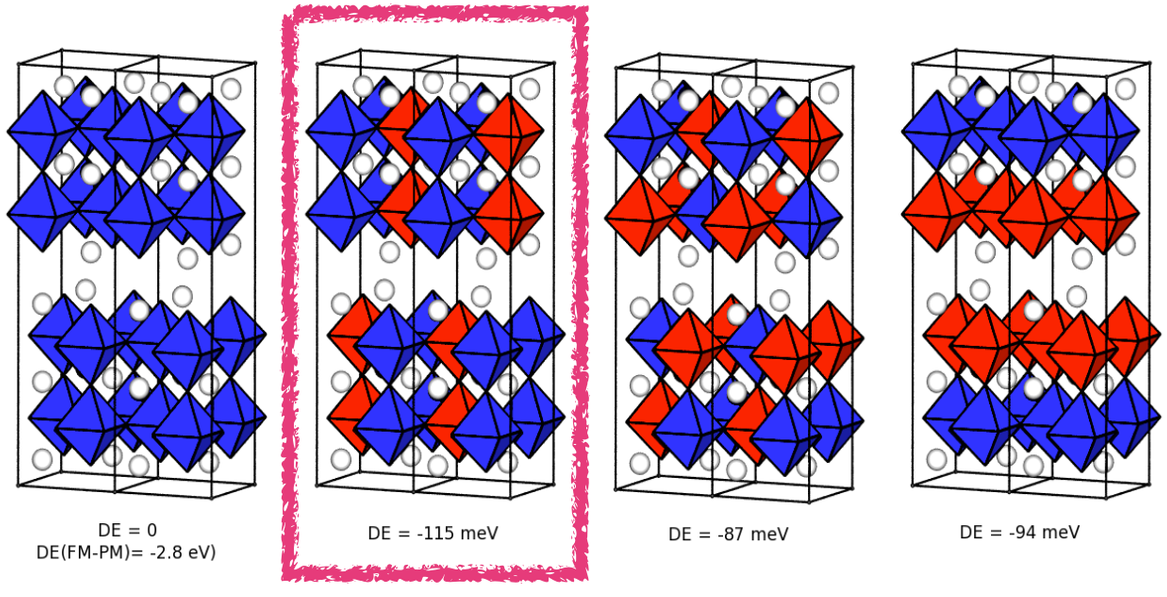

$Sr_3Cr_2O_7$

Neutron Powder diffraction

ILL, D1B & D2B instruments

D1B : Claire Colin & Vivian Nassif
D2B : Emmanuelle Suard

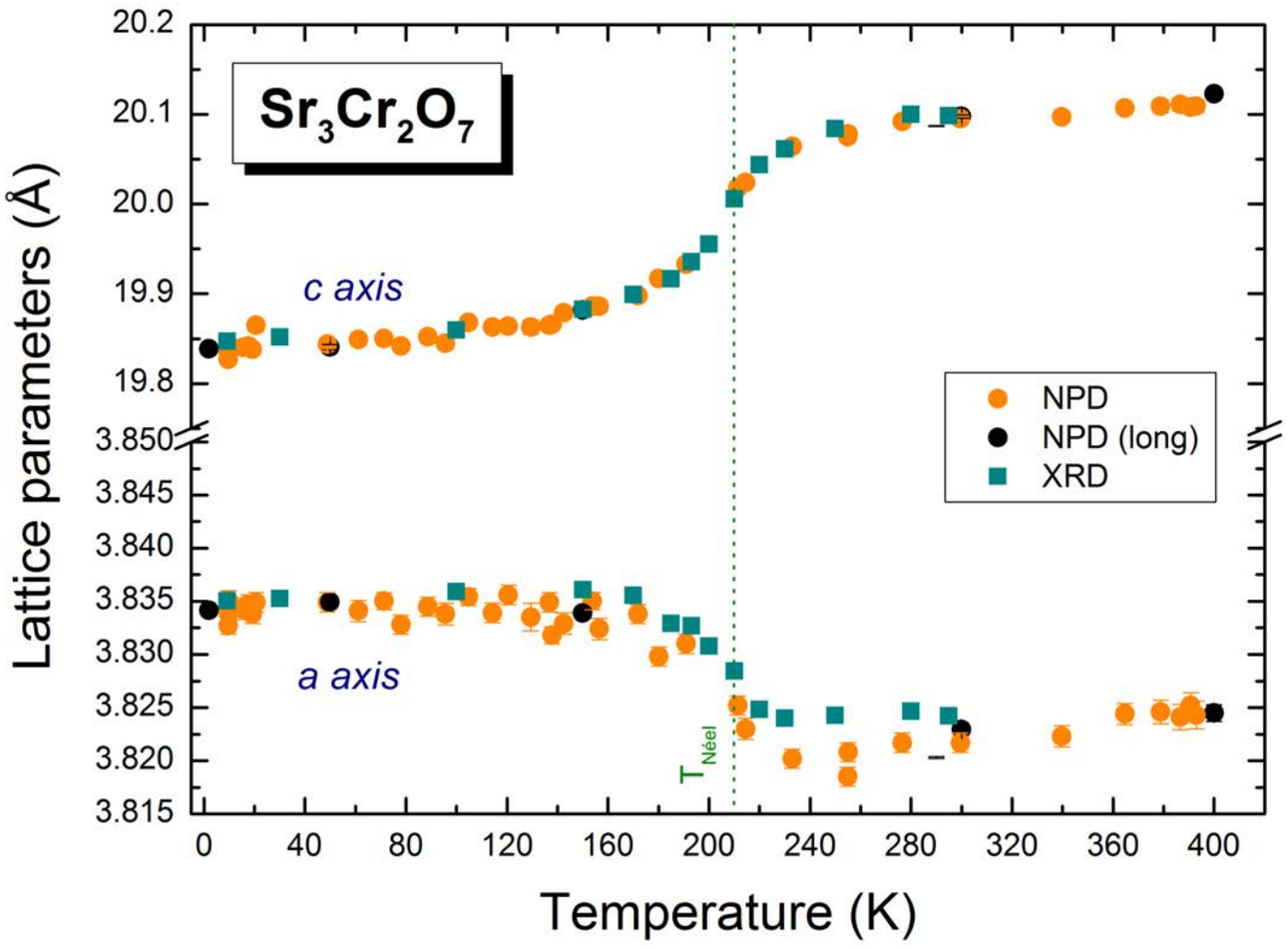

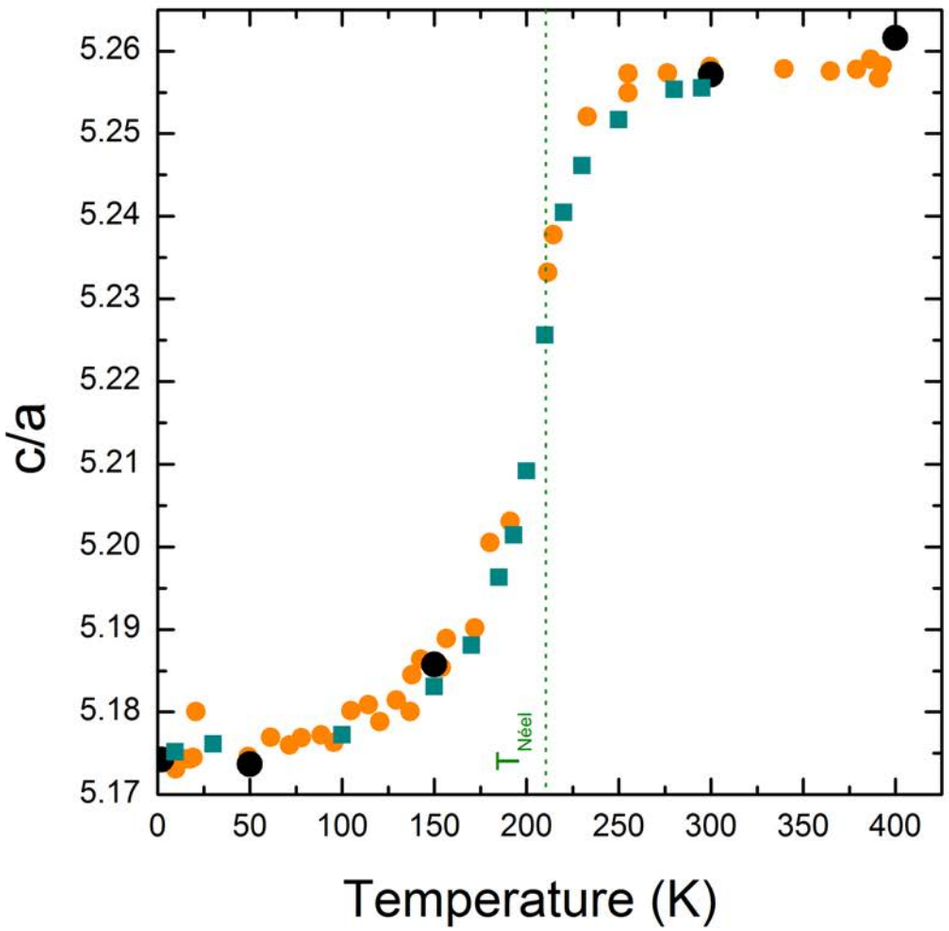

Huge anomaly at T_N : strong magneto-structural coupling

c axis : -1.33%

a axis : +0.33%

$Sr_3Cr_2O_7$

Neutron Powder diffraction

ILL, D1B & D2B instruments

D1B : Claire Colin & Vivian Nassif
D2B : Emmanuelle Suard

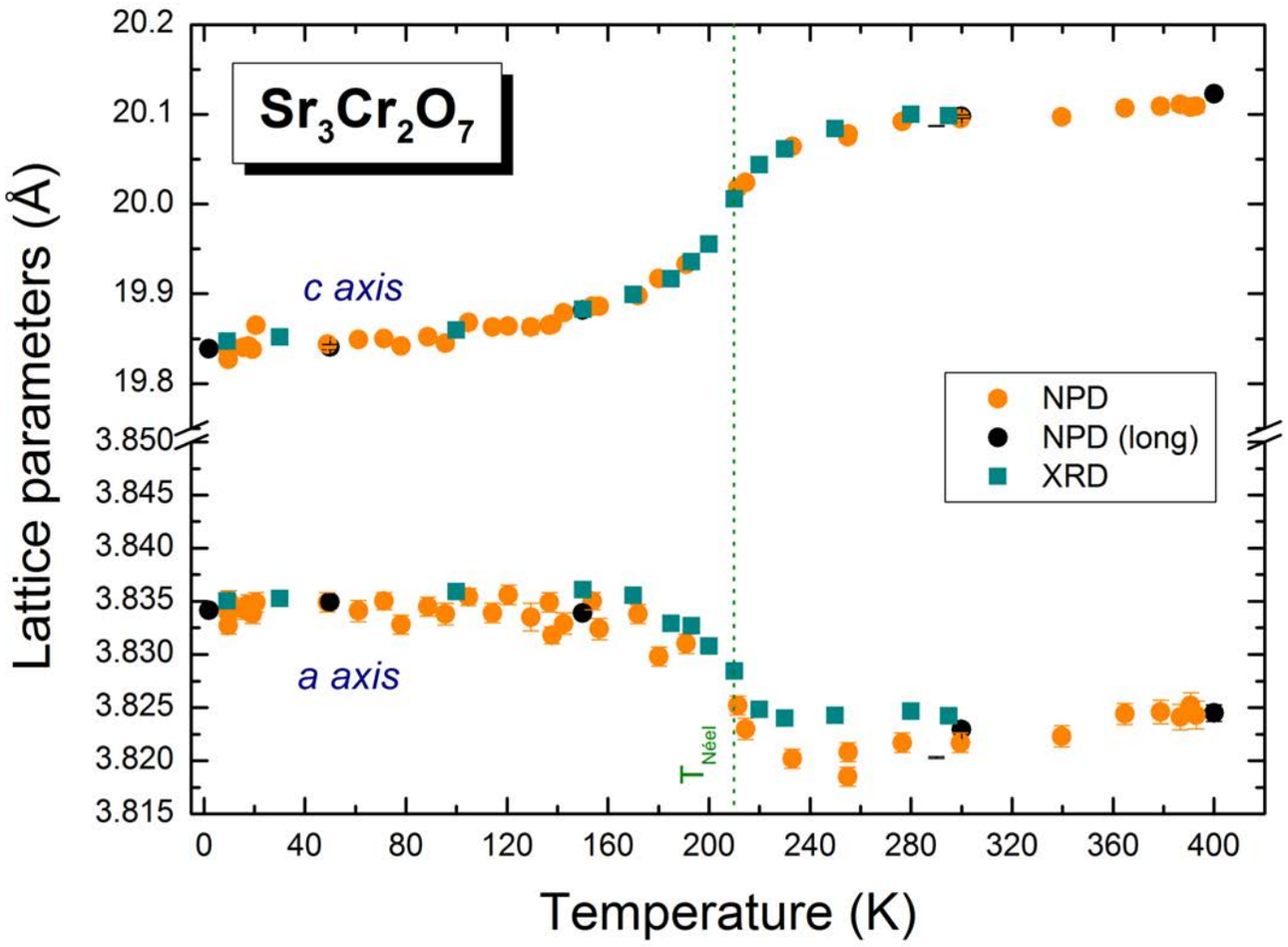

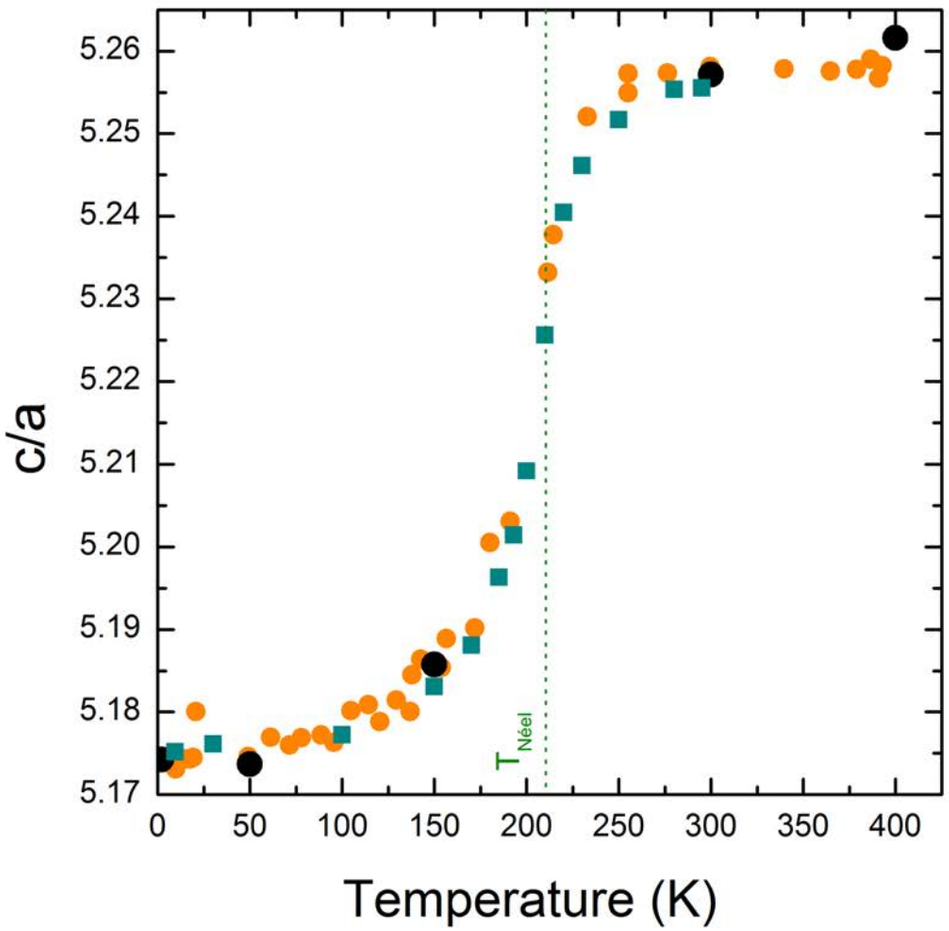

Huge anomaly at T_N : strong magneto-structural coupling

c axis : -1.33%

a axis : +0.33%

$LaMnO_3$: a +0.8% at $T_{Néel}$=141K
b -0.05%

$CaCrO_3$: c +0.5% at $T_{Néel}$=90K

$Sr_3Cr_2O_7$

Specific Heat

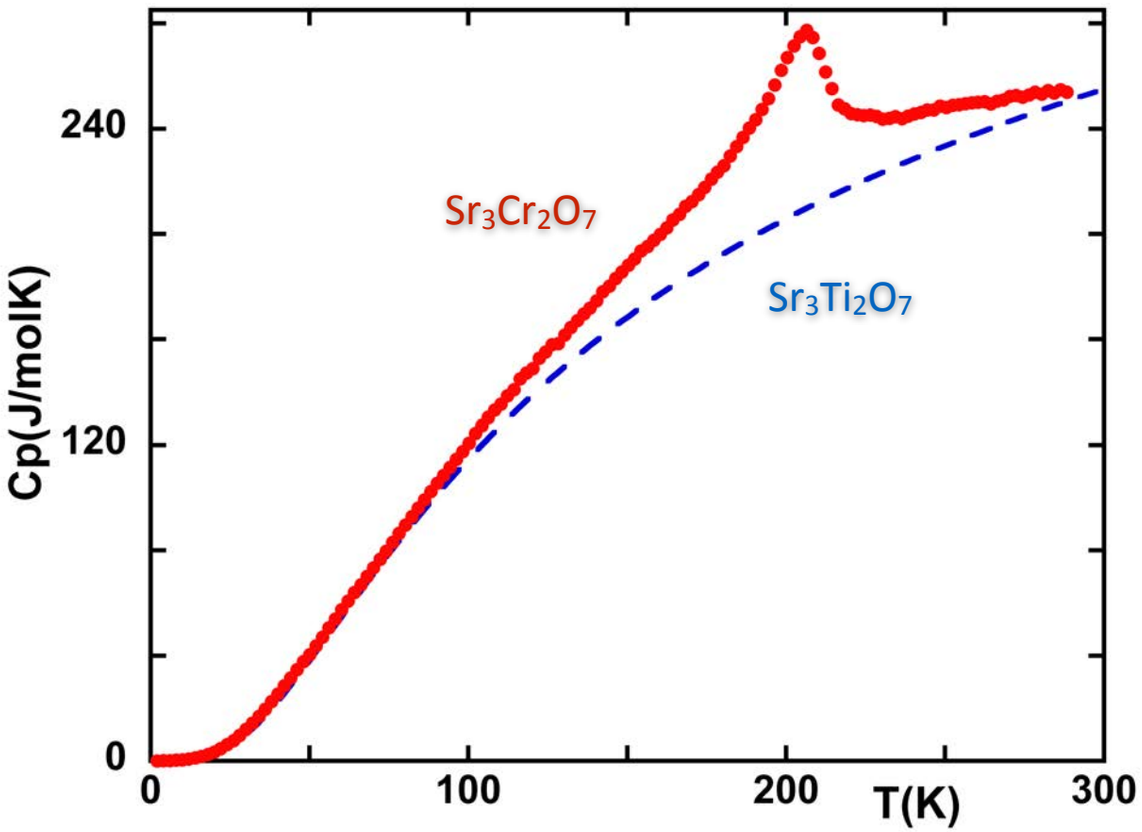

$Sr_3Cr_2O_7$

Specific Heat

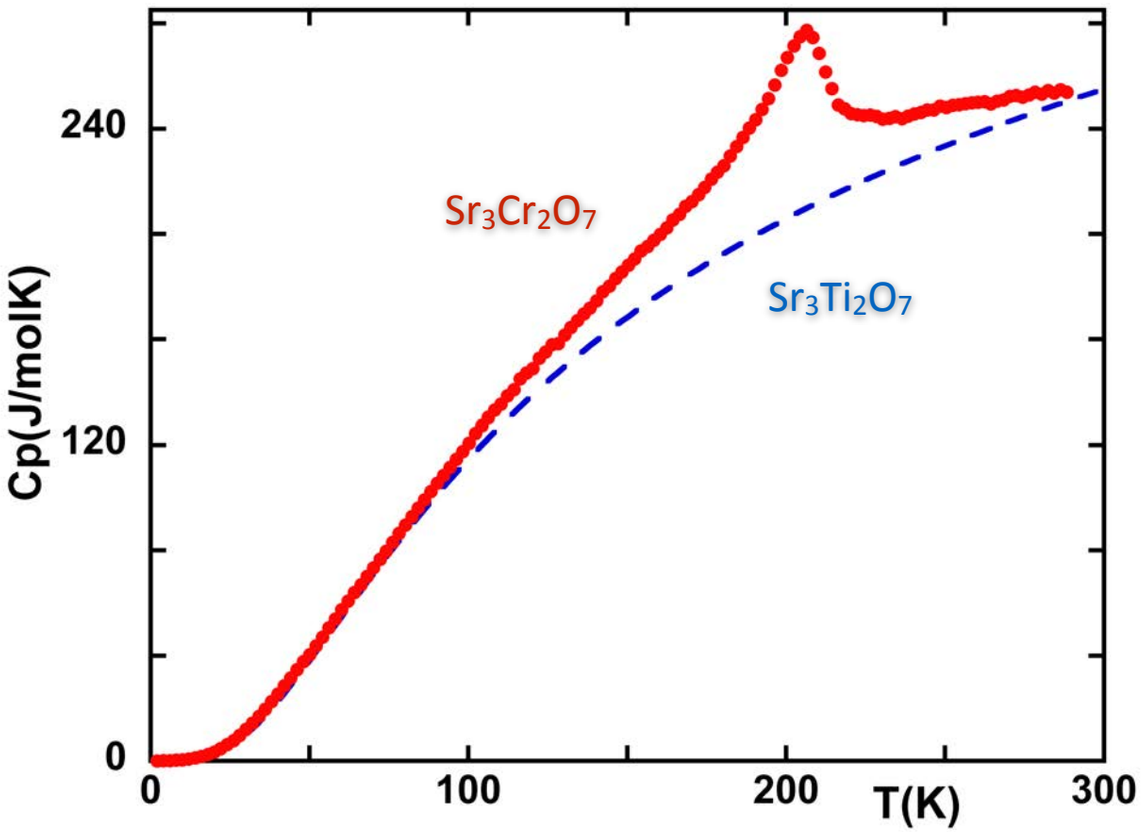

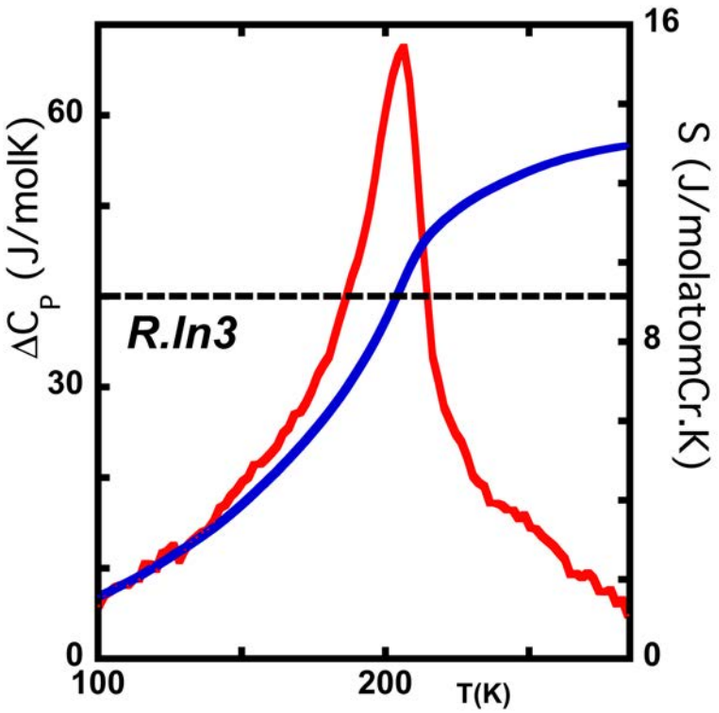

$Sr_3Cr_2O_7$

Specific Heat

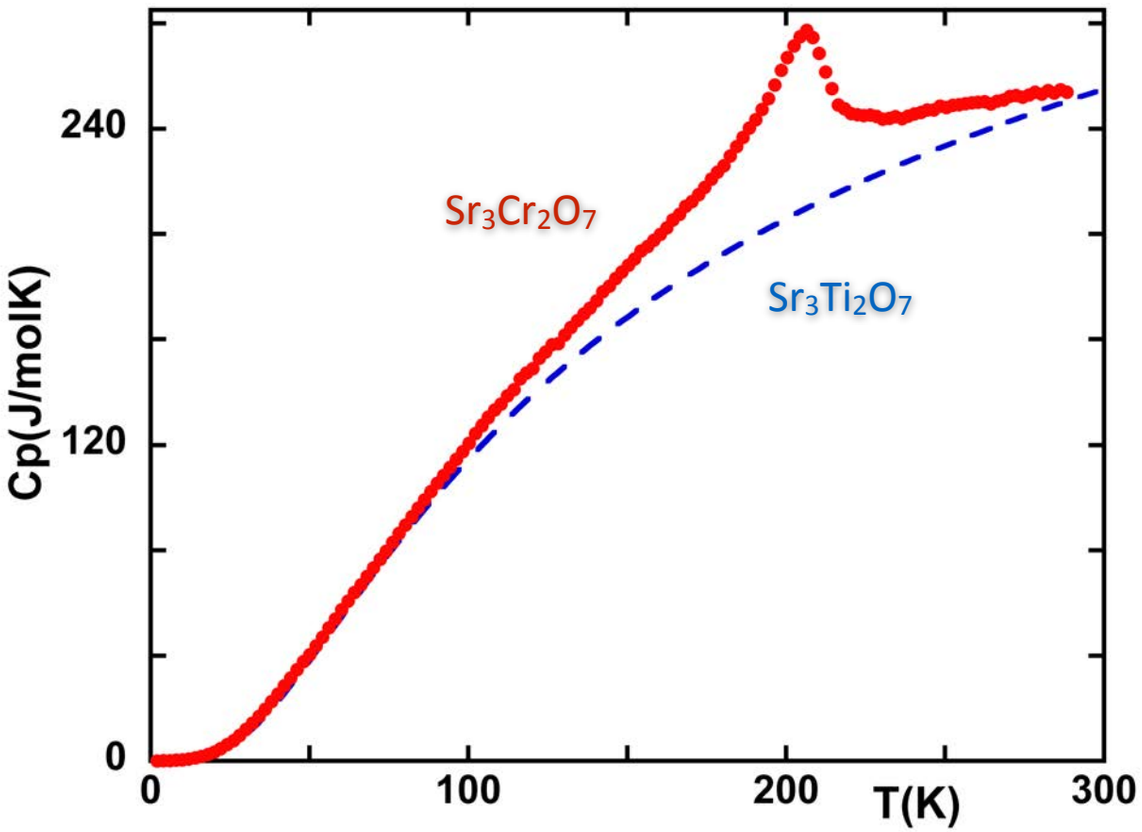

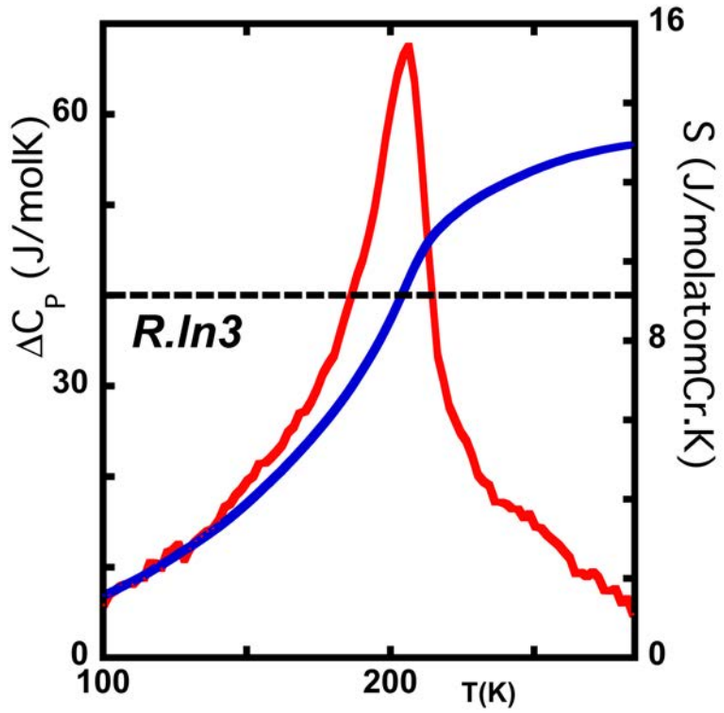

Transition entropy : near to **R*ln6***

(if only magnetic ordering : R*ln3)*

$Sr_3Cr_2O_7$

Specific Heat

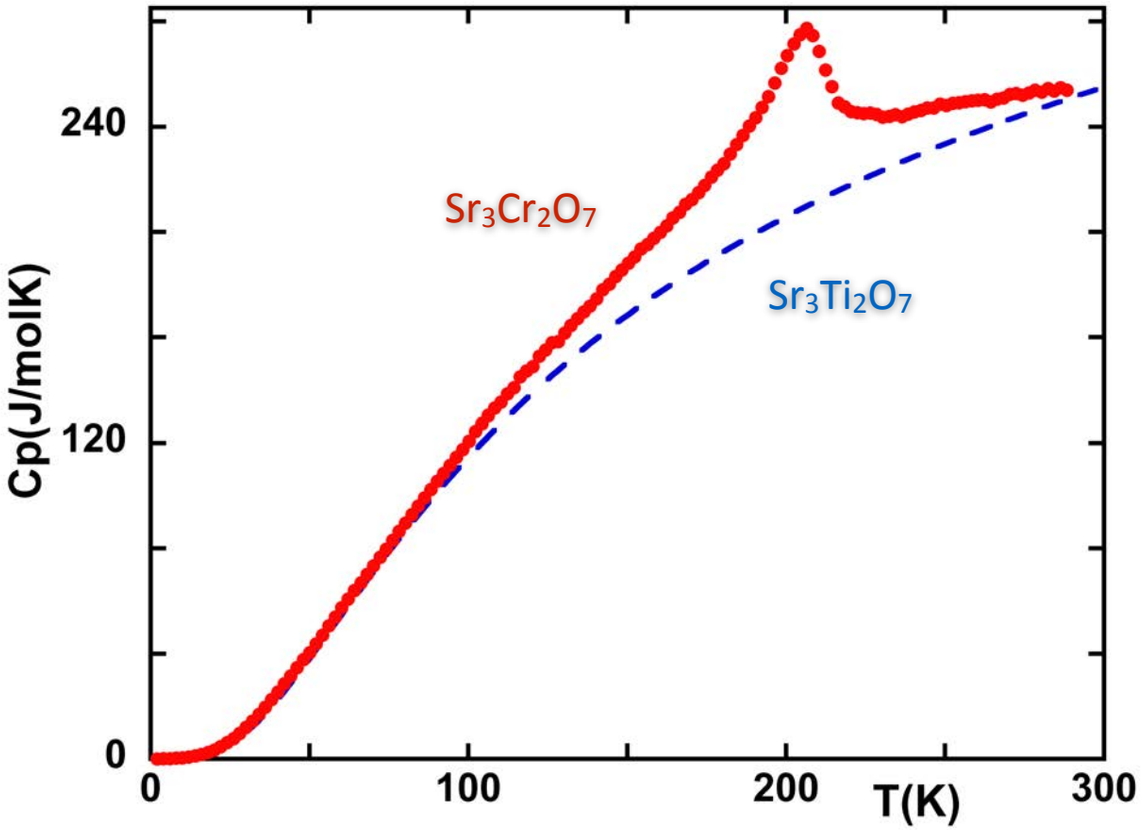

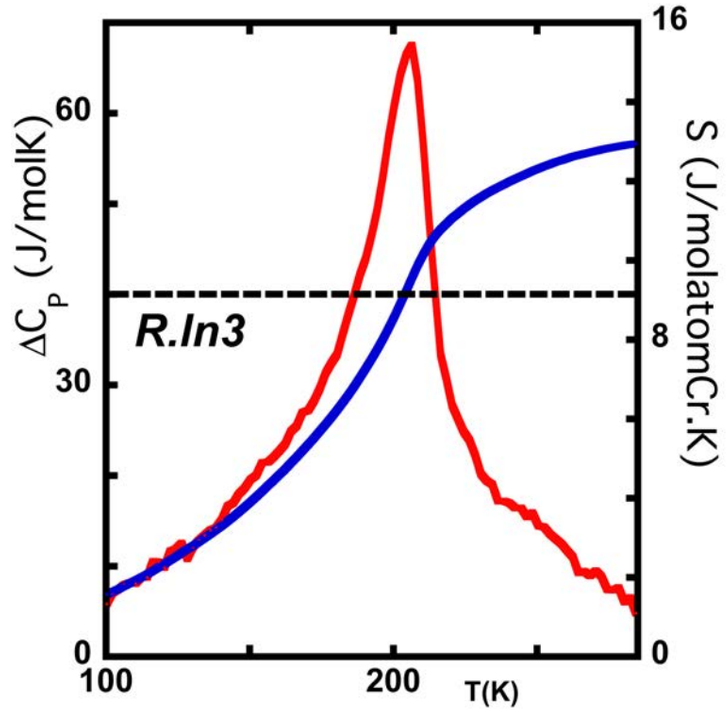

Transition entropy : near to **R*ln6***

(if only magnetic ordering : R*ln3)*

Magnetic AND Orbital Ordering

$Sr_3Cr_2O_7$

Specific Heat

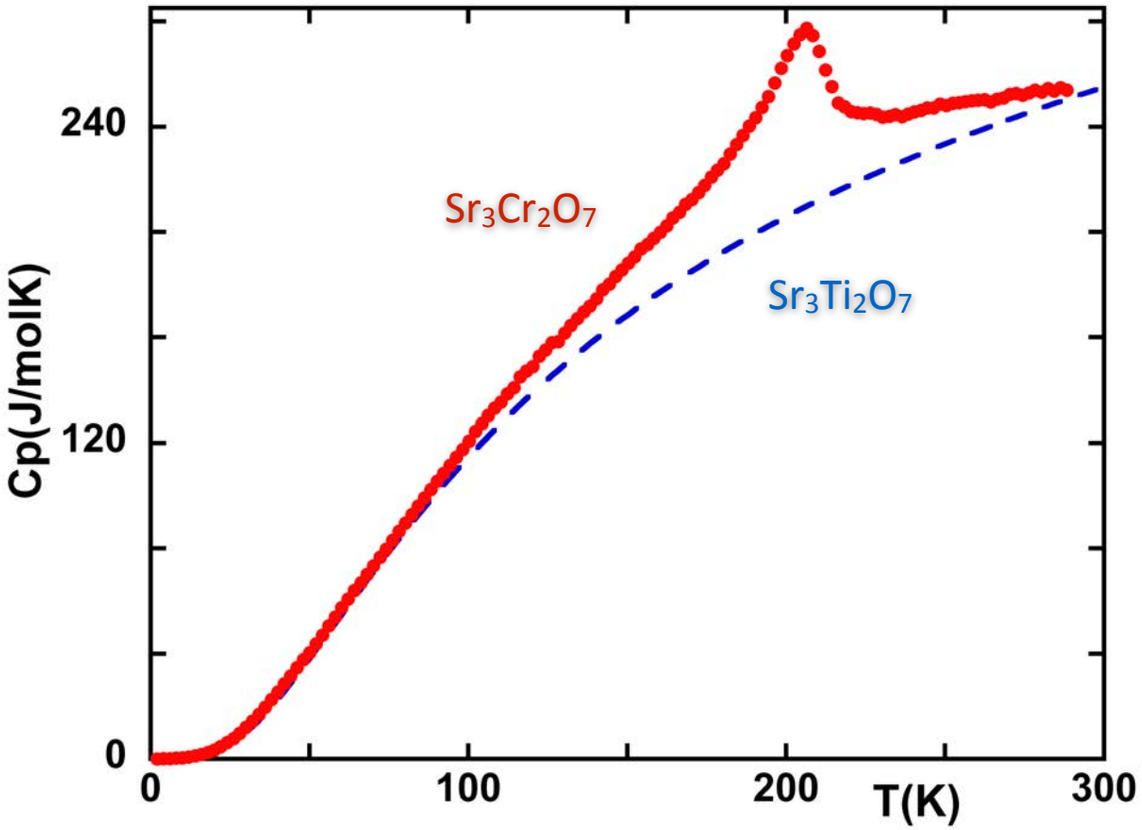

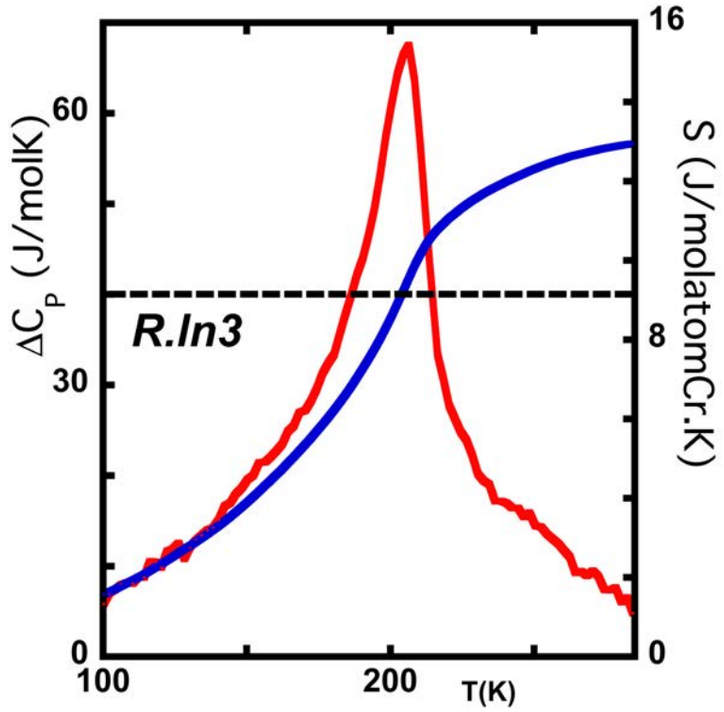

Transition entropy : near to **R*ln6***

(if only magnetic ordering : R*ln3)*

↓

Magnetic AND Orbital Ordering

↓

partial or full?

$Sr_3Cr_2O_7$

Specific Heat

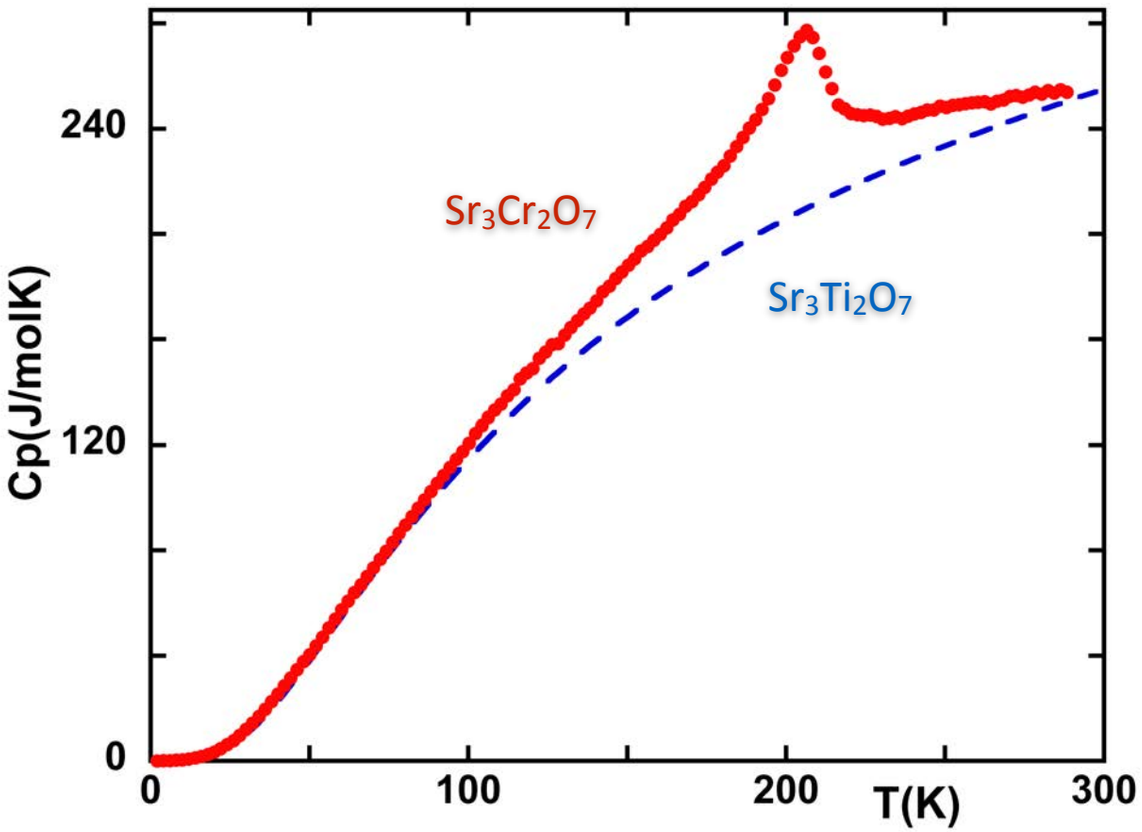

Transition entropy : near to **R*ln6***

(if only magnetic ordering : R*ln3)*

Magnetic AND Orbital Ordering

partial or full?

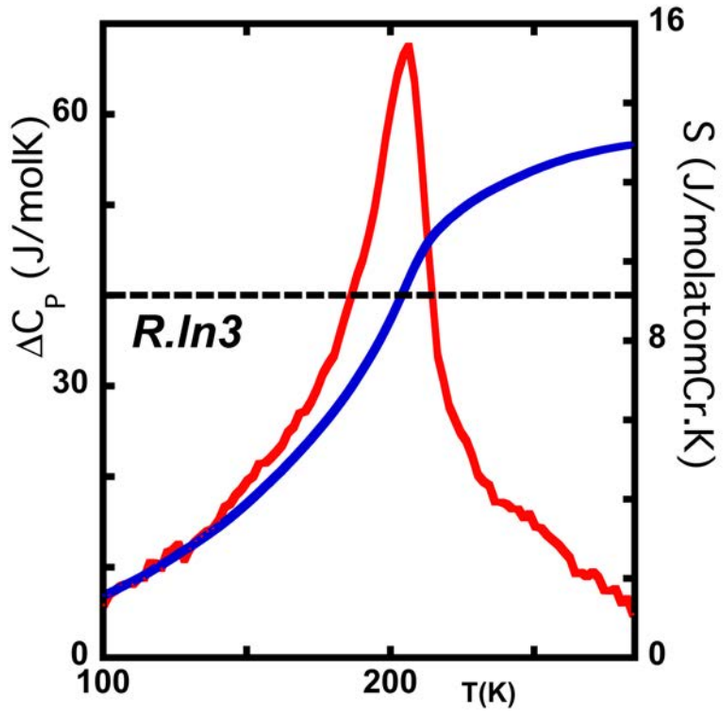

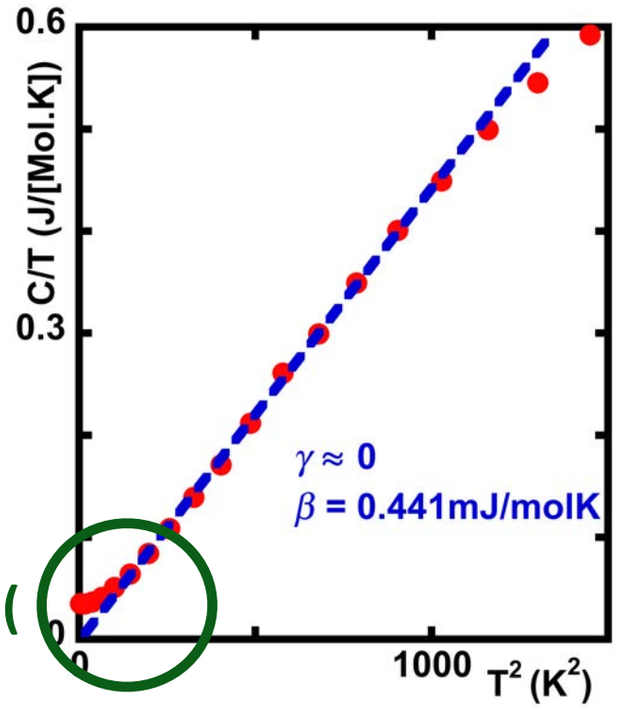

non metallic :'(

$Sr_3Cr_2O_7$

Neutron Powder diffraction

ILL, D1B & D2B instruments

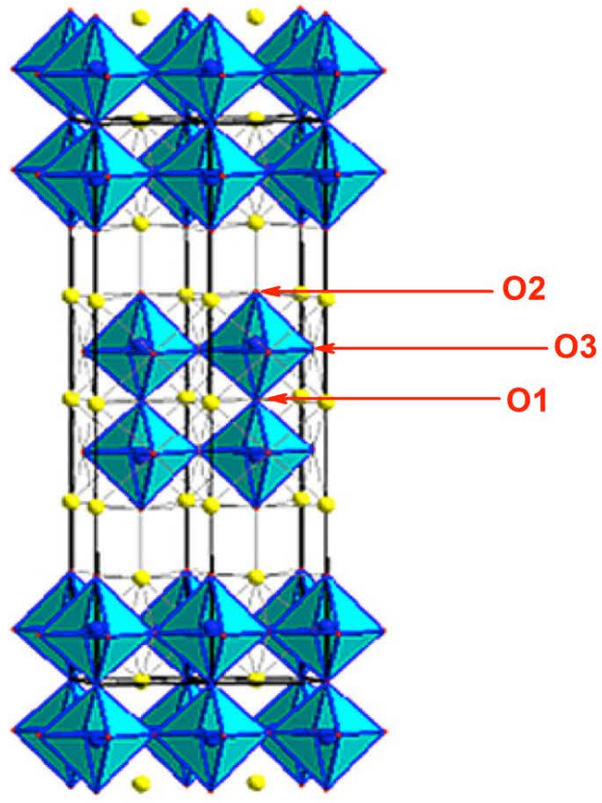

$Sr_3Cr_2O_7$

Neutron Powder diffraction

ILL, D1B & D2B instruments

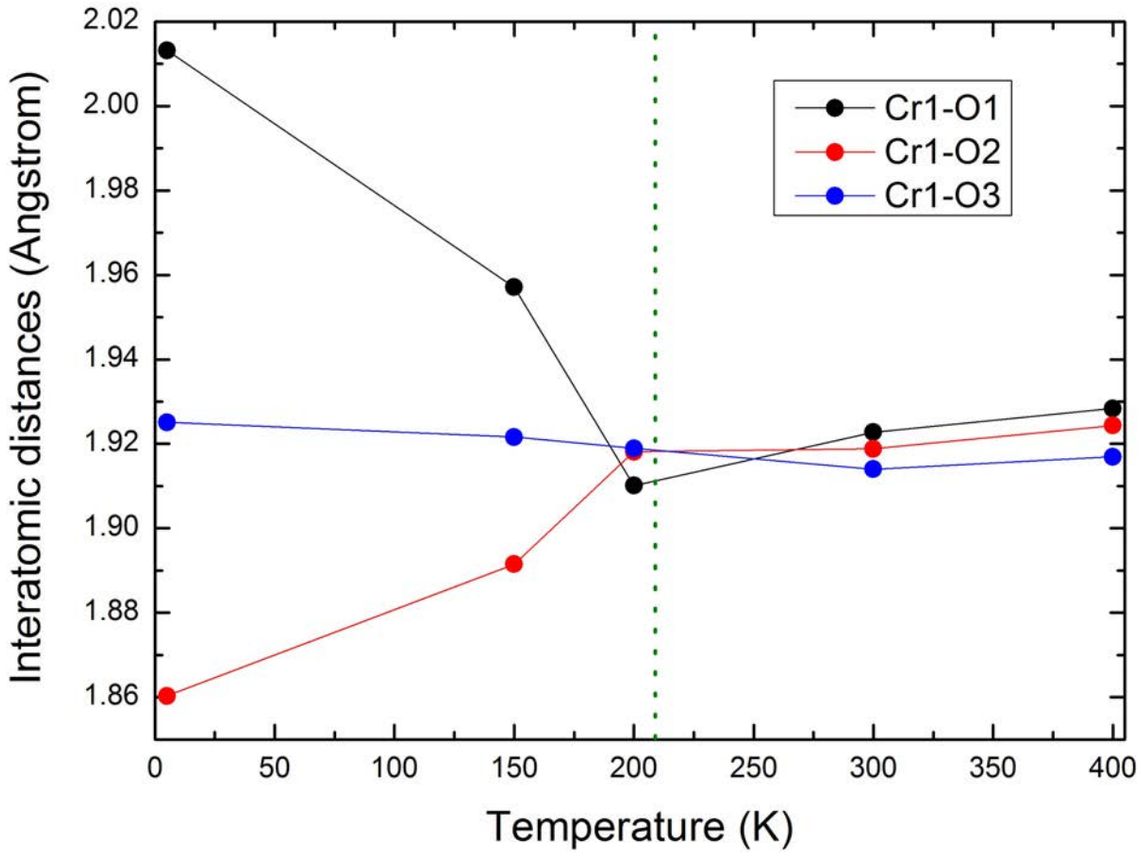

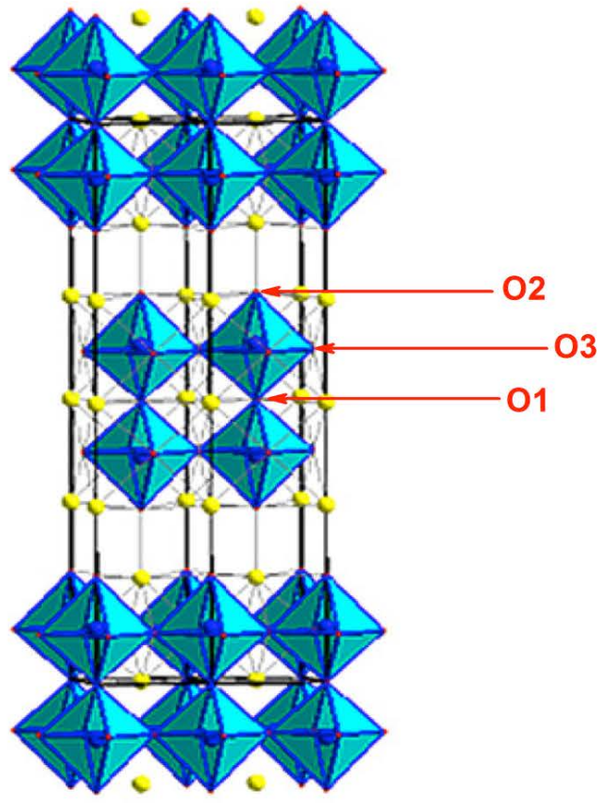

$Sr_3Cr_2O_7$

Neutron Powder diffraction

ILL, D1B & D2B instruments

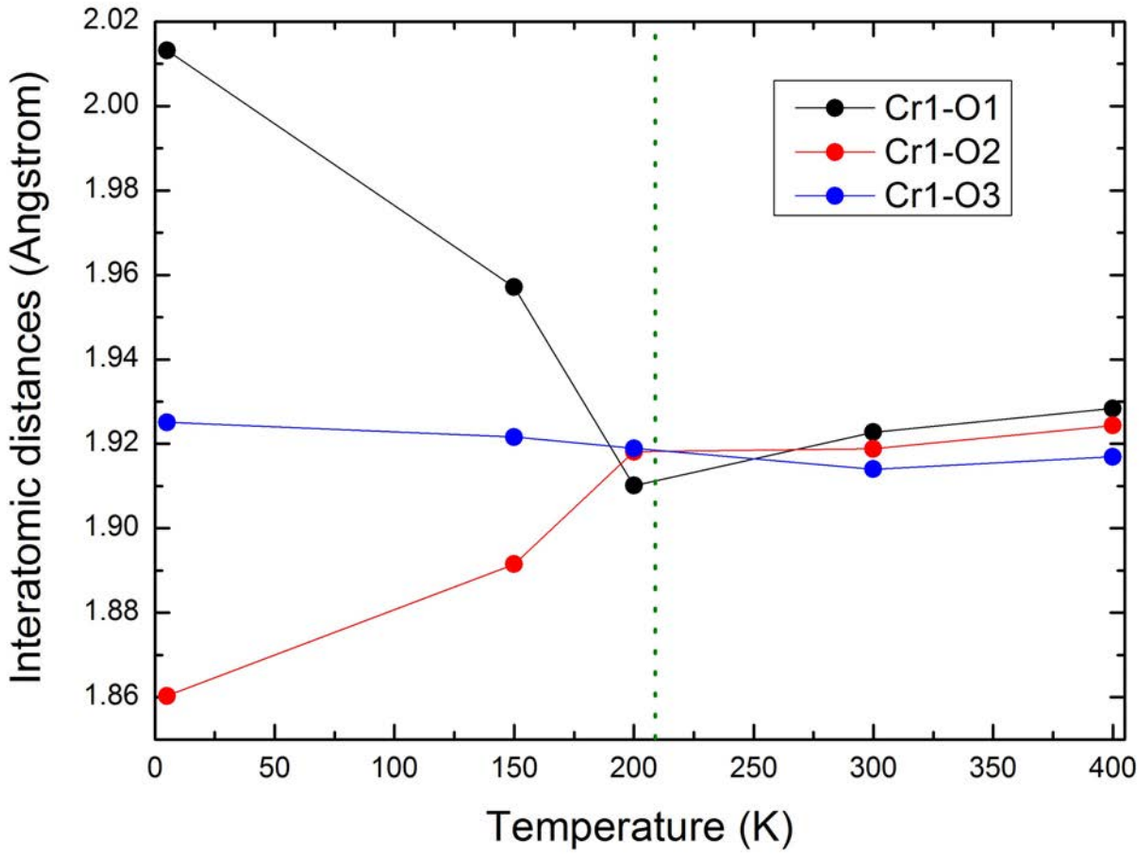

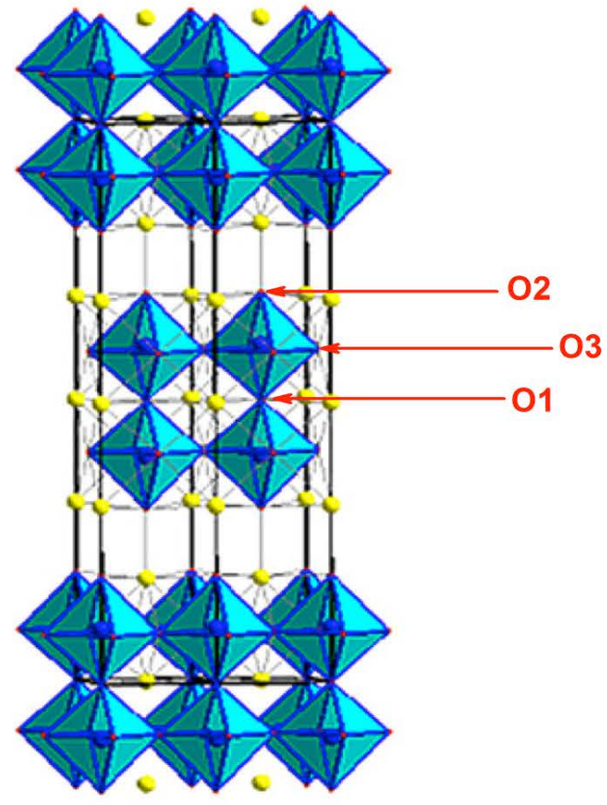

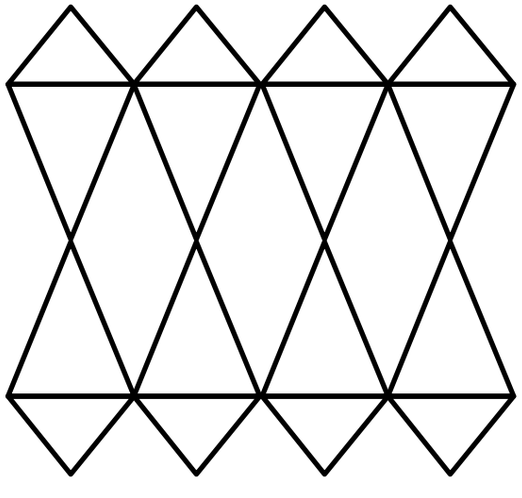

Low temperature

non symmetric

CrO_6 octahedron distortion

210K

AF order

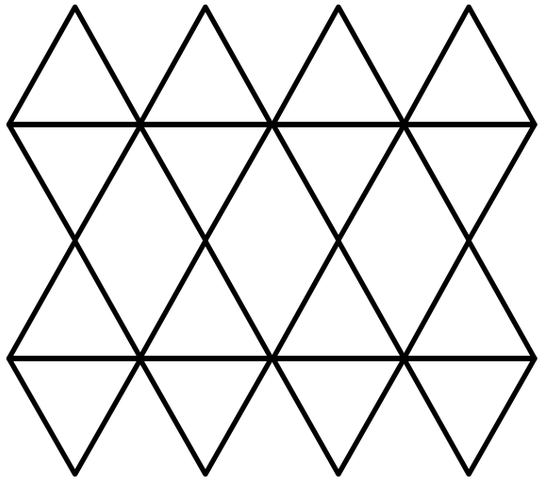

High temperature

Orbital model

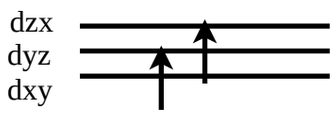

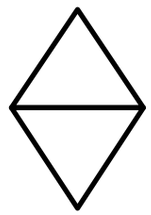

orbital degenerescence **regular octahedra**

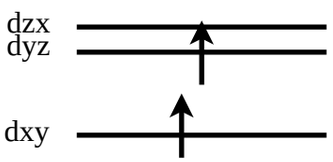

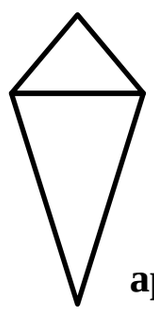

partial orbital ordering **apical distortion**

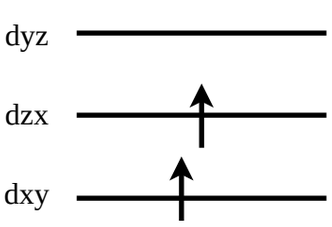

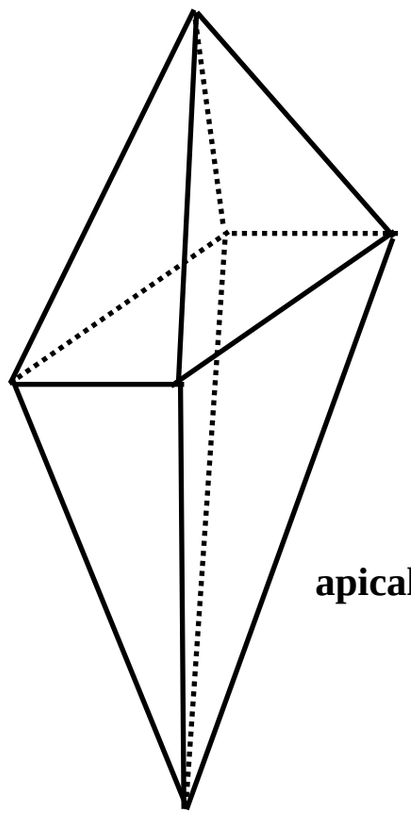

total orbital ordering **apical & in-plane distortion**

Orbital model

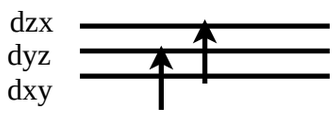

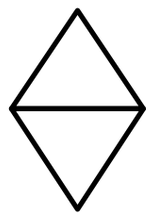

orbital degeneresccence **regular octahedra**

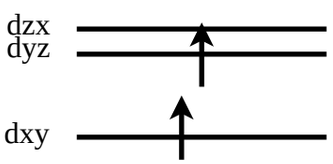

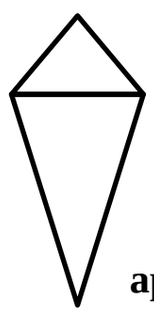

partial orbital ordering **apical distortion**

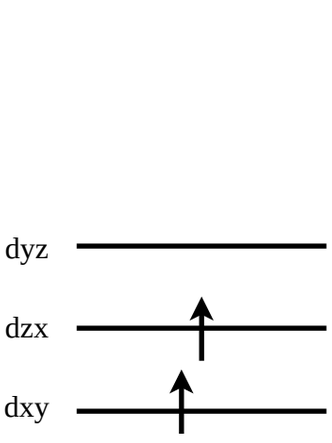

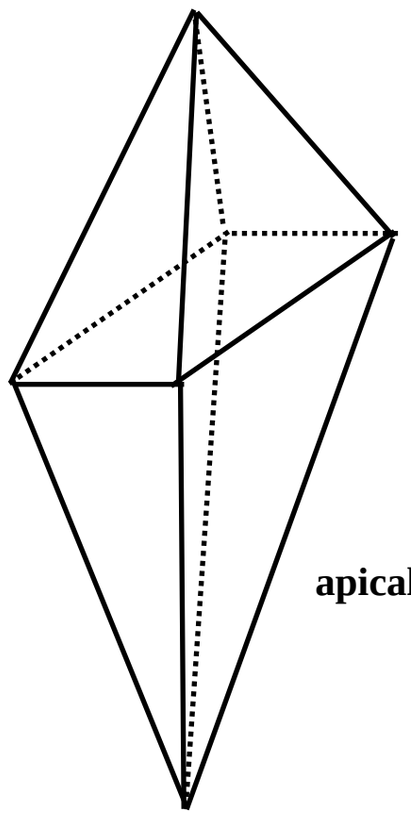

total orbital ordering

apical & in-plane distortion → **ESRF & lab XRD : no in-plane distortion observed**

Orbital model

orbital degenerescence

regular octahedra

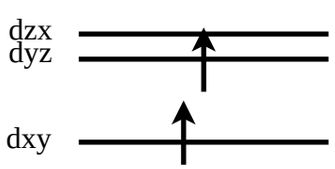

partial orbital ordering

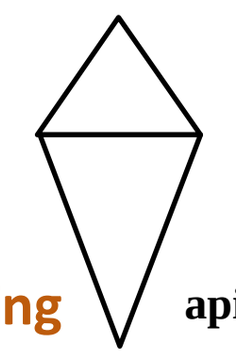

apical distortion

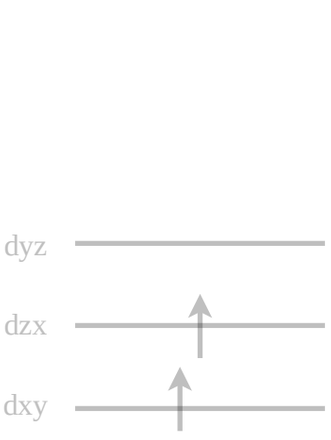

total orbital ordering

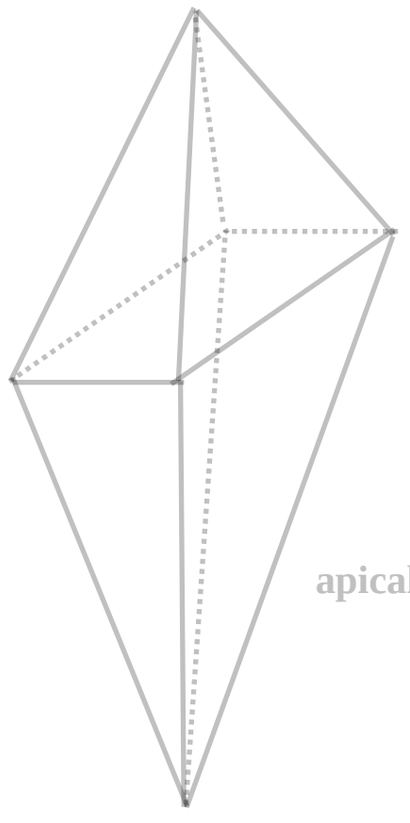

apical & in-plane distortion → ESRF & lab XRD : no in-plane distortion observed

Orbital model

orbital degenerescence

regular octahedra

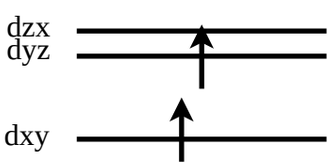

partial orbital ordering

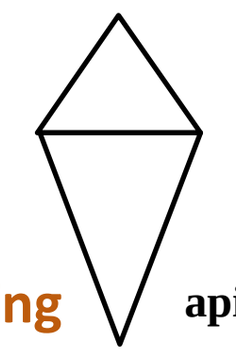

apical distortion

Clément Février
Claudine Lacroix
Arnaud Ralko

Armando A. Aligia

Kugel-Khomski Hamiltonian

$$\mathbf{H}_{eff} = \mathbf{S}_i.\mathbf{S}_j \times f(\boldsymbol{\tau}_i;\boldsymbol{\tau}_j) + g$$

spin **pseudo-spin**

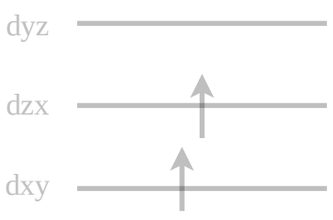

total orbital ordering

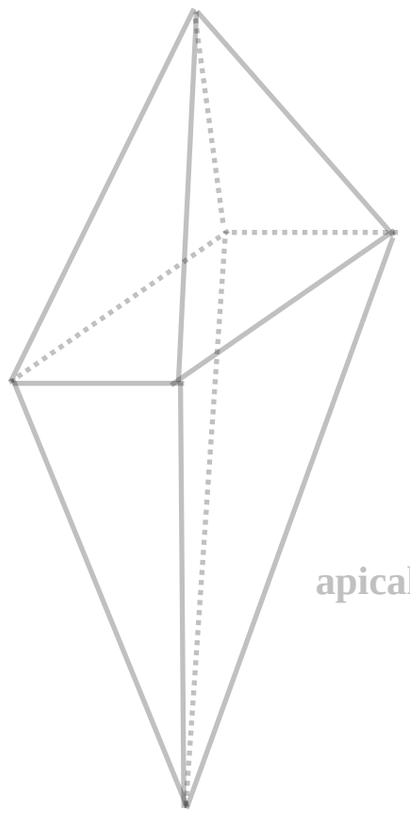

apical & in-plane distortion

ESRF & lab XRD : no in-plane distortion observed

Orbital model

orbital degenerescence

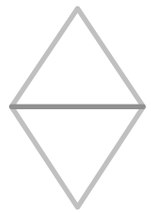

regular octahedra

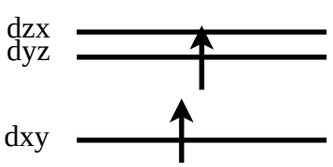

partial orbital ordering

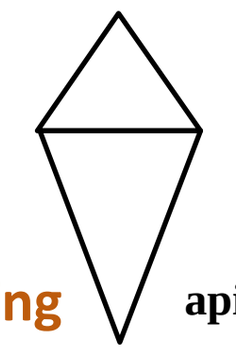

apical distortion

Clément Février
Claudine Lacroix
Arnaud Ralko

Armando A. Aligia

Kugel-Khomski Hamiltonian

$$\mathbf{H}_{eff} = \mathbf{S}_i.\mathbf{S}_j \times f(\boldsymbol{\tau}_i;\boldsymbol{\tau}_j) + g$$

spin pseudo-spin

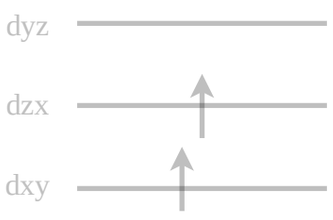

total orbital ordering

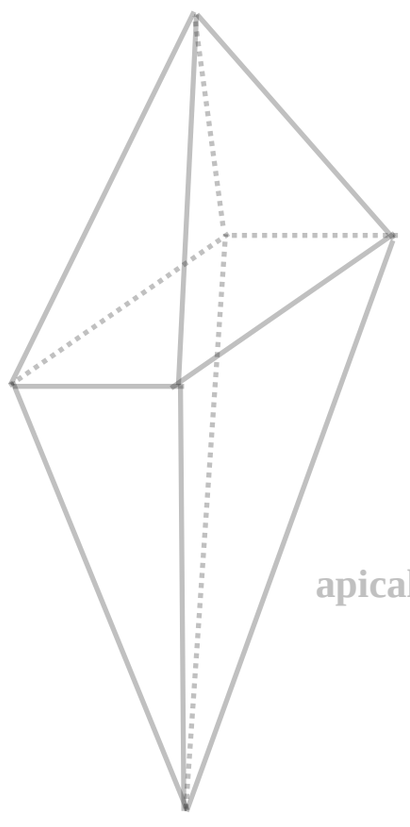

apical & in-plane distortion

Total orbital ordering
AF in-plane and between adjacent Cr planes

ESRF & lab XRD : no in-plane distortion observed

New Ca-based phases

$Ca_3Cr_2O_7$

New Ca-based phases

$Ca_3Cr_2O_7$

Magnetic measurement

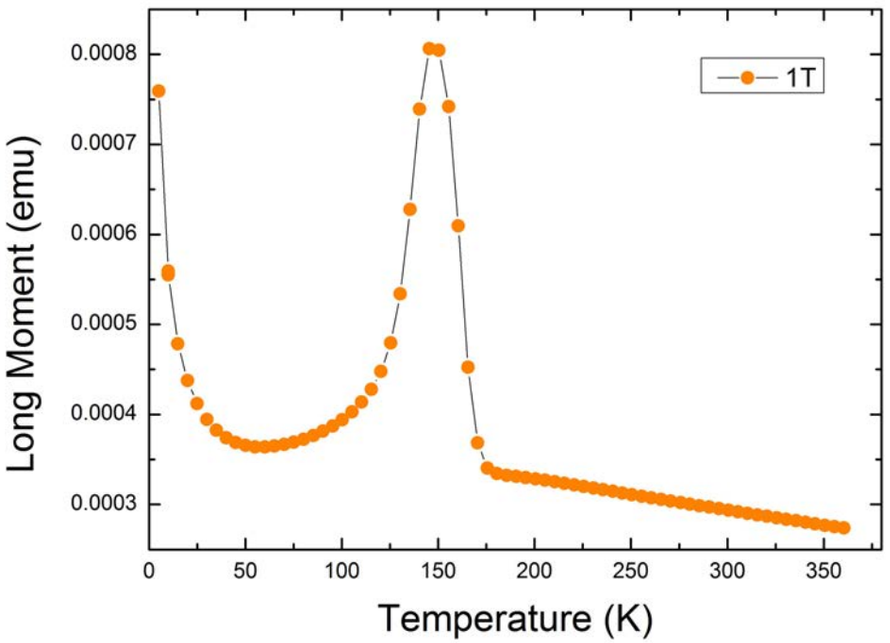

Specific heat measurement

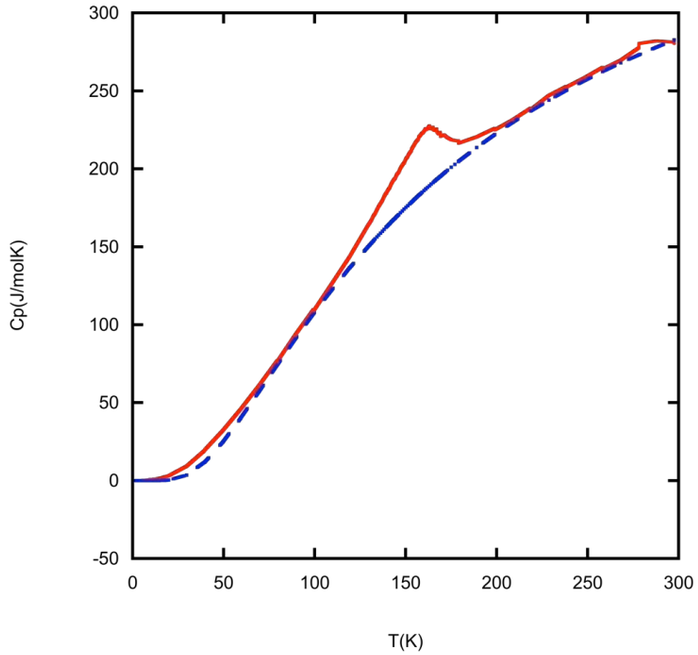

$T_{Néel\ (Ca327)}$ = 150K

<

$T_{Néel(Sr327)}$ = 210K

New Ca-based phases

$Ca_3Cr_2O_7$

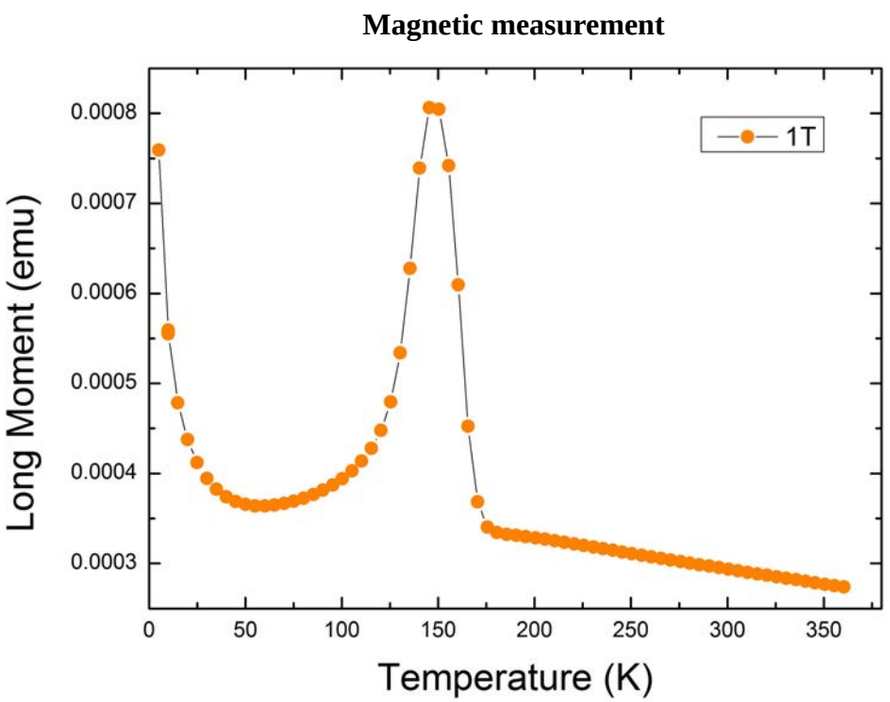

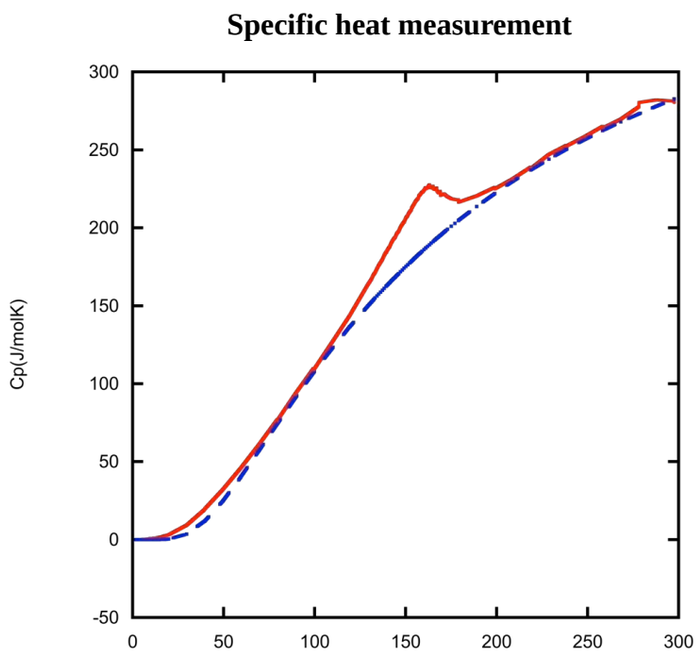

$T_{Néel\ (Ca327)}$ = 150K

<

$T_{Néel(Sr327)}$ = 210K

$S_{(Ca327)}$ = Rln2

<

$S_{(Sr327)}$ = Rln6

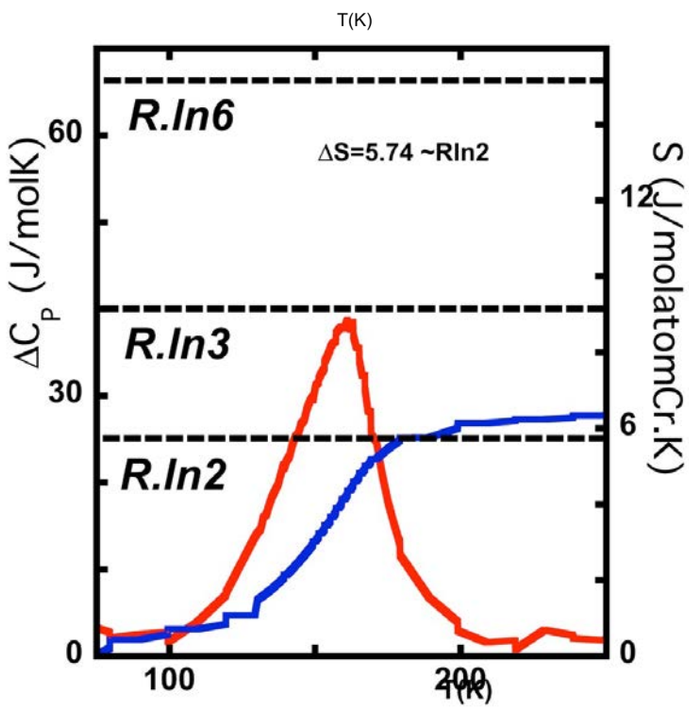

New Ca-based phases

$Ca_3Cr_2O_7$

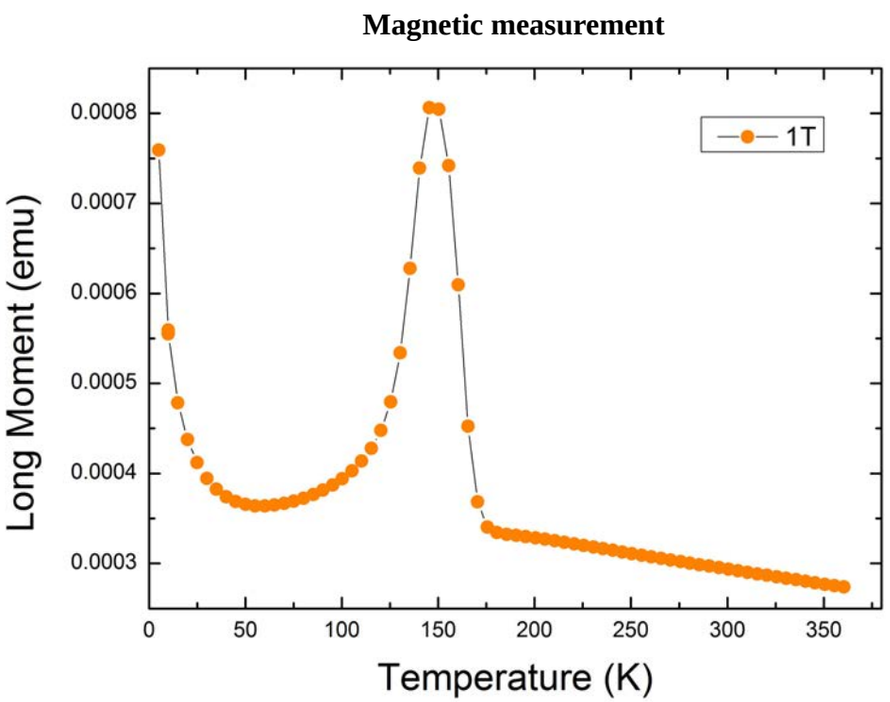

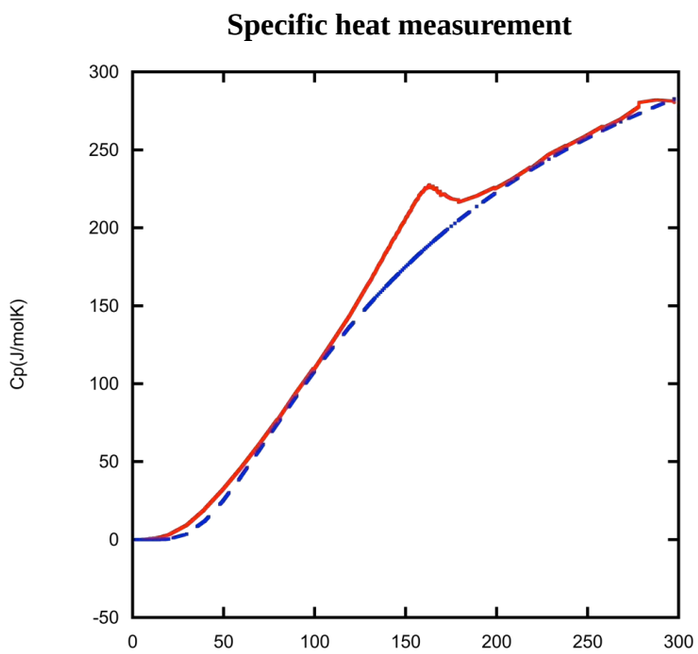

$T_{Néel\ (Ca327)}$ = 150K

<

$T_{Néel(Sr327)}$ = 210K

$S_{(Ca327)}$ = Rln2

<

$S_{(Sr327)}$ = Rln6

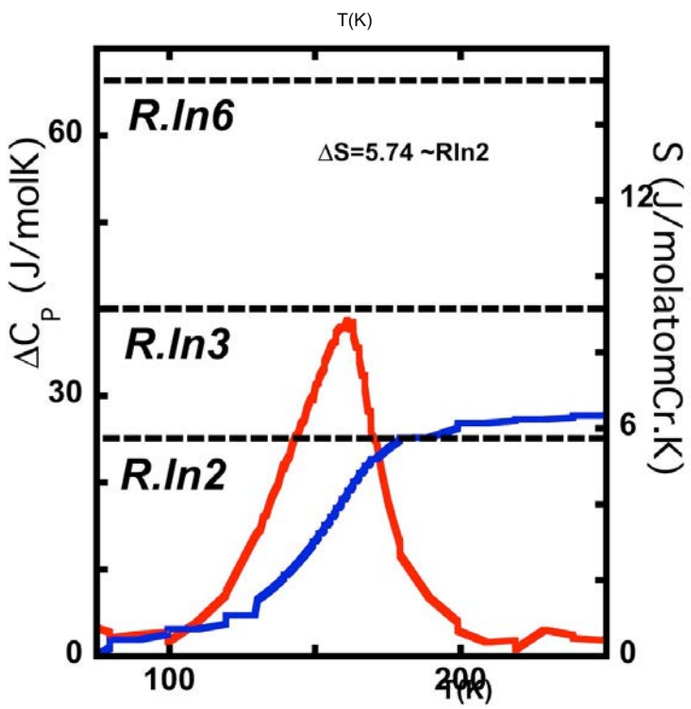

metallic :)

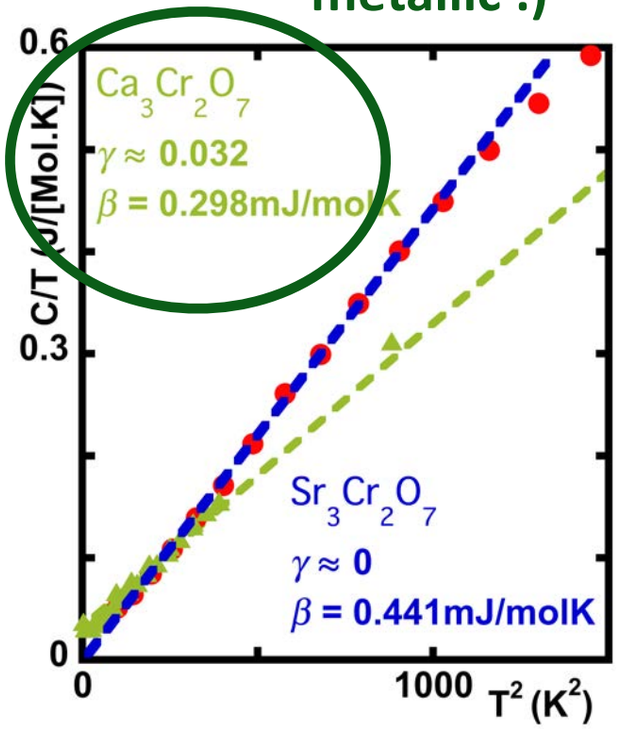

Conclusion

$Sr_3Cr_2O_7$

strong magneto-structural coupling

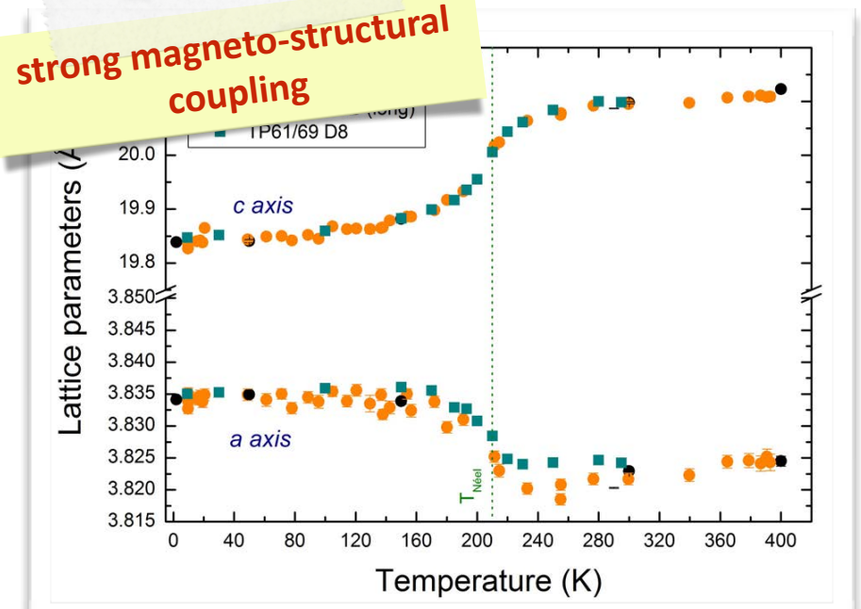

octahedra distortion

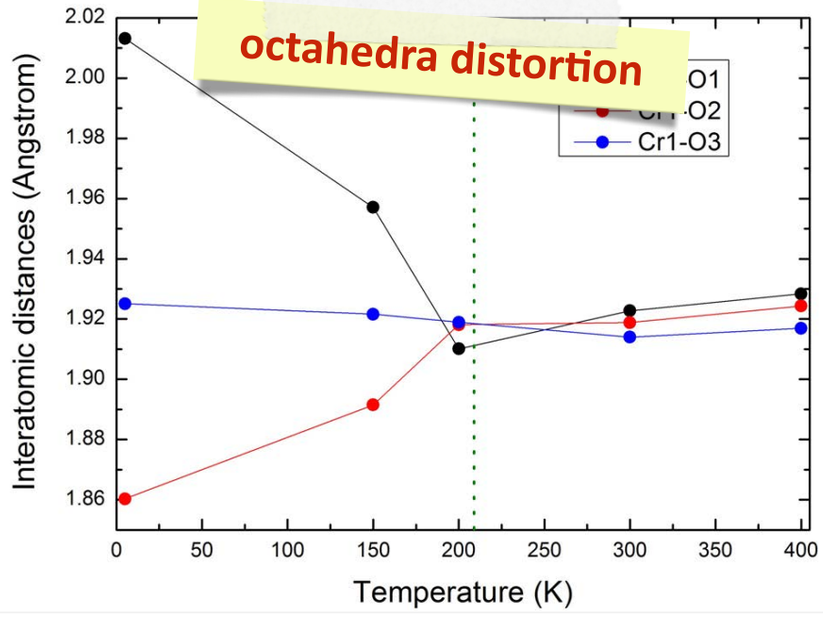

AFM structure determined

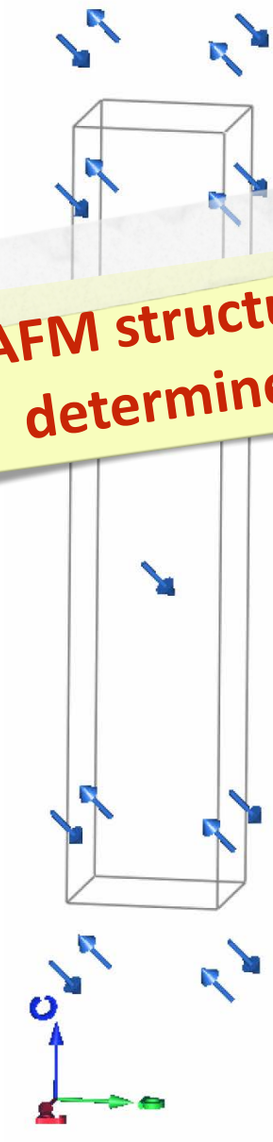

Orbital ordering..

Big thank to..

Pierre Bouvier
Frédéric Gay
Gaétan Giriat
Céline Goujon
Claudine Lacroix
Christophe Lepoittevin
Murielle Legendre
Olivier Leynaud
José-Emilio Lorenzo-Diaz
Gyorgy Remenyi
Pierre Rodiere
Denis Testemale
Pierre Strobel
André Sulpice
Ruben Weht

D1B
Claire Collin
Vivan Nassif
D2B
Emmanuelle Suard

and you!

New Ca-based phases

Ca_2CrO_4

New Ca-based phases

Ca_2CrO_4

Magnetic measurement

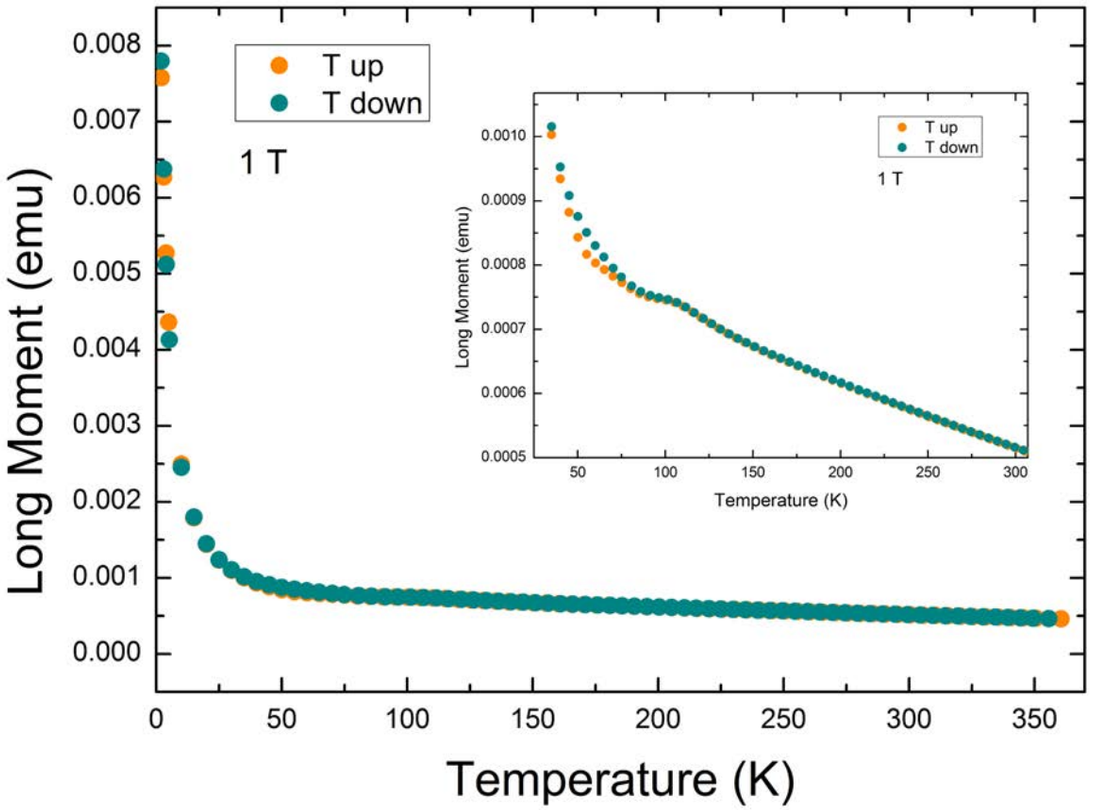

Specific heat measurement

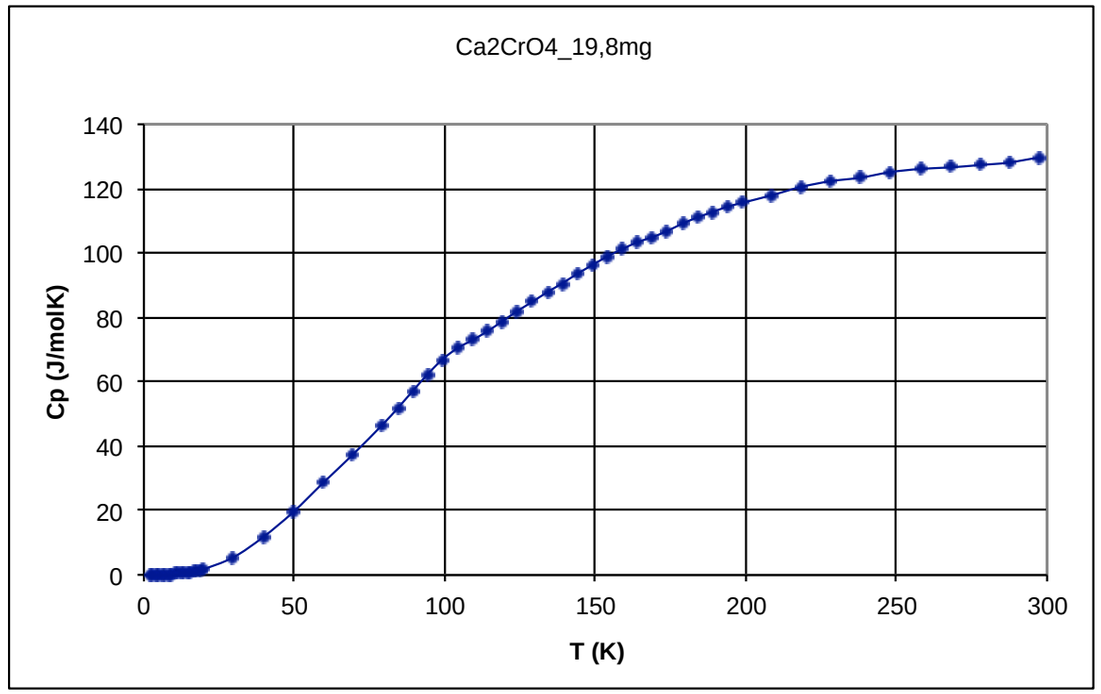

- **No AFM anomaly at high temperature (Sr-based:T_N=305 K)**
- **Weak AFM anomaly on magnetic measurement and specific heat around 100 K**

New Ca-based phases

Ca_2CrO_4

Magnetic measurement

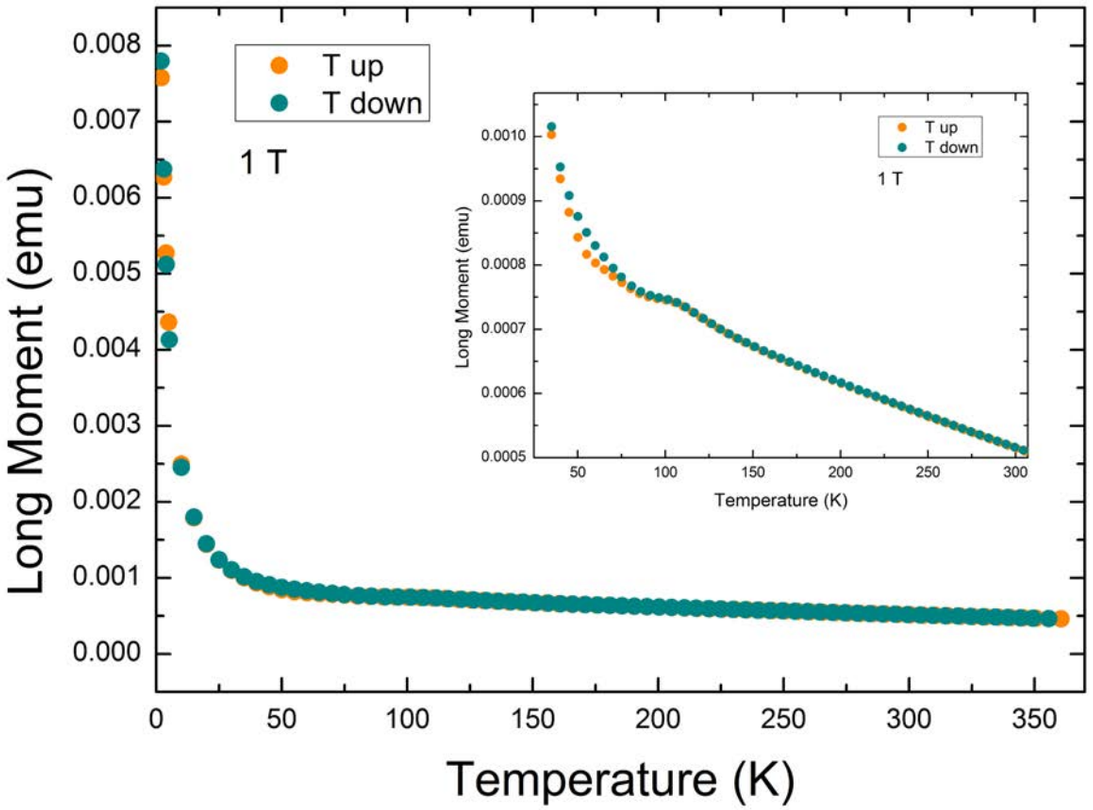

Specific heat measurement

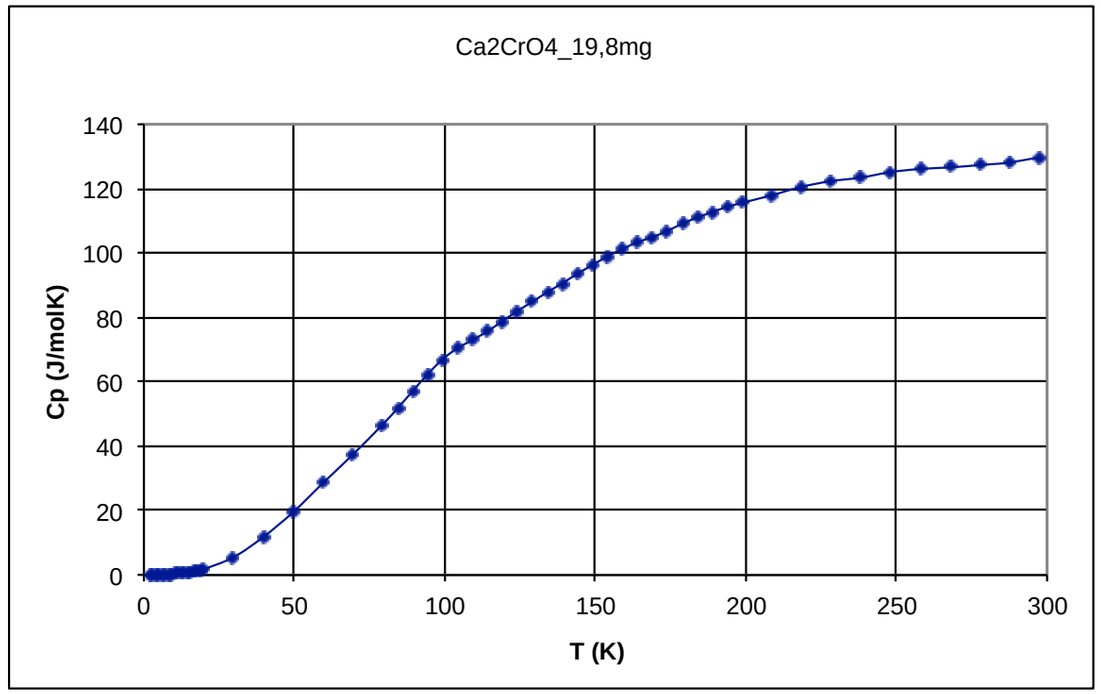

- **No AFM anomaly at high temperature (Sr-based:T_N=305 K)**
- **Weak AFM anomaly on magnetic measurement and specific heat around 100 K**

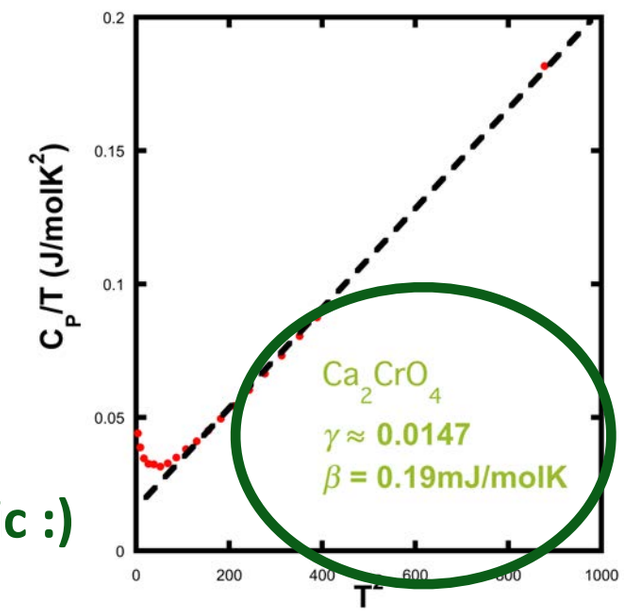

metallic :)

$CrSb_2$

CrAs motivation

$CrSb_2$

CrAs motivation

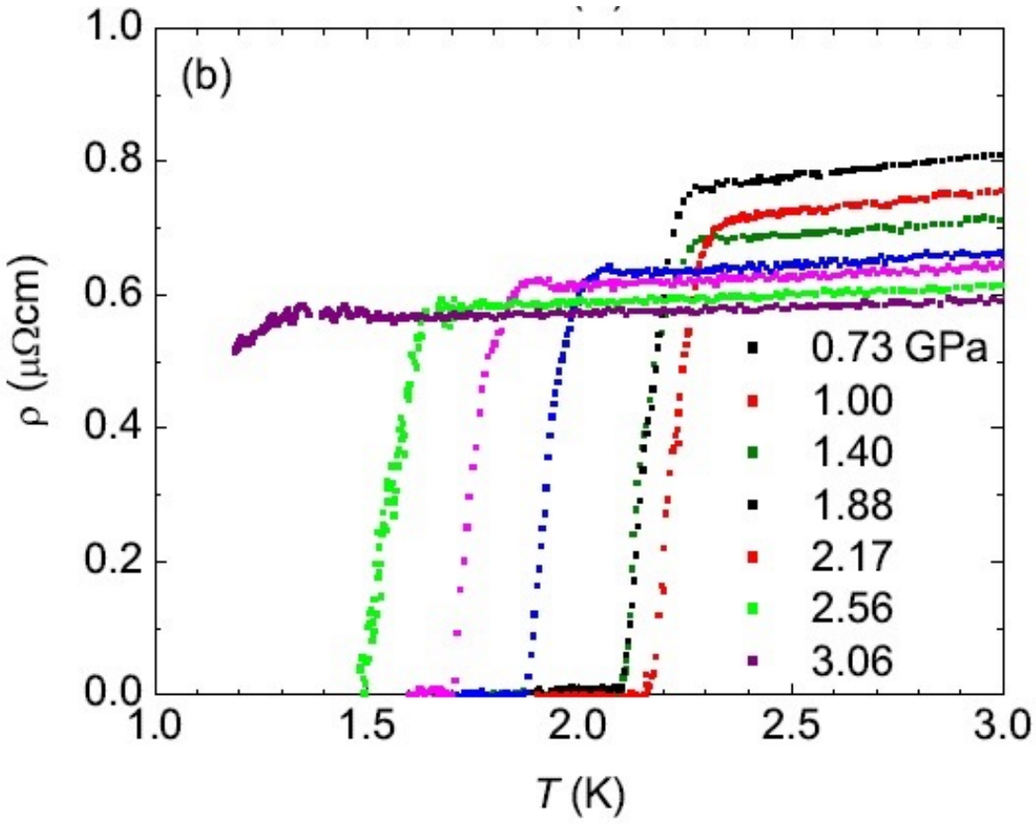

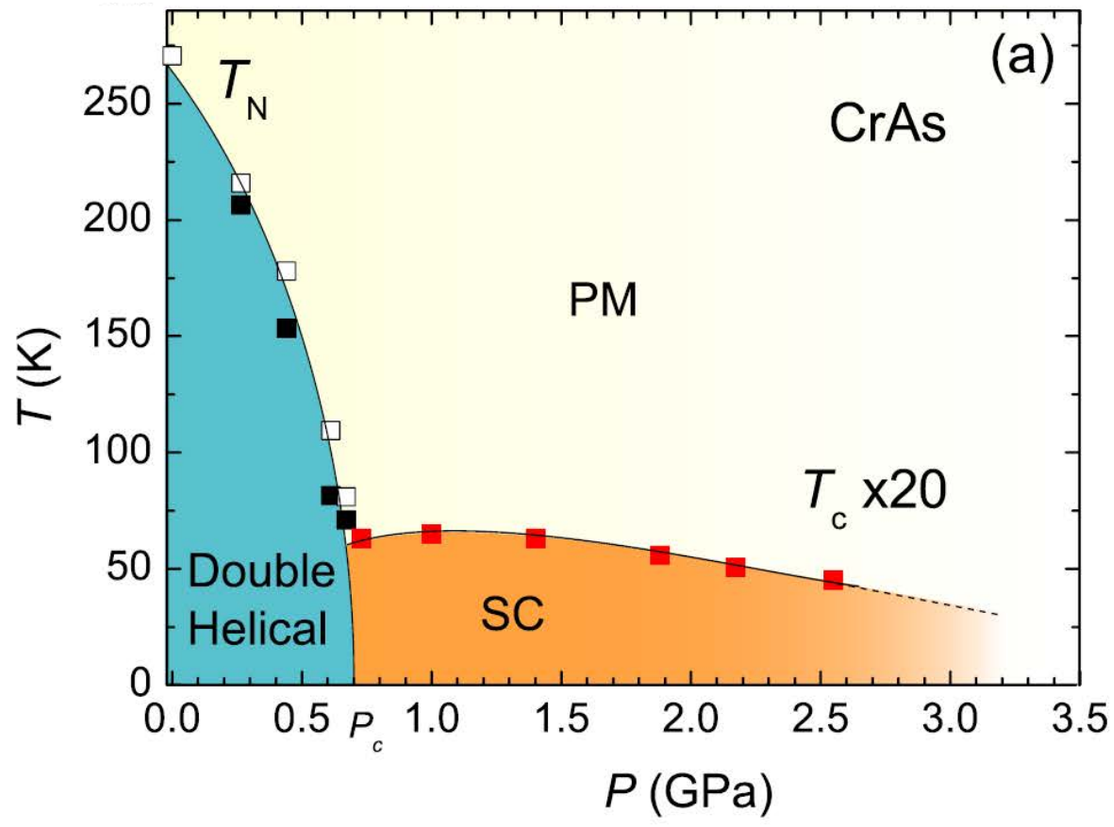

3D compound : orthorhombic (MnP-type structure)

double helical magnetic structure (Cr moment = 1.7 μb)

T_N = 265K

T_c = 2K (at 0.7 GPa)

$CrSb_2$

CrAs motivation

CrSb2

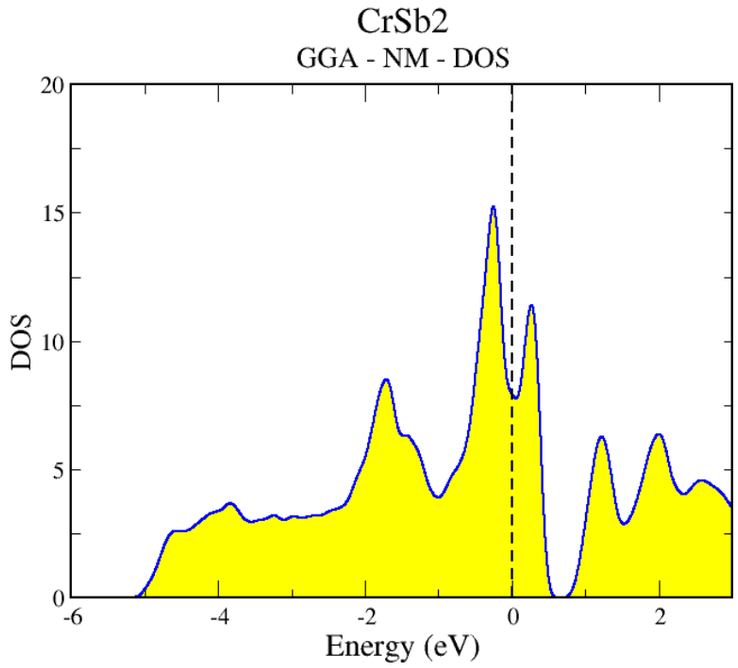

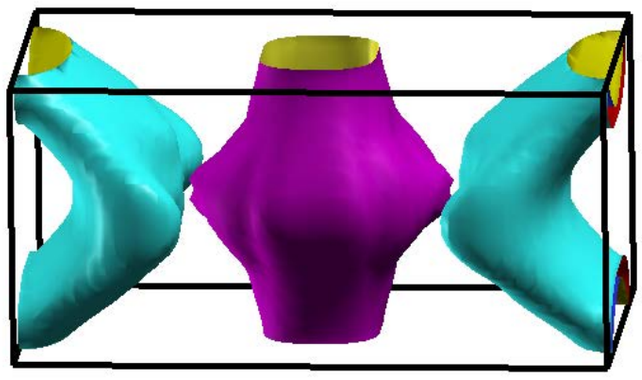

CrAs

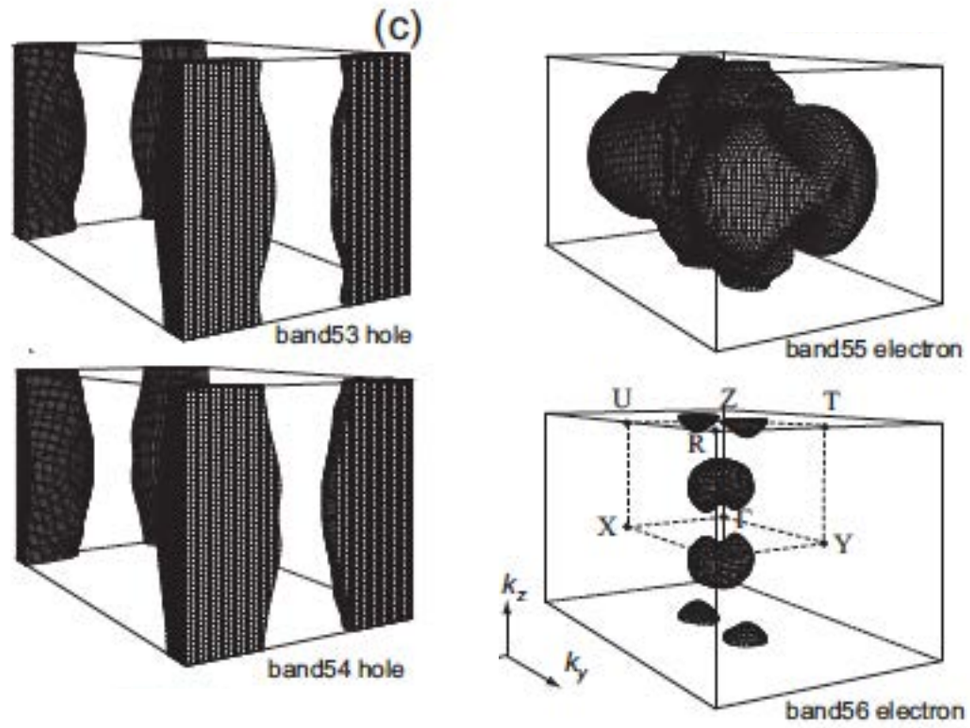

3D compounds but quasi-2D band

$CrSb_2$

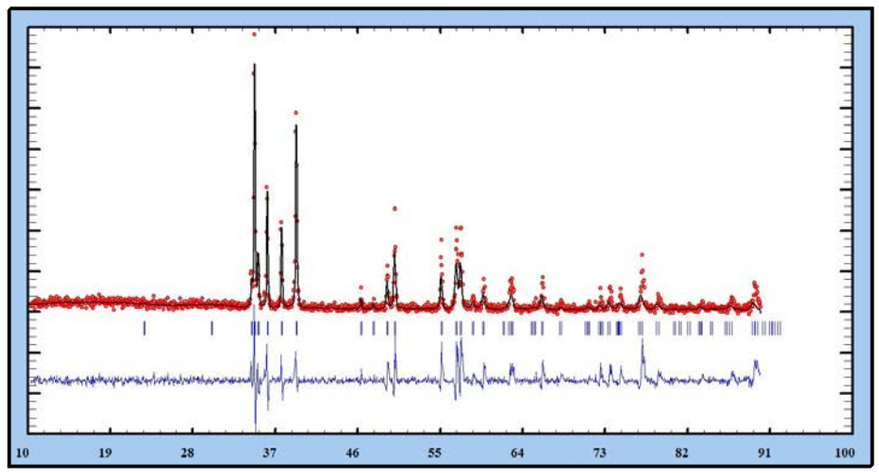

Marcasite-type structure
(space group Pnnm)

a = 6.04 Æ
b = 6.89 Æ
c = 3.28 Æ

$T_{Néel}$ = 273 K

Pure polycrystal & singlecrystal synthesis

$CrSb_2$

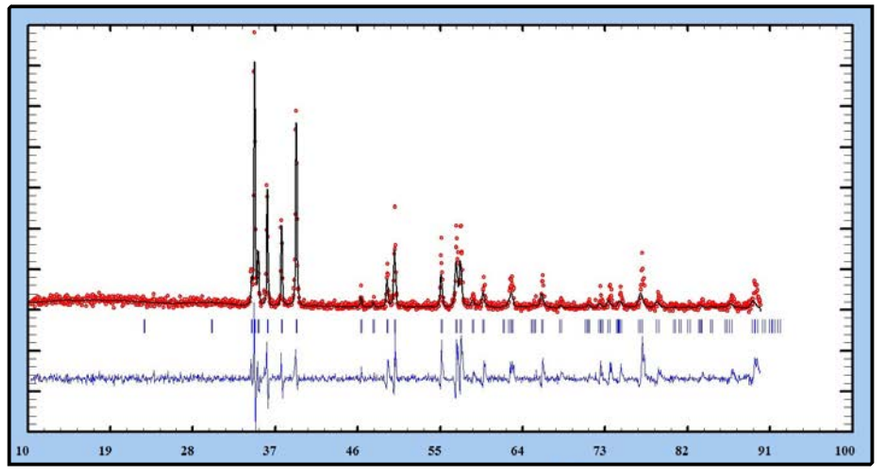

Marcasite-type structure
(space group Pnnm)

a = 6.04 Æ
b = 6.89 Æ
c = 3.28 Æ

$T_{Néel}$ = 273 K

Pure polycrystal & singlecrystal synthesis

Transport measurement (ambiant pressure)

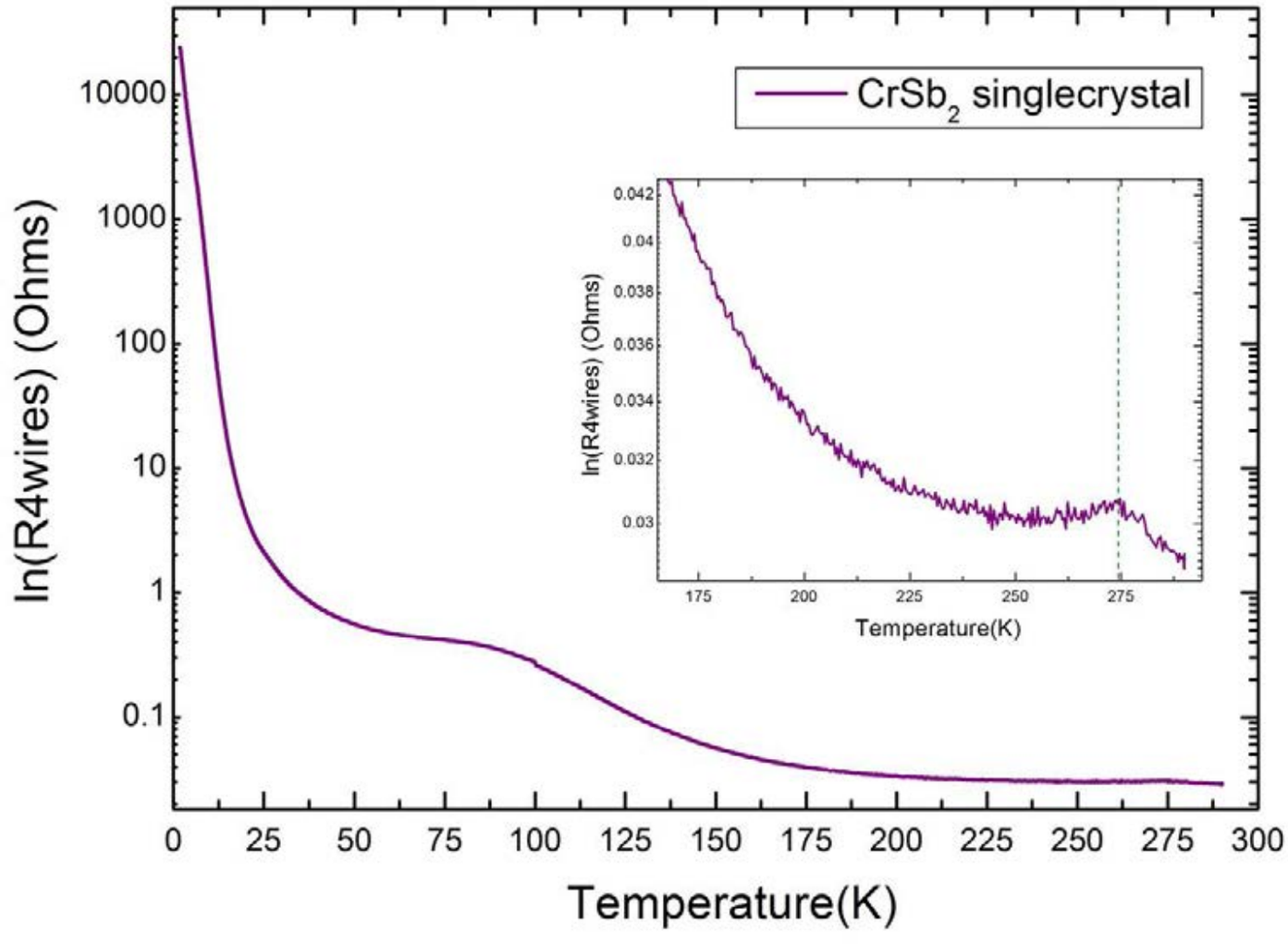

$CrSb_2$

High pressure transport measurement

$CrSb_2$

High pressure transport measurement

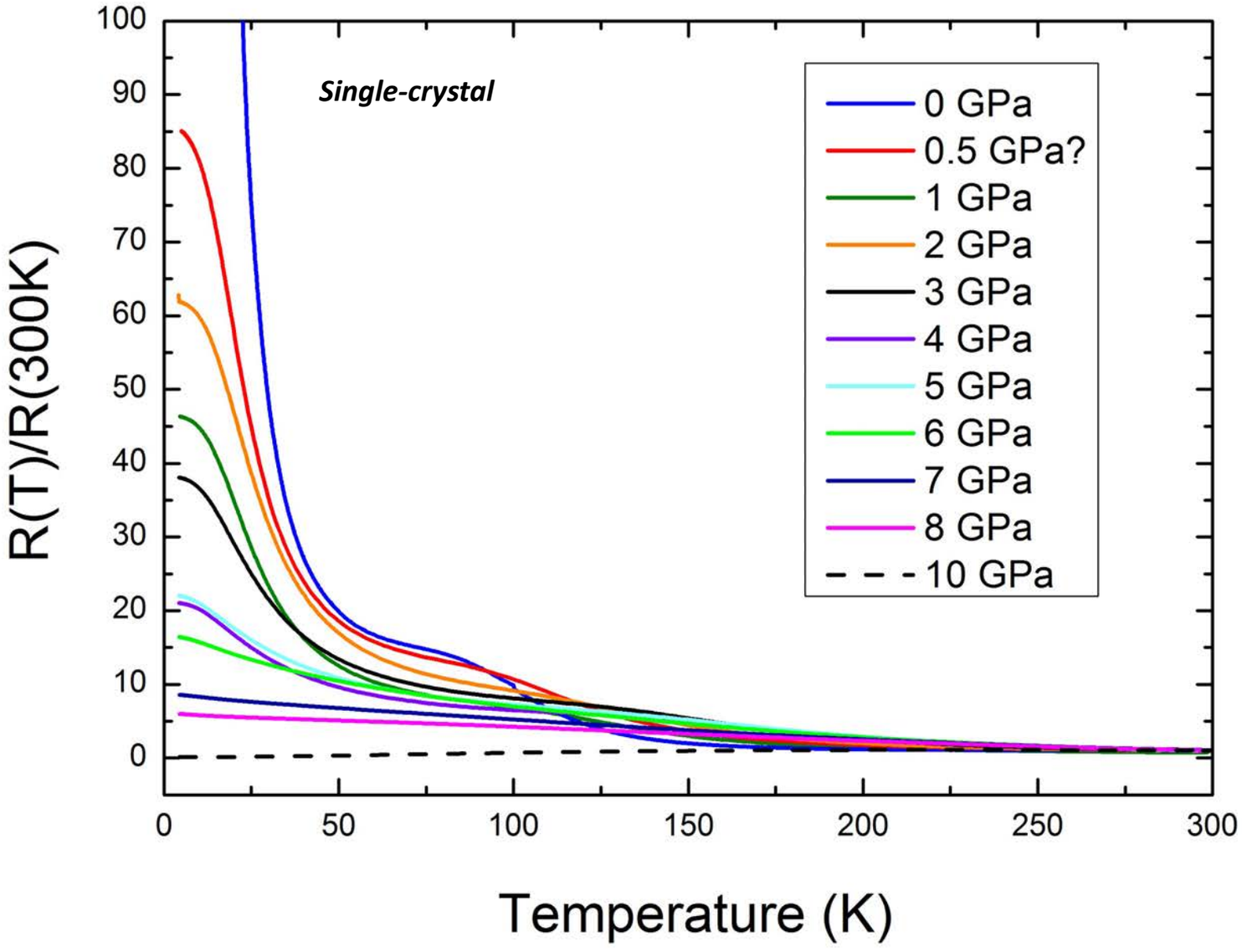

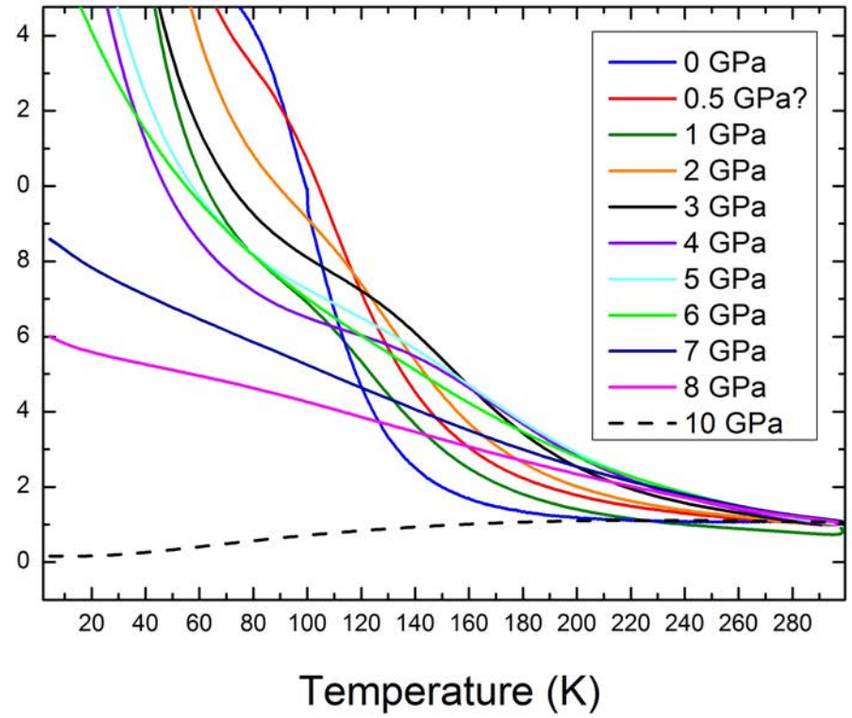

Transition metal-insulator at 10 GPa

No SC up to 20 GPa and down to 2k

$CrSb_2$

High pressure transport measurement

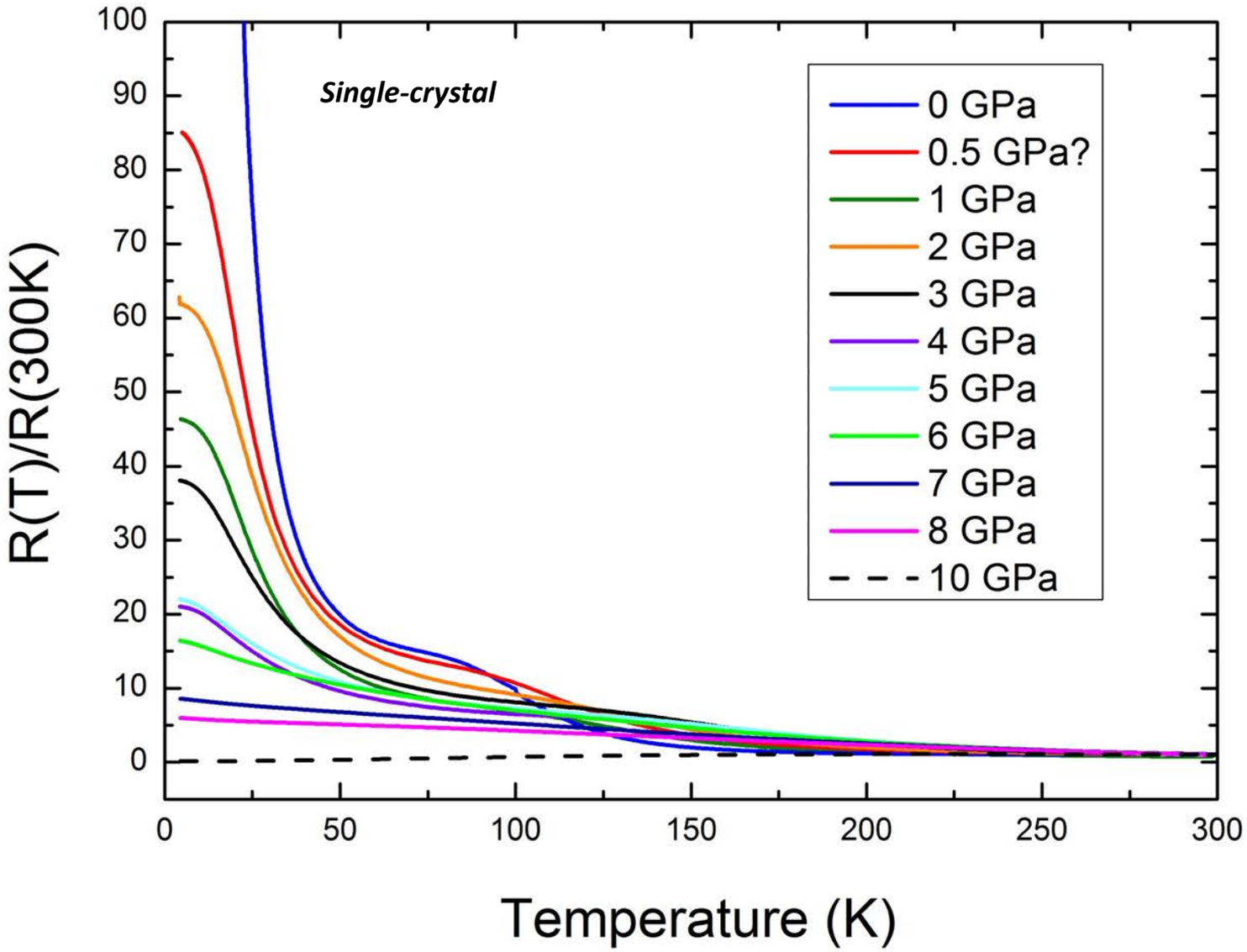

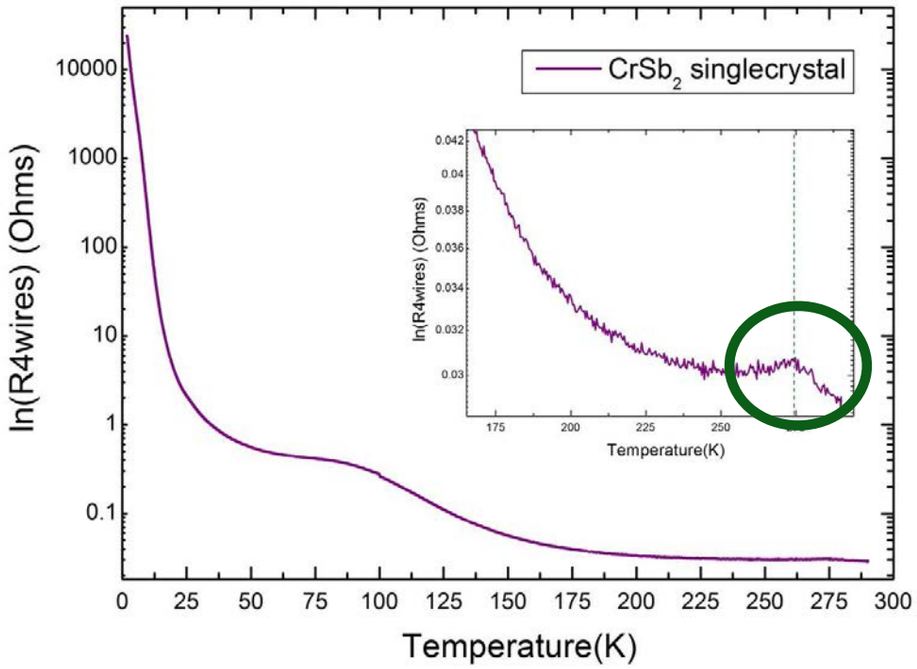

Transition metal-insulator at 10 GPa

No SC up to 20 GPa and down to 2k

$CrSb_2$ High pressure transport measurement

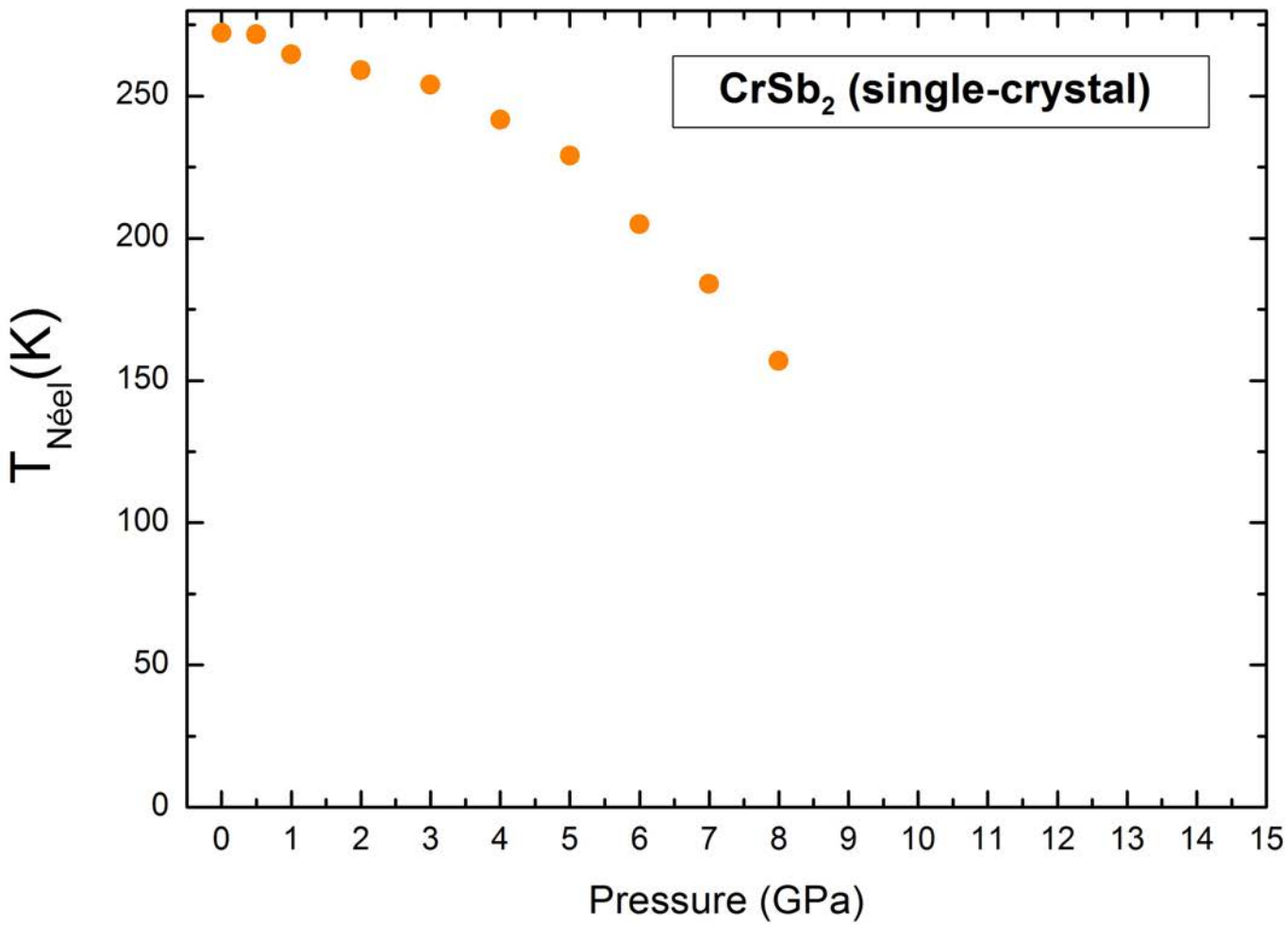

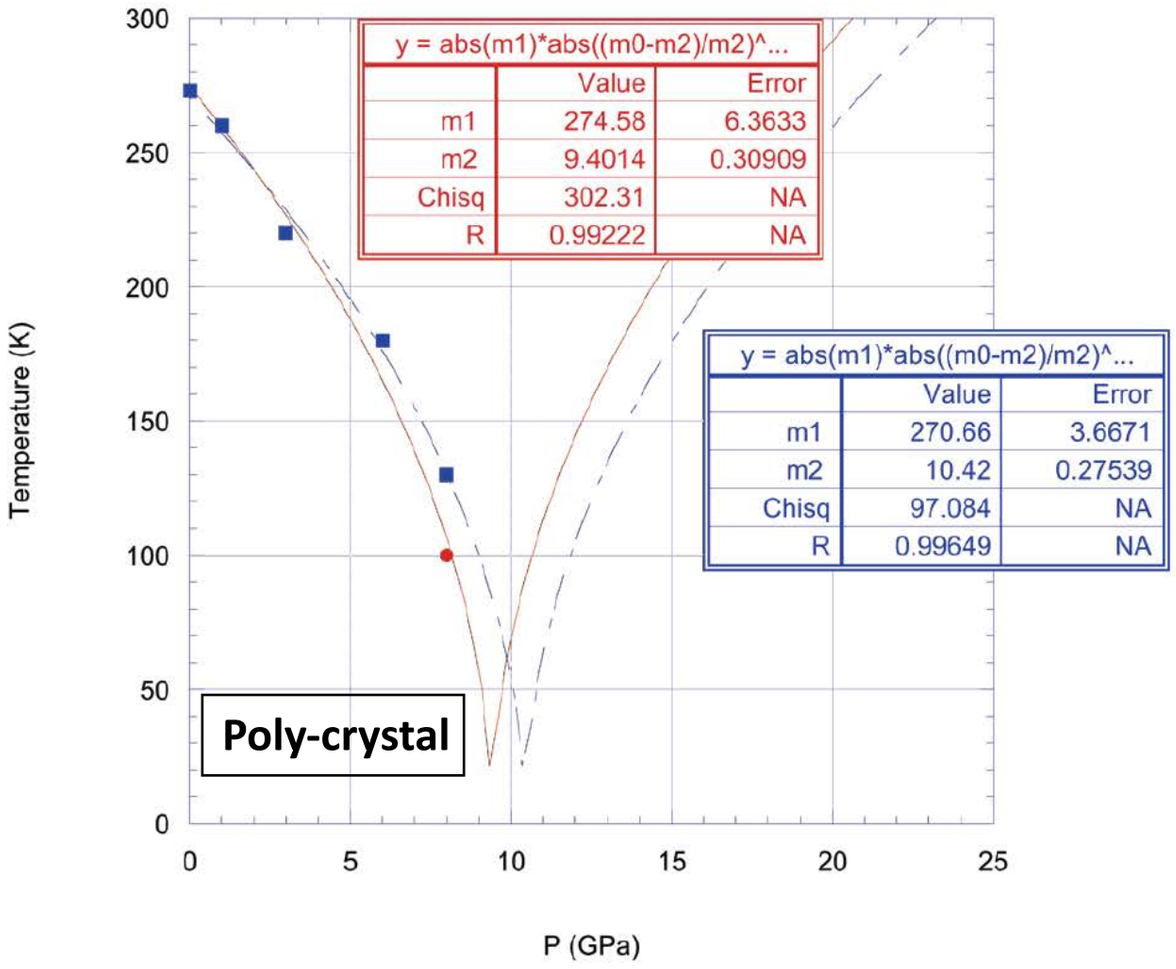

$CrSb_2$ High pressure transport measurement

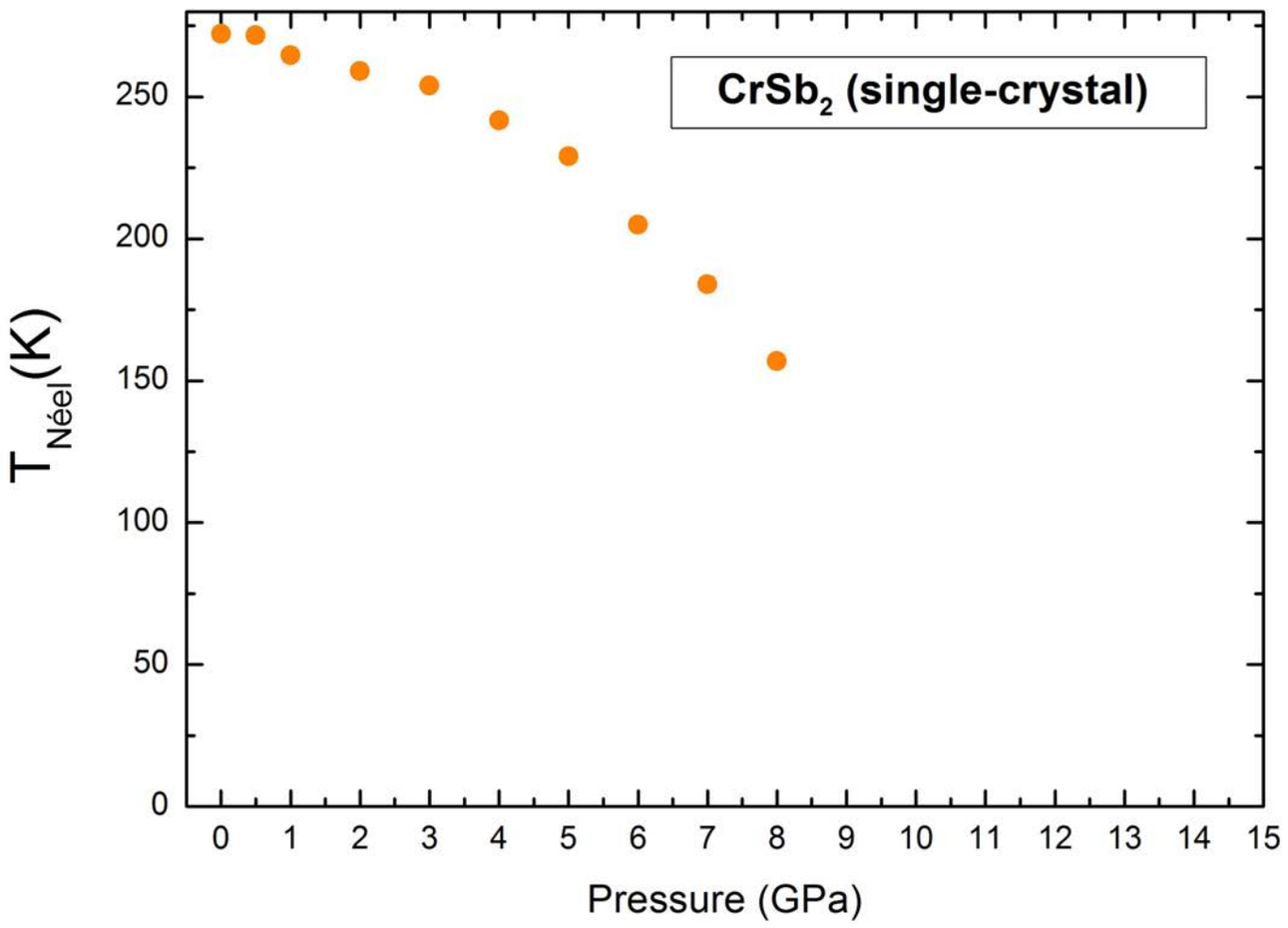

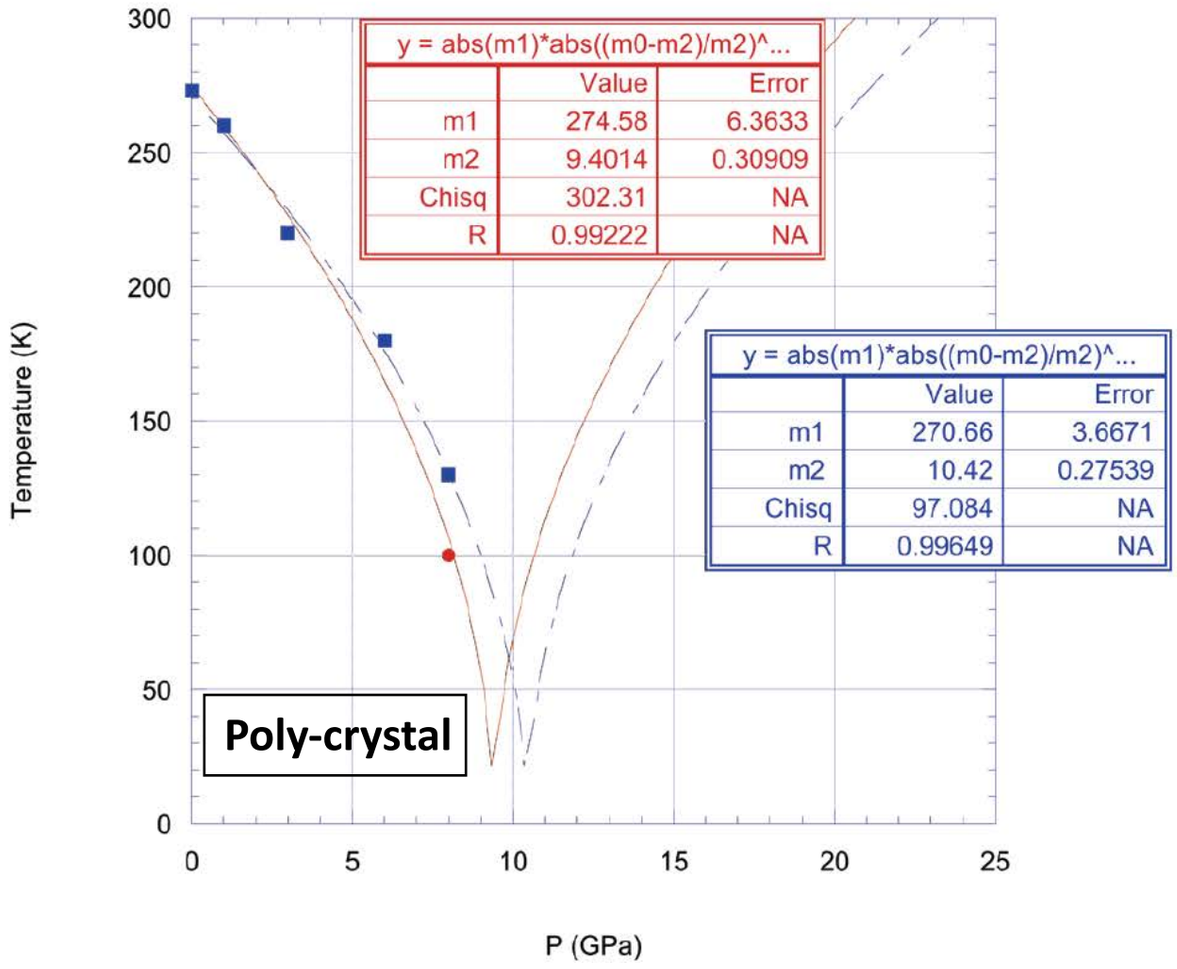

AFM should be destroyed around 10 GPa according to HP transport measurements : OK with metal-insulator pressure transition

$CrSb_2$

Neutron Powder Diffraction under pressure (D1B instrument)

$CrSb_2$

Neutron Powder Diffraction under pressure (D1B instrument)

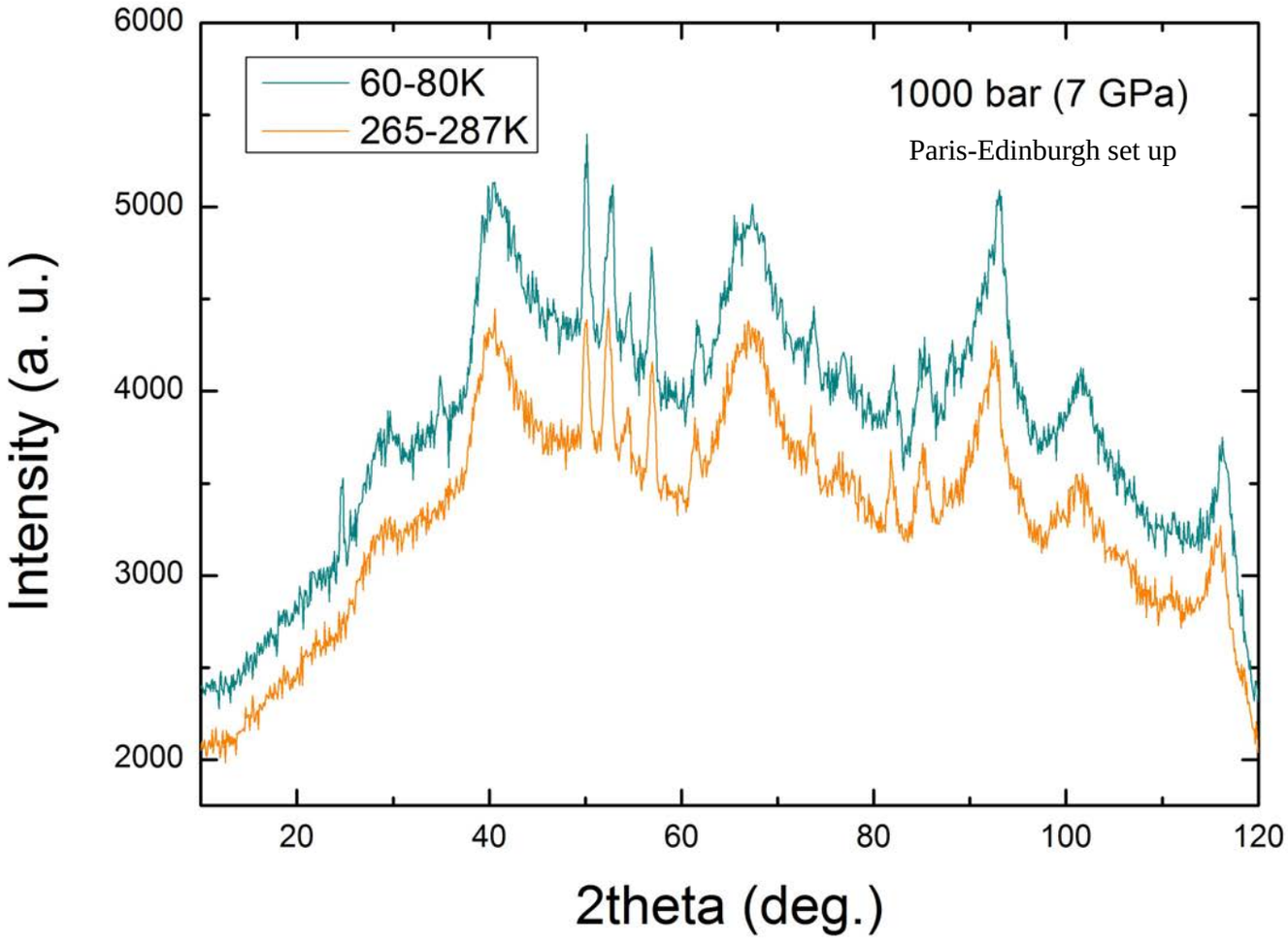

No phase transition observed until 10 GPa (limit of PE press)

$CrSb_2$

Neutron Powder Diffraction under pressure (D1B instrument)

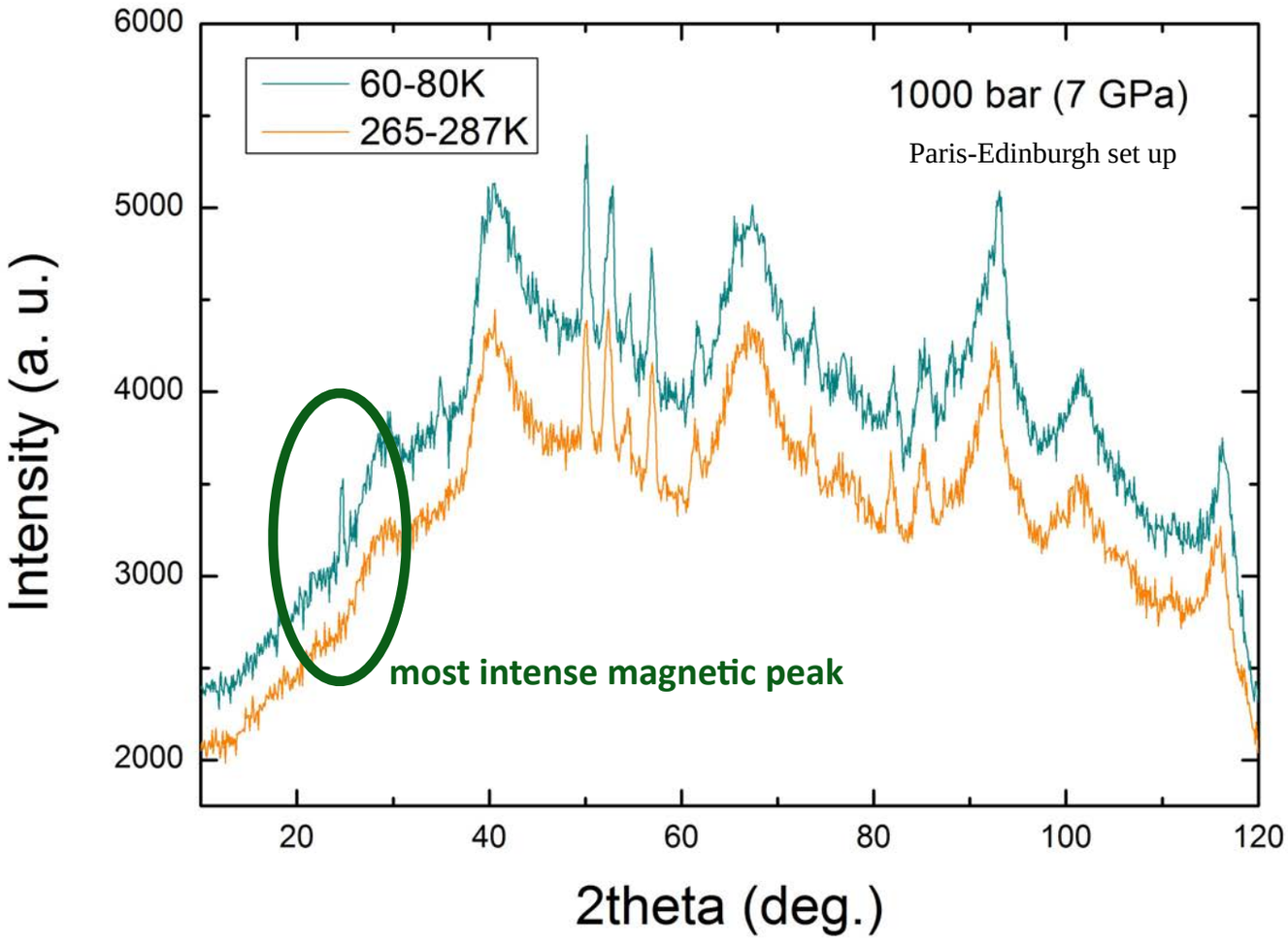

No phase transition observed until 10 GPa (limit of PE press)

Following the AFM order under pressure

$CrSb_2$

Neutron Powder Diffraction under pressure (D1B instrument)

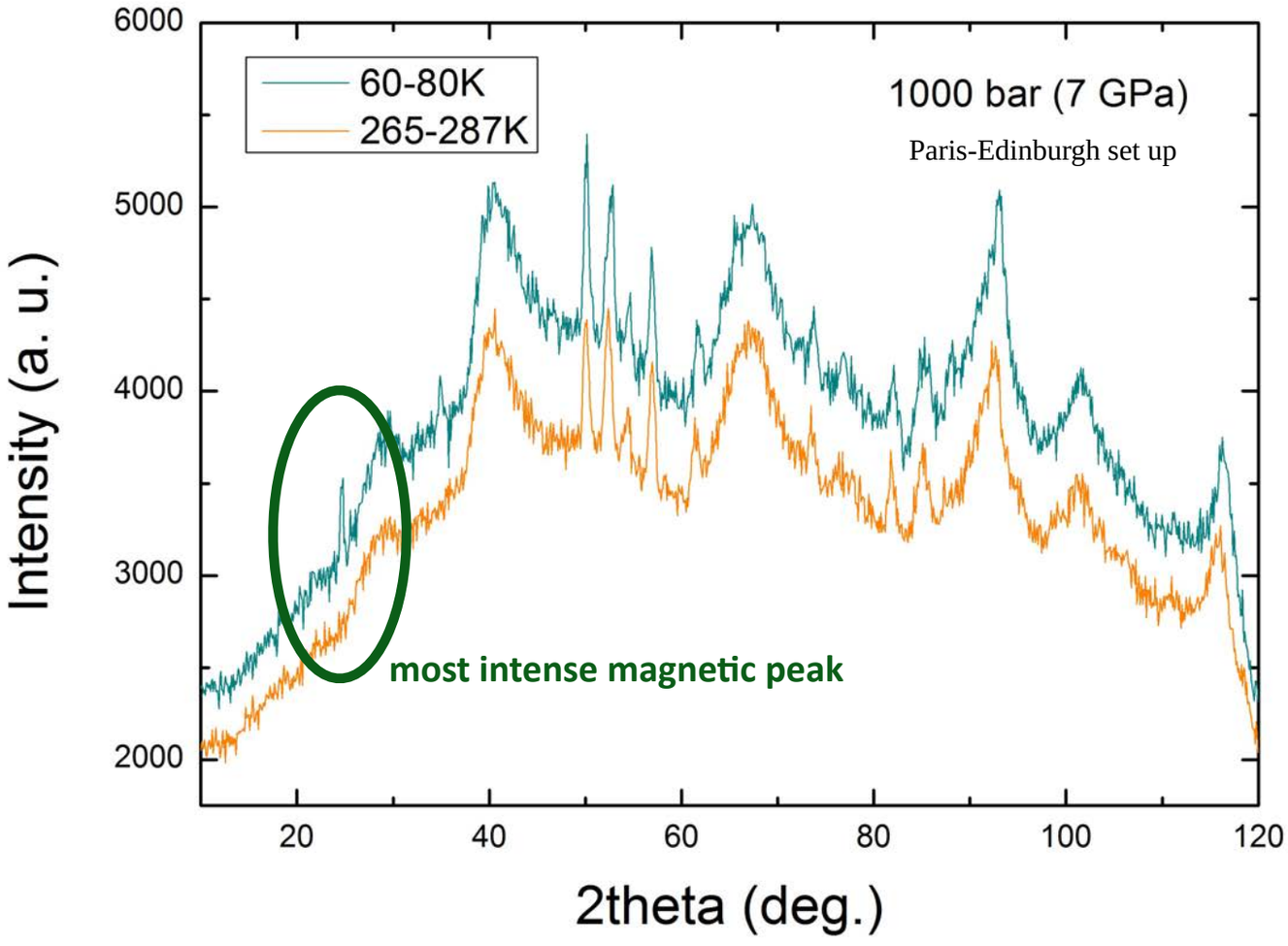

No phase transition observed until 10 GPa (limit of PE press)

Following the AFM order under pressure

—> seems much difficult to kill (more pressure needed)

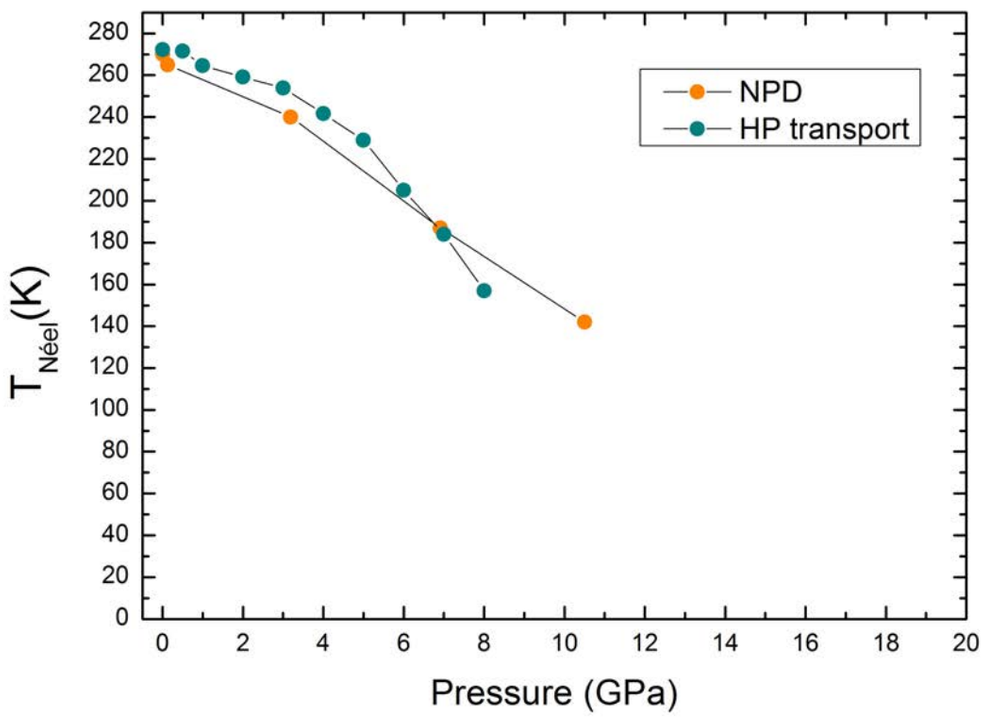

$CrSb_2$

Neutron Powder Diffraction under pressure (D1B instrument)

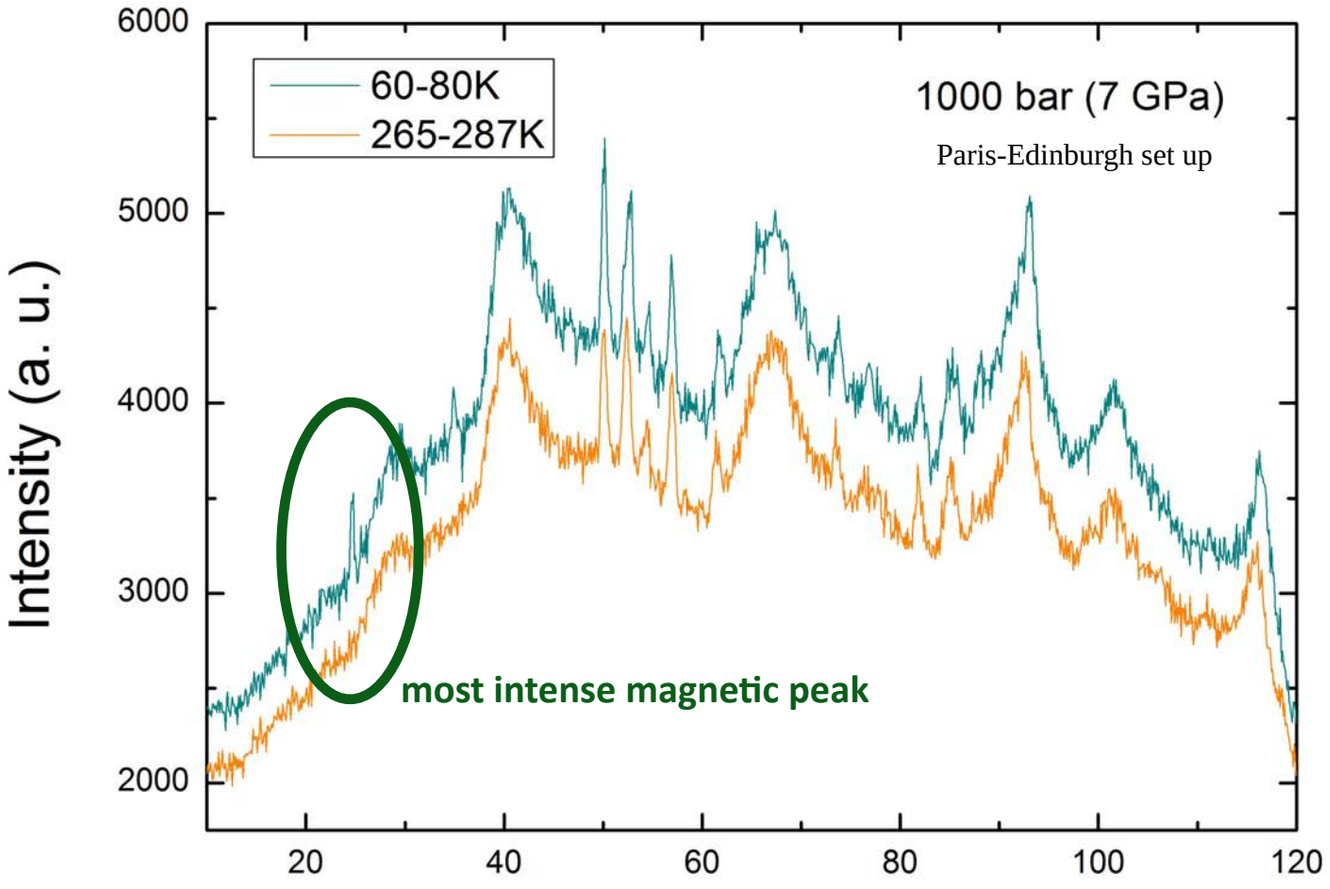

CrSb2, AF most stable solution
(DFT Ruben W.)
—> strong AFM order

CrAs, AF and FM orders almost degenerated
(DFT Ruben W.)
—> helicoidal order

No phase transition observed until 10 GPa (limit of PE press)

Following the AFM order under pressure

—> seems much difficult to kill (more pressure needed)

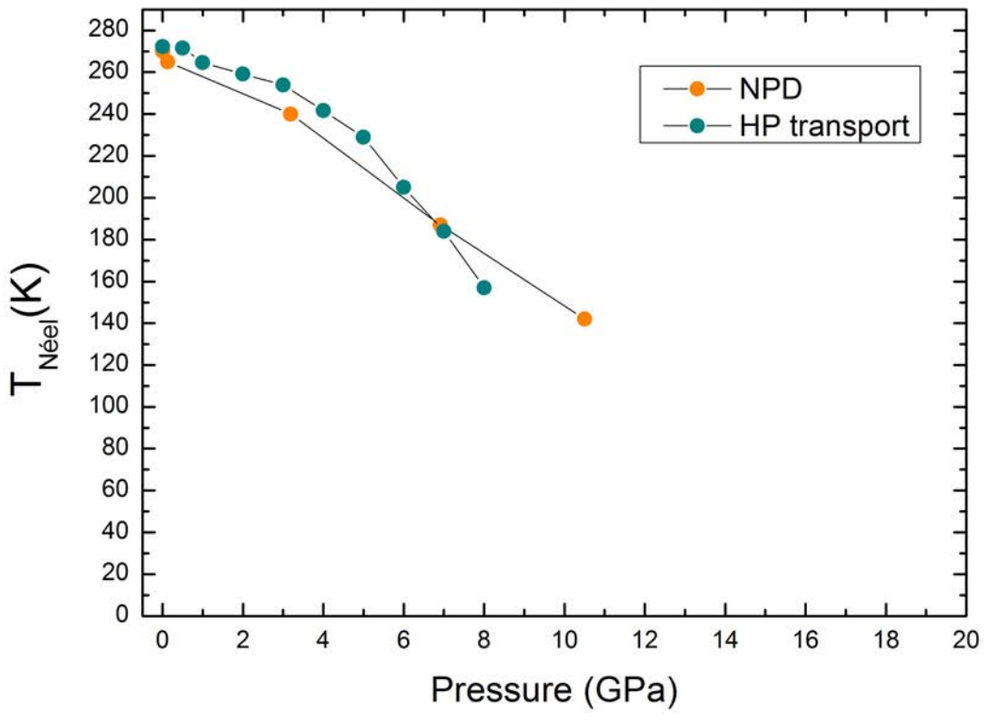

$CrSb_2$

XRD /HP at RT (ESRF, id27)

$CrSb_2$

XRD /HP at RT (ESRF, id27)

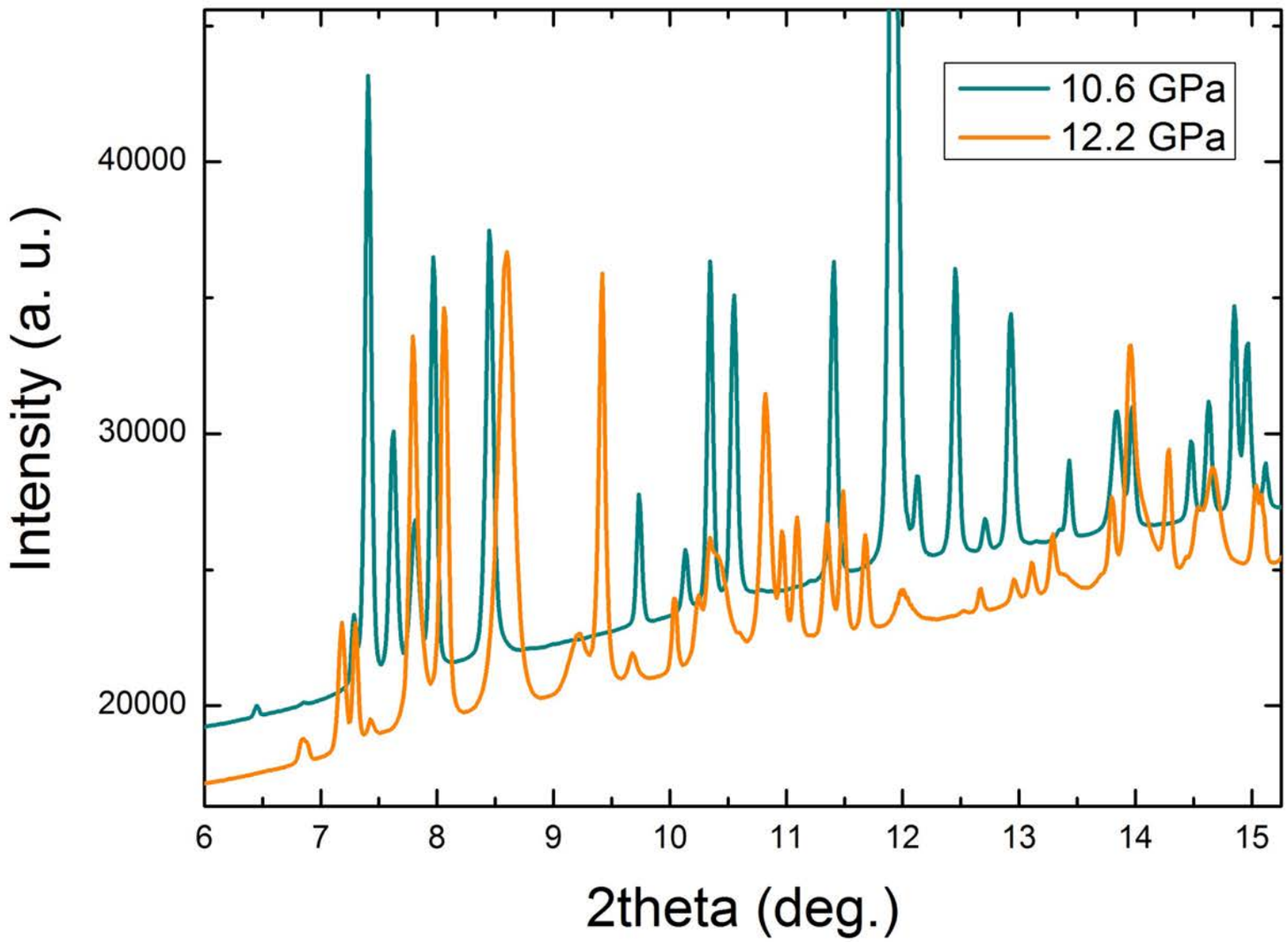

$CrSb_2$

XRD /HP at RT (ESRF, id27)

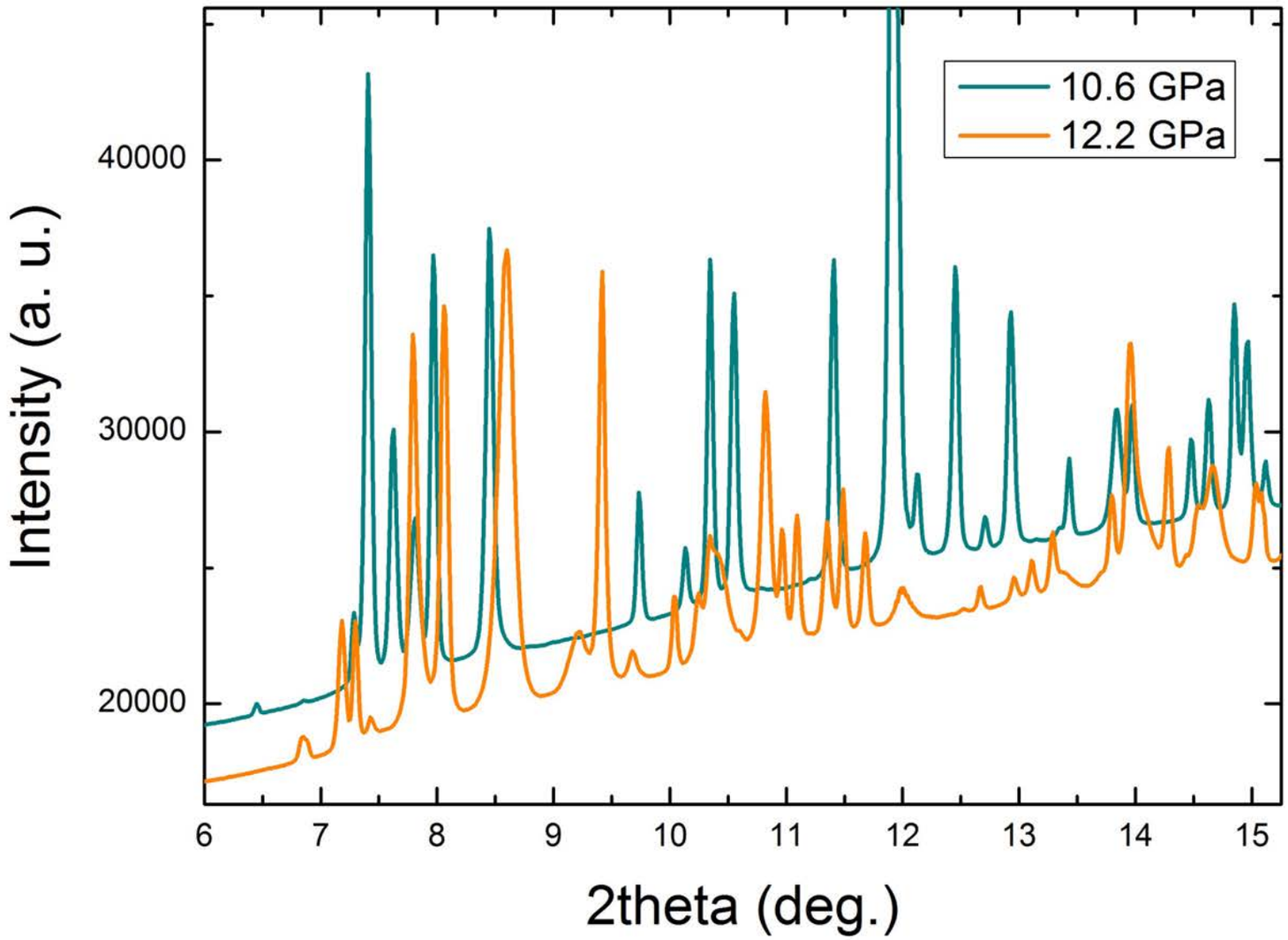

CrSb2 marcasite-type structure

$CrSb_2$

XRD /HP at RT (ESRF, id27)

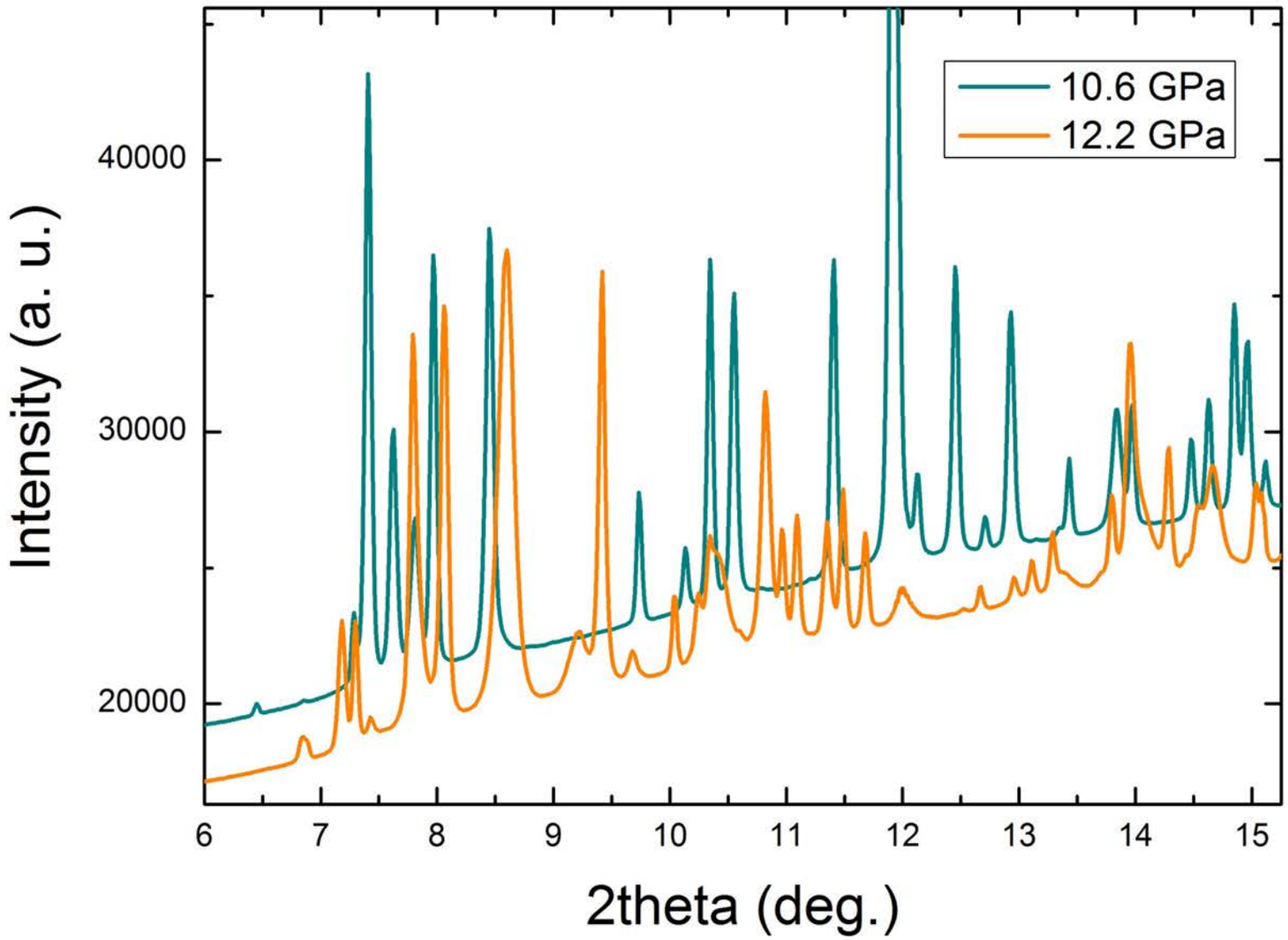

CrSb2 marcasite-type structure

12 GPa

Phase transition

??

$CrSb_2$

XRD /HP at RT (ESRF, id27)

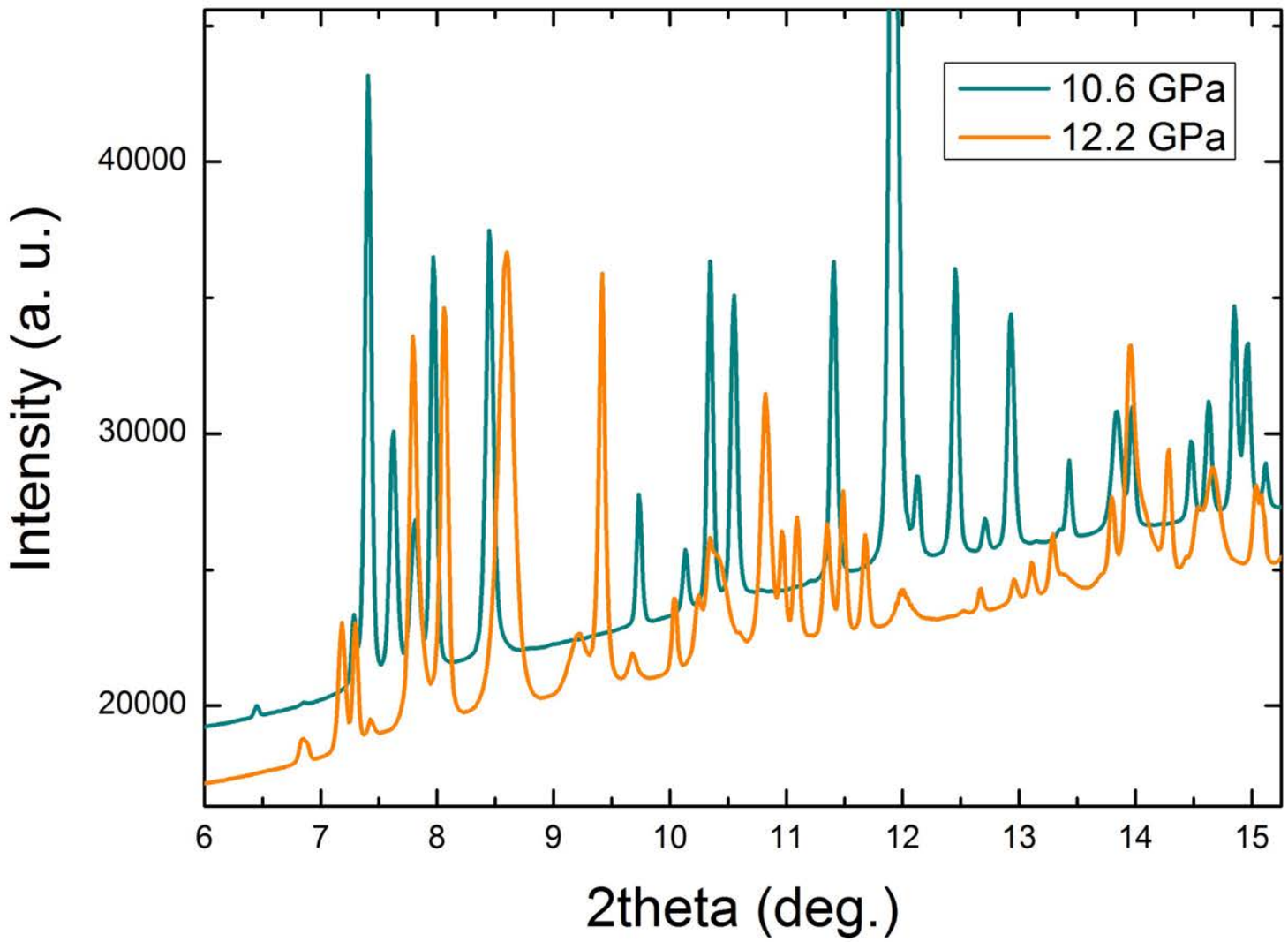

CrSb2 marcasite-type structure

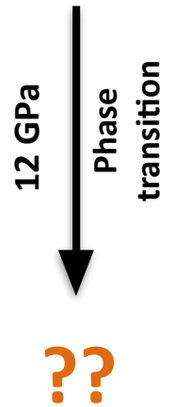

??

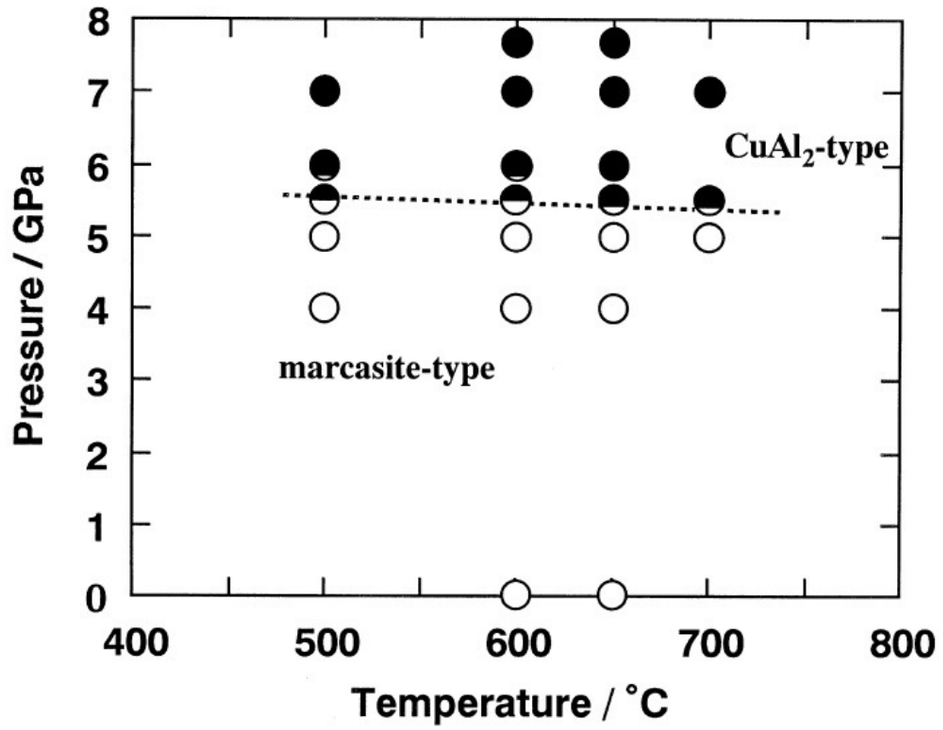

auteurs

$CrSb_2$

XRD /HP at RT (ESRF, id27)

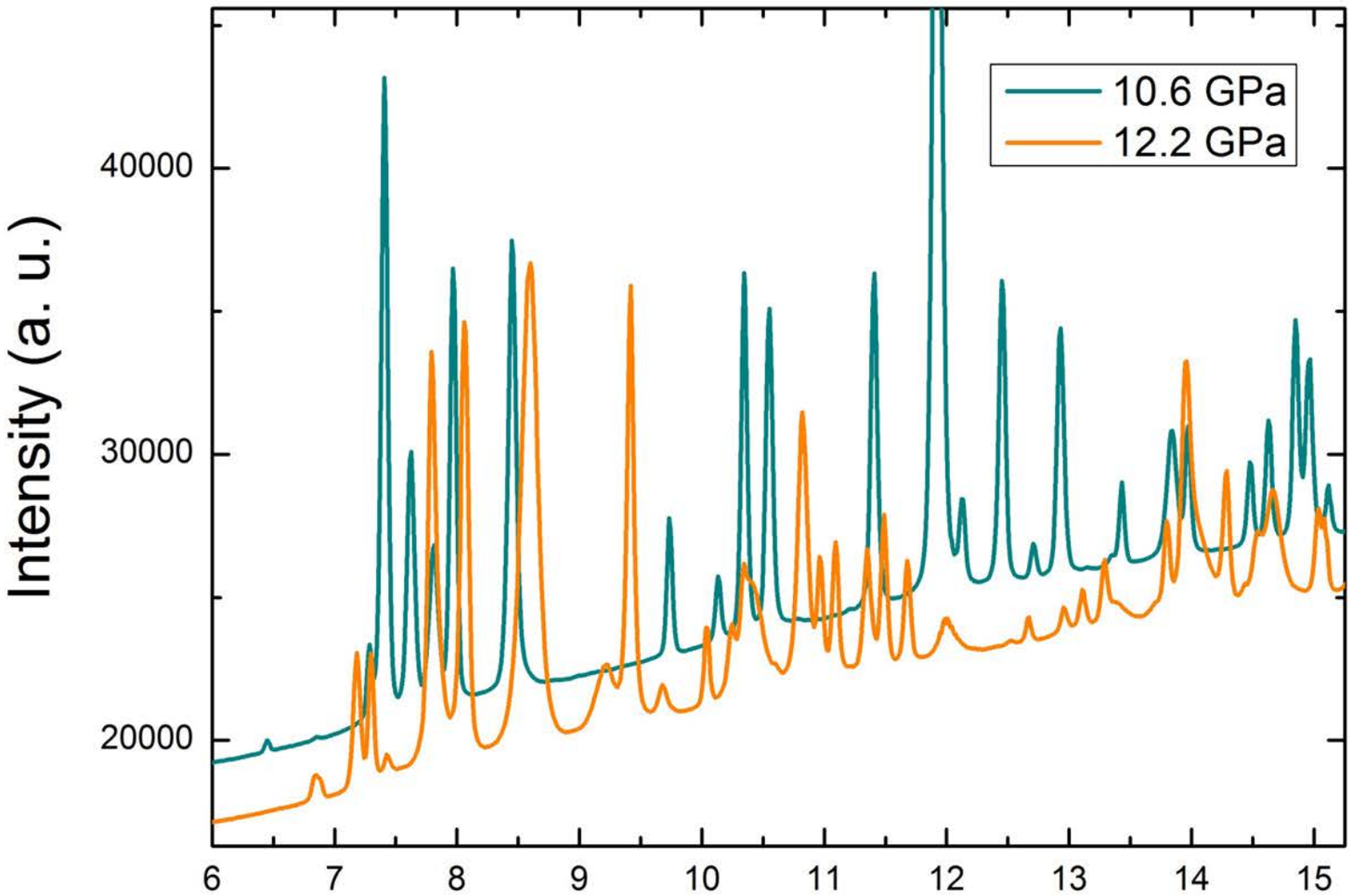

First refinement tried with :

CuAl2-type + deformed Marcasite-type = not bad but needs other(s) phase(s)

CrSb2 marcasite-type structure

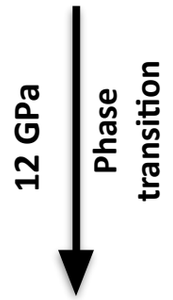

??

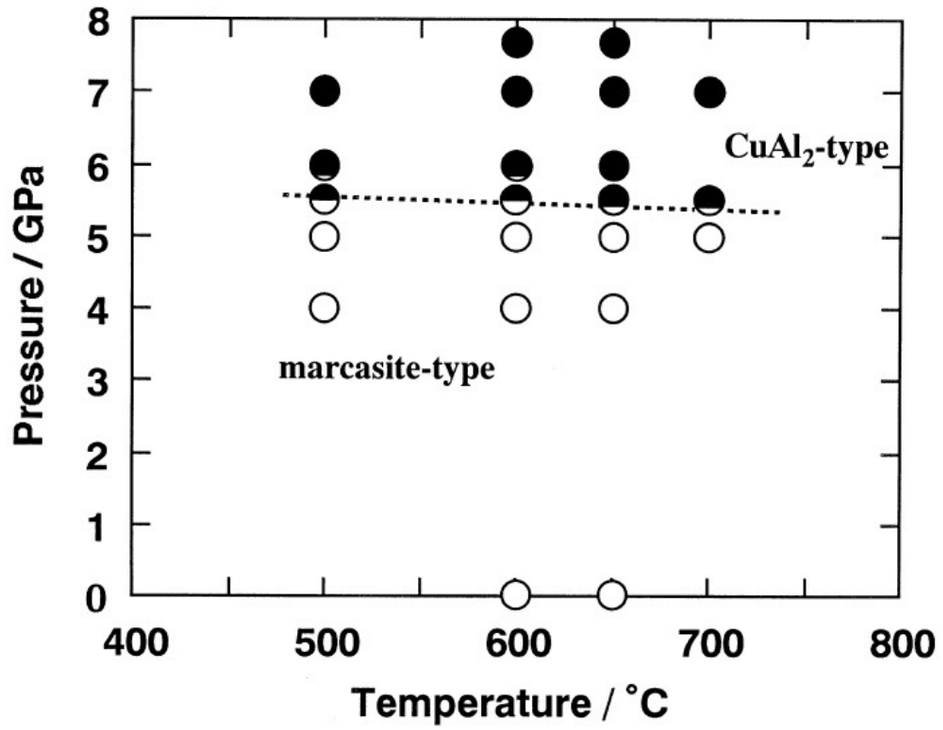

auteurs

$CrSb_2$

XRD /HP at RT (ESRF, id27)

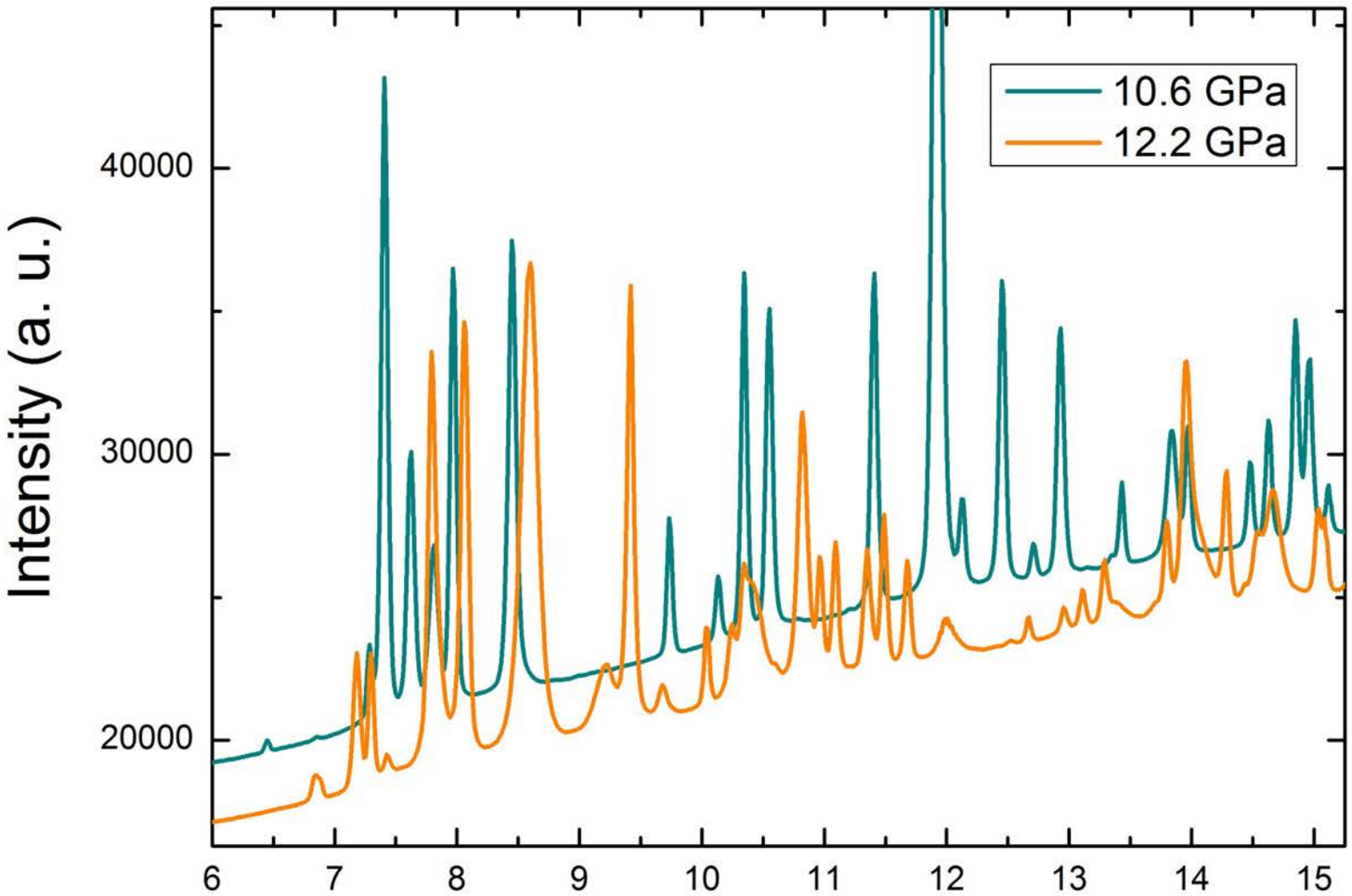

CrSb2 marcasite-type structure

12 GPa
Phase transition

??

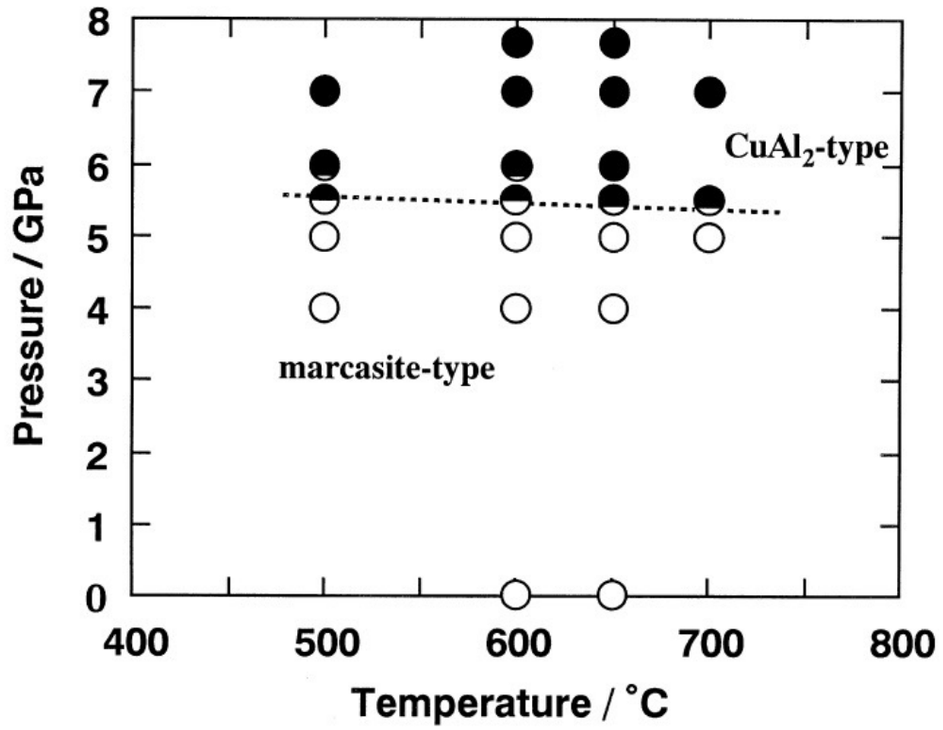

First refinement tried with :

CuAl2-type + deformed Marcasite-type = not bad but needs other(s) phase(s)

Metallic and FM

auteurs

$CrSb_2$

CrAs motivation

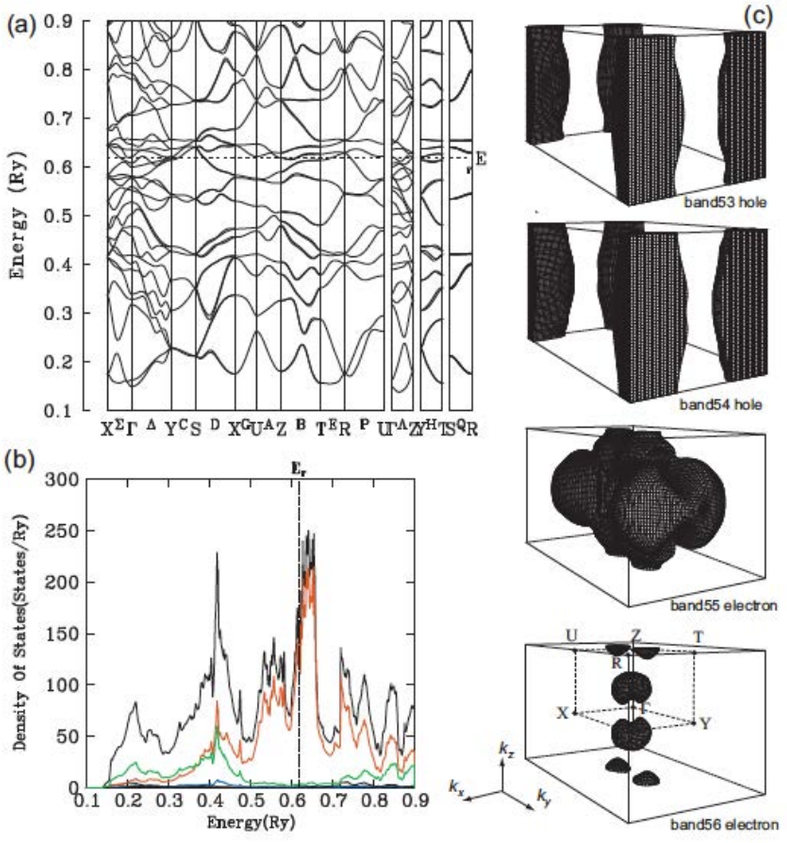

CrAs

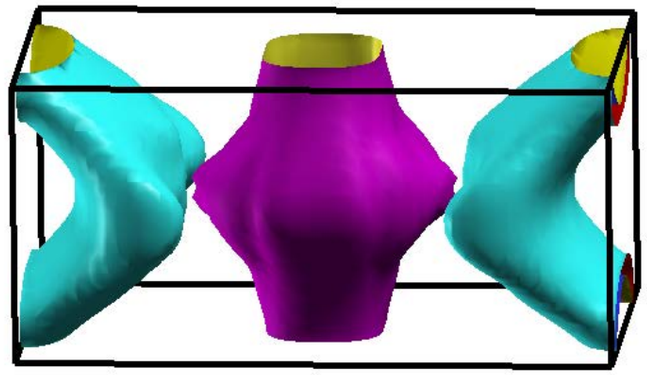

CrSb2

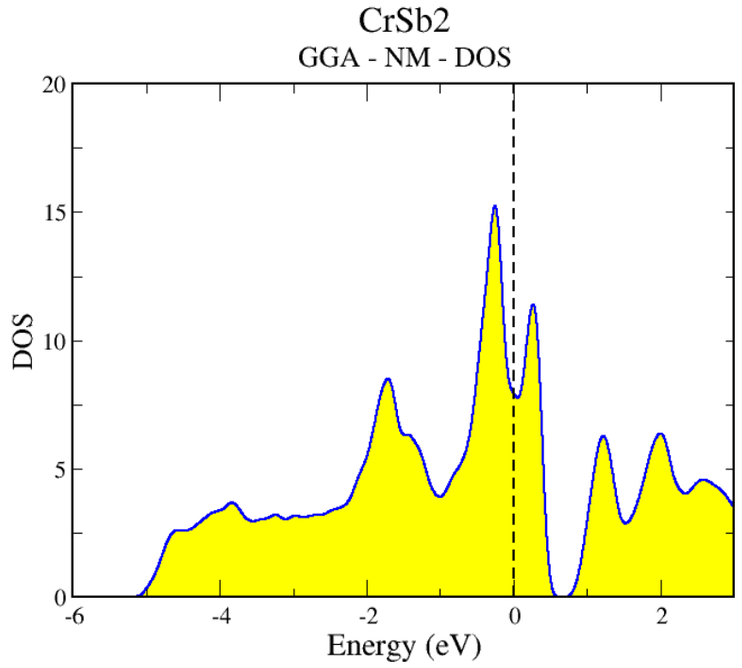

CrSb2

DIAPO QUESTION

AJOUTER MAG-CURIE POUR VOIR CE PIC À BASSE T

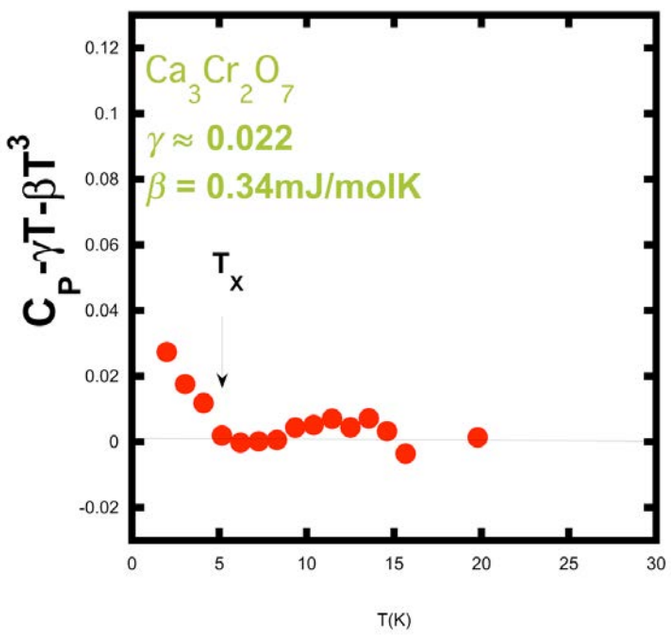

Sr3Cr2O7-2K-Non Magnetic

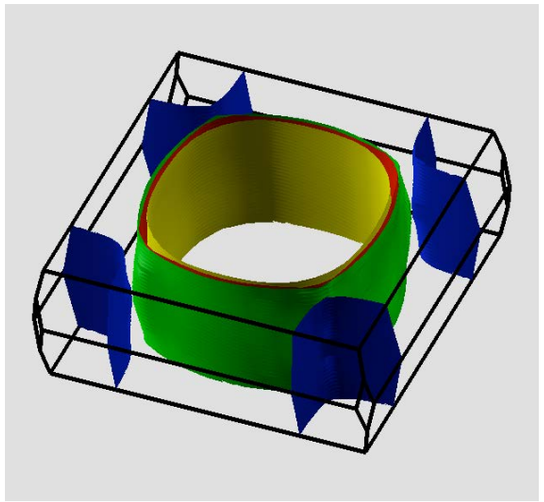

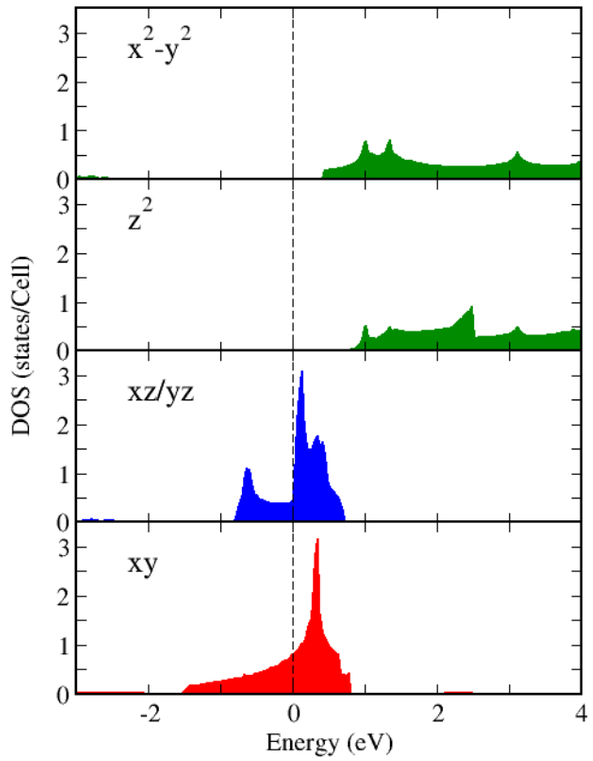

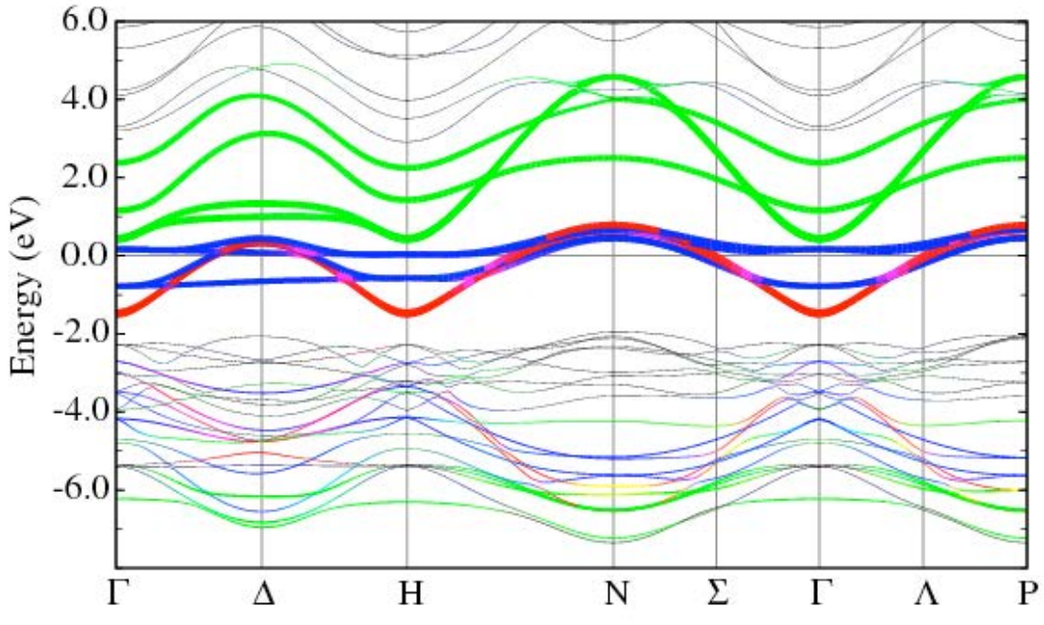

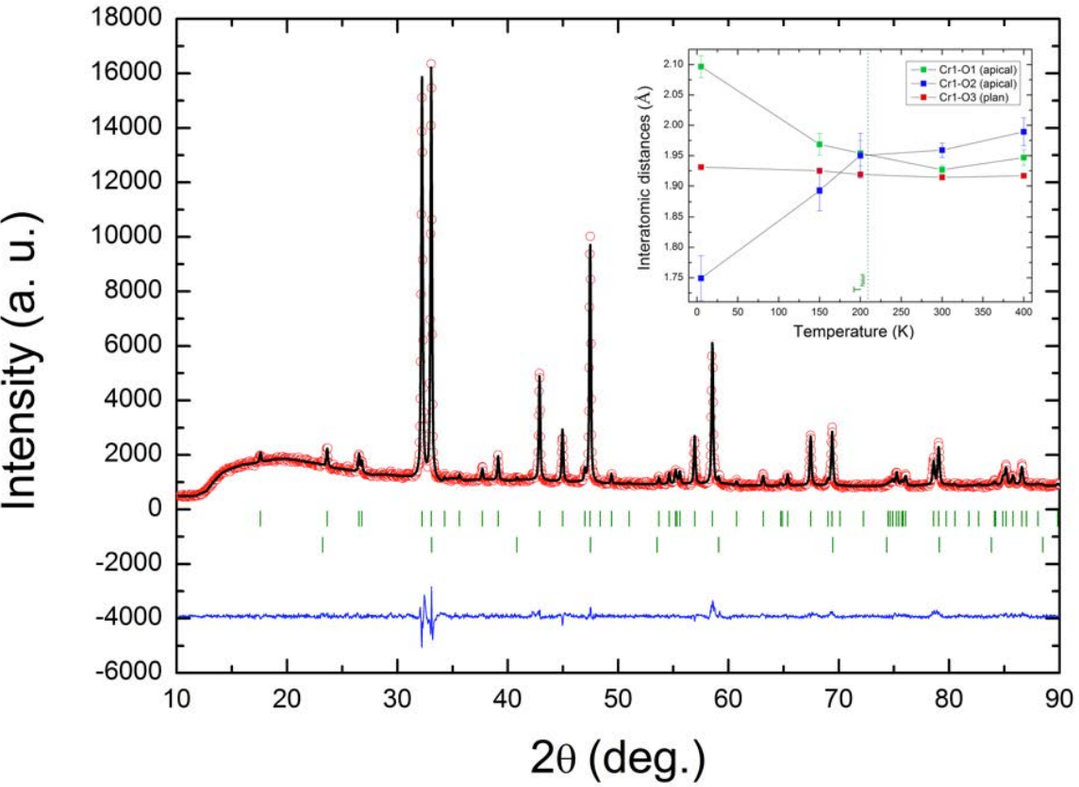
Intensity (a. u.)
2θ (deg.)
Cr1-O1 (apical)
Cr1-O2 (apical)
Cr1-O3 (plan)
Interatomic distances (Å)
Temperature (K)

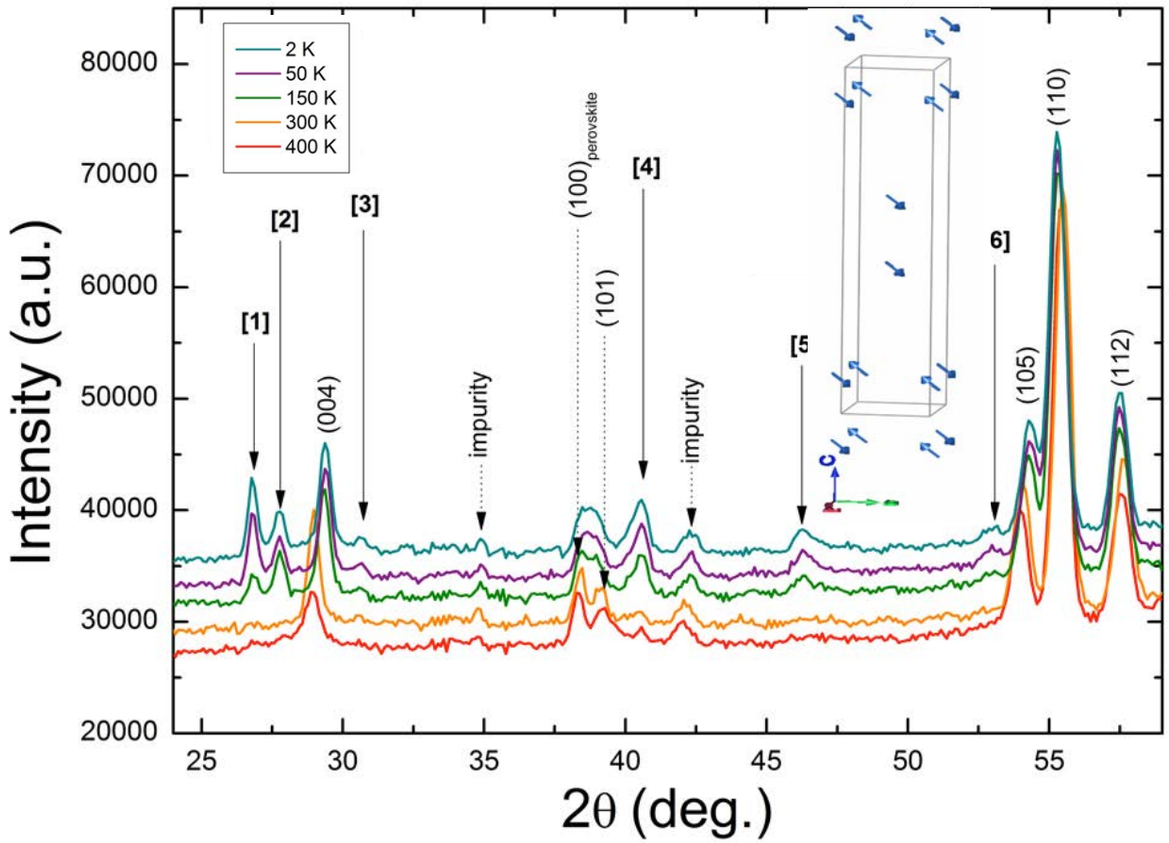
Intensity (a.u.)
2θ (deg.)
2 K
50 K
150 K
300 K
400 K
[1]
[2]
[3]
(004)
impurity
(100)perovskite
(101)
[4]
impurity
[5
6]
(105)
(110)
(112)

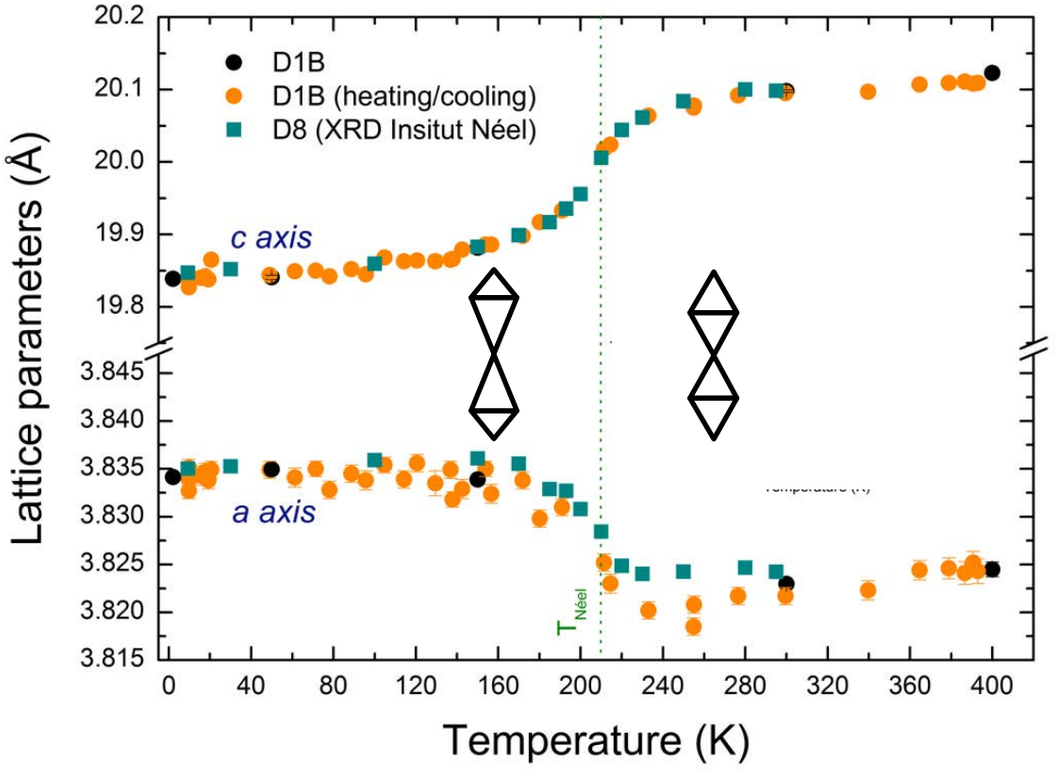
Lattice parameters (Å)
Temperature (K)
D1B
D1B (heating/cooling)
D8 (XRD Insitut Néel)
c axis
a axis
T Néel

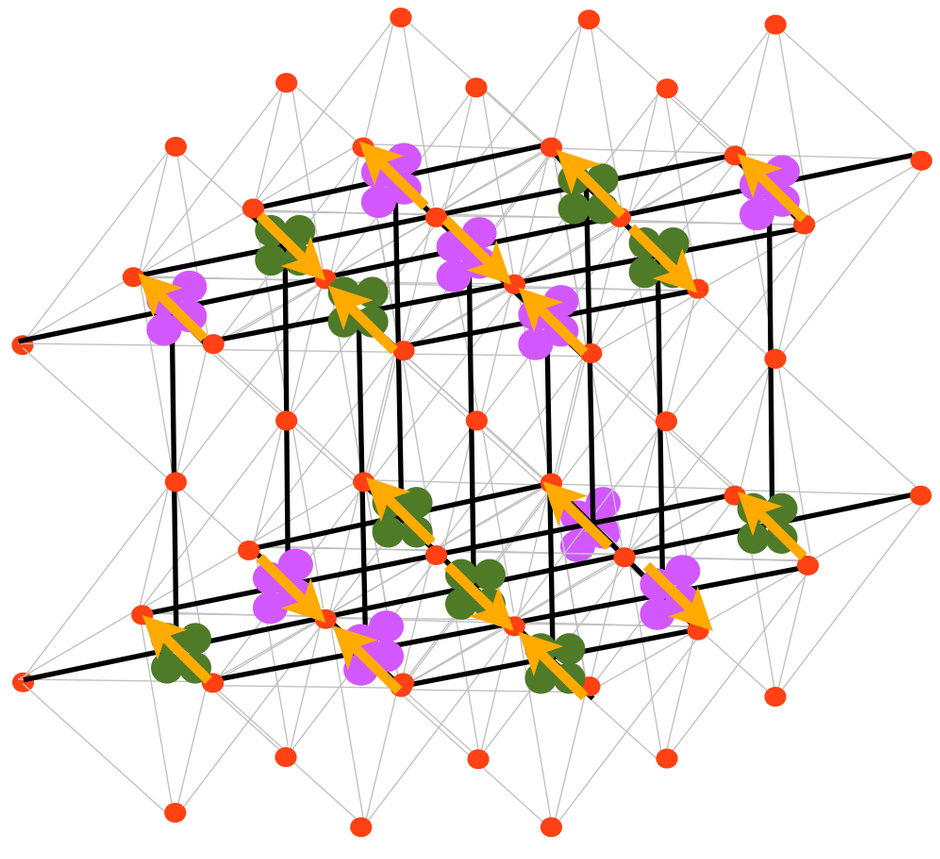

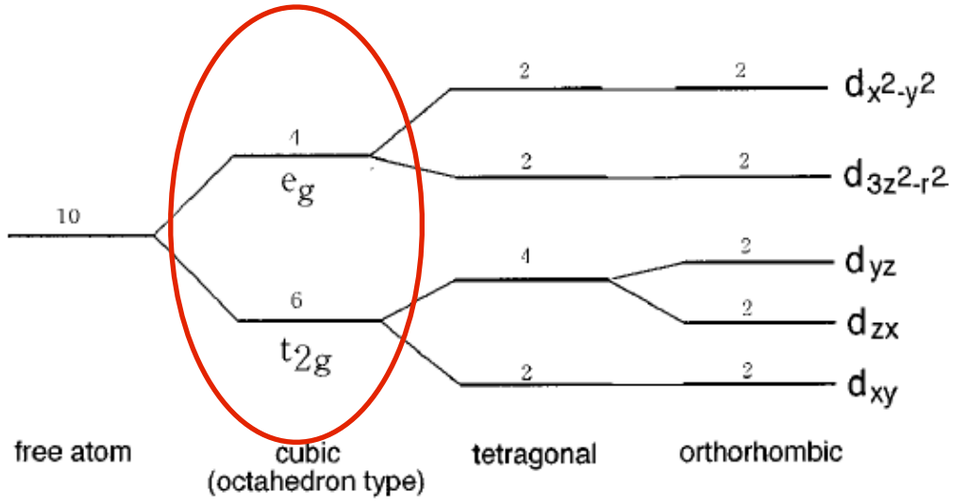

FIG. 2. Crystal-field splitting of $3d$ orbitals under cubic, tetragonal, and orthorhombic symmetries. The numbers cited near the levels are the degeneracy including spins.

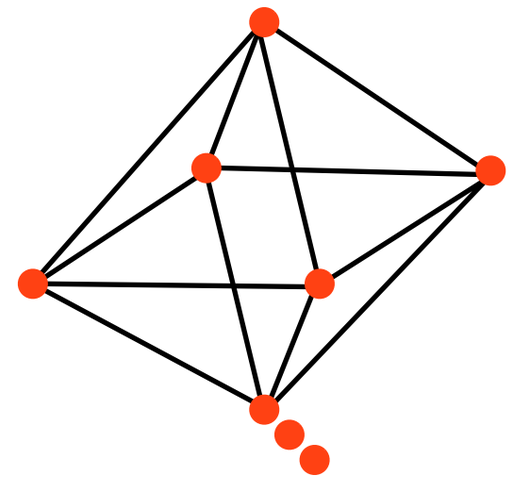

d^7

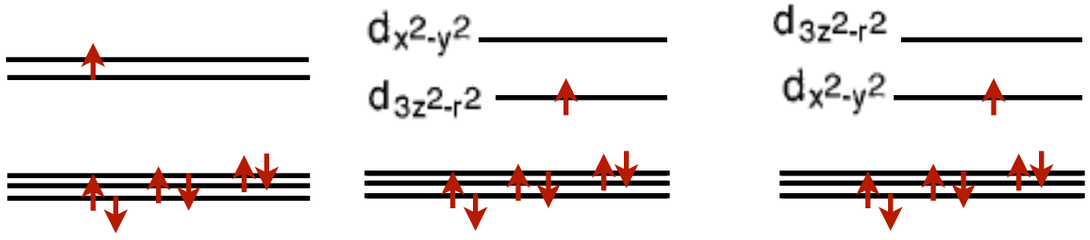

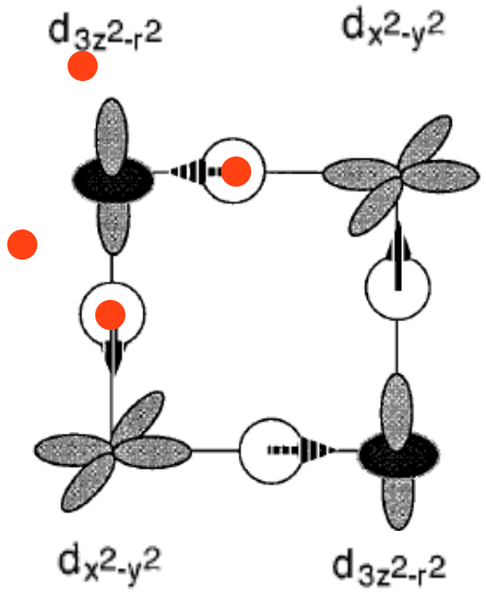

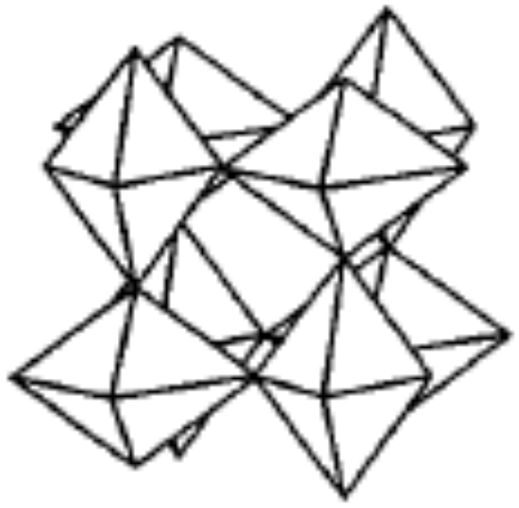

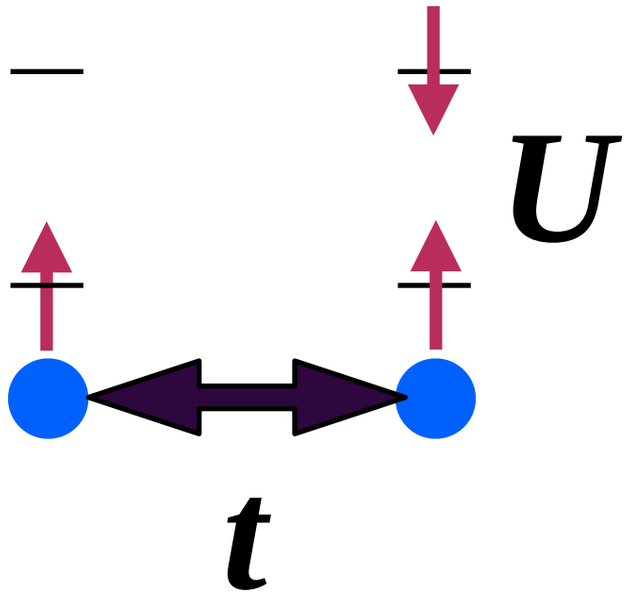

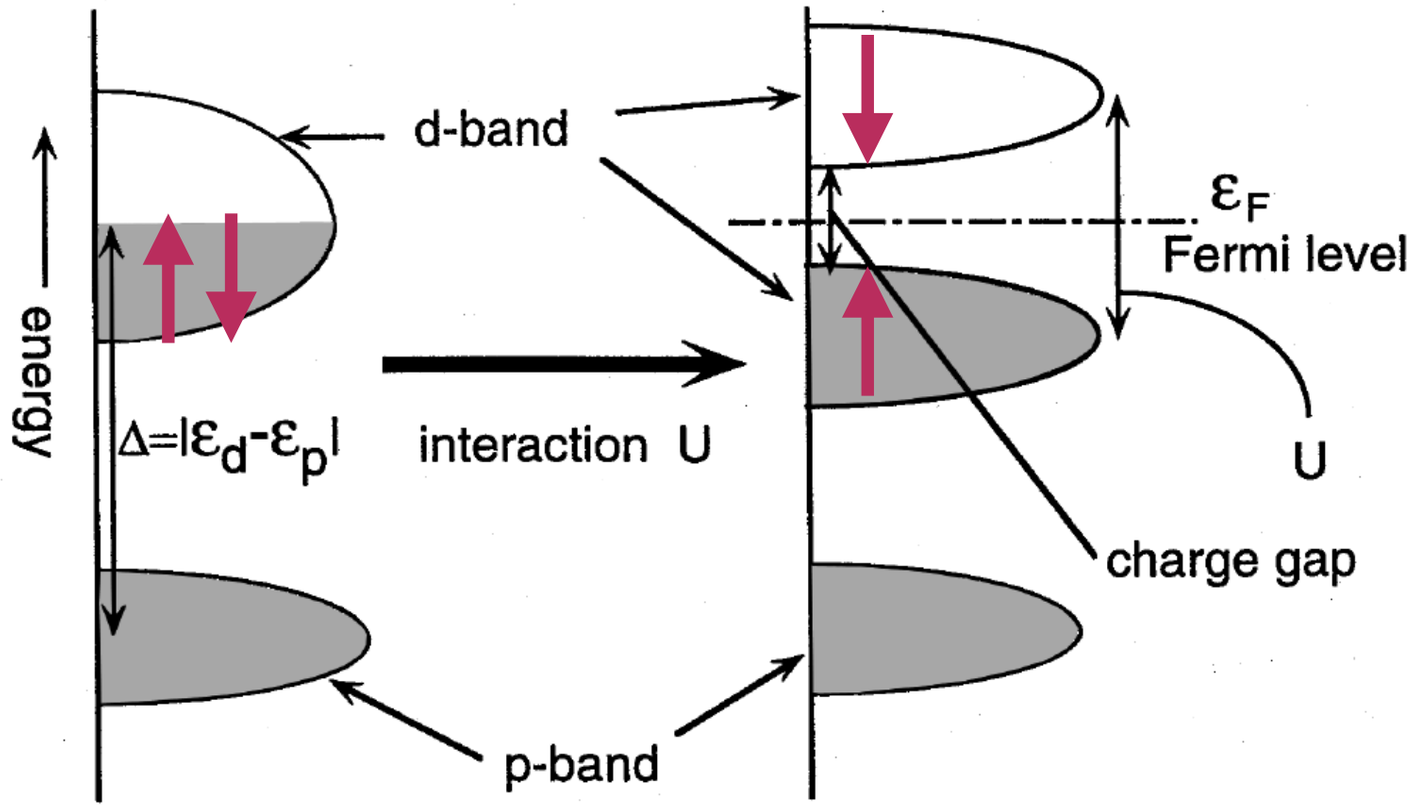

(a) Mott-Hubbard Insulator

FIG. 1. Metal-insulator phase diagram based on the Hubbard model in the plane of U/t and filling n. The shaded area is in principle metallic but under the strong influence of the metal-insulator transition, in which carriers are easily localized by extrinsic forces such as randomness and electron-lattice coupling. Two routes for the MIT (metal-insulator transition) are shown: the FC-MIT (filling-control MIT) and the BC-MIT (bandwidth-control MIT).

Superexchange

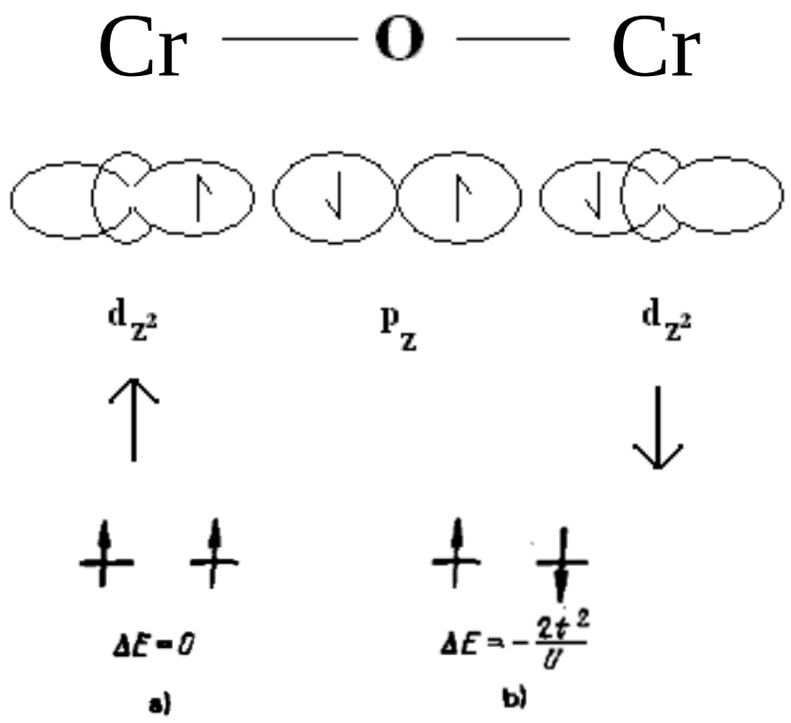

FIG. 10. Scheme for superexchange in the nondegenerate case. Shown here is the energy increase due to virtual transitions of an electron to a neighboring center. An antiparallel orientation of the spins is seen to be preferred from the energy standpoint.

Same orbitals

Different orbitals

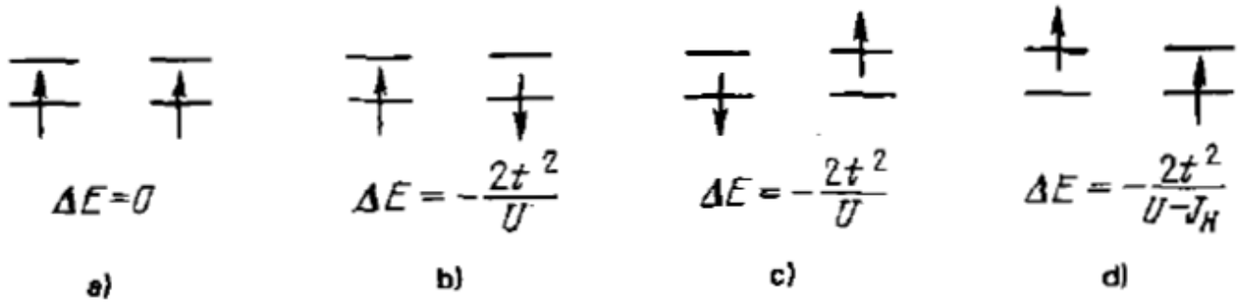

FIG. 12. Superexchange in the case of twofold-degenerate orbitals. Shown here is the energy increase if only diagonal transitions are possible ($t_{11} = t_{22} + t$, $t_{12} = 0$). Intraatomic (Hund) exchange is also taken into account.

Sr_2CrO_4

Sr214
I4/mmm

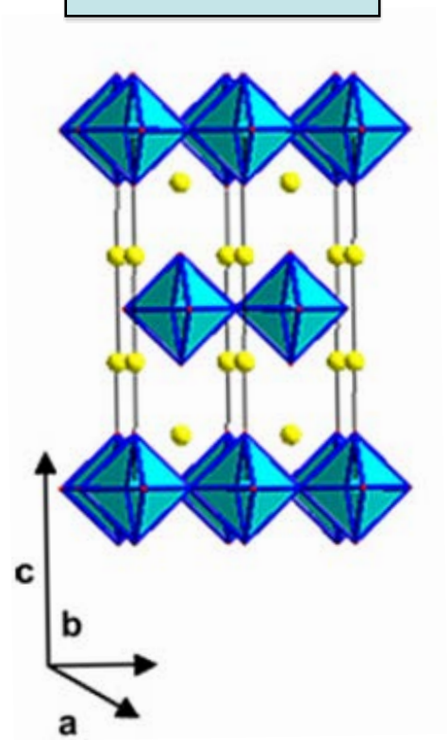

a ~ 3.81 Å

c ~ 12.52 Å

Sr_2CrO_4

Sr214
I4/mmm

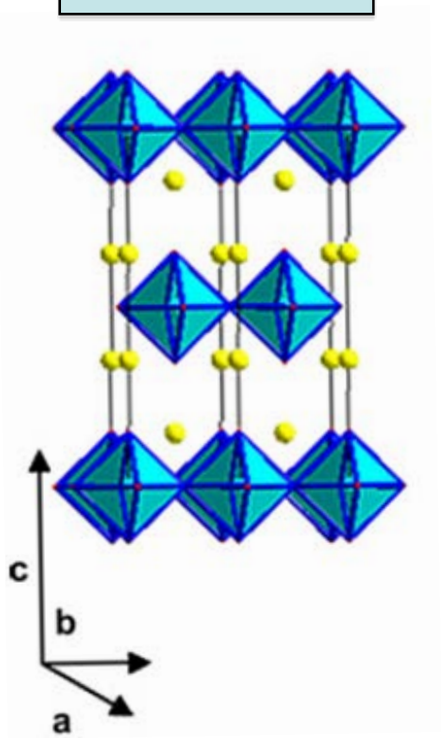

a ~ 3.81 Å

c ~ 12.52 Å

X-ray diffraction

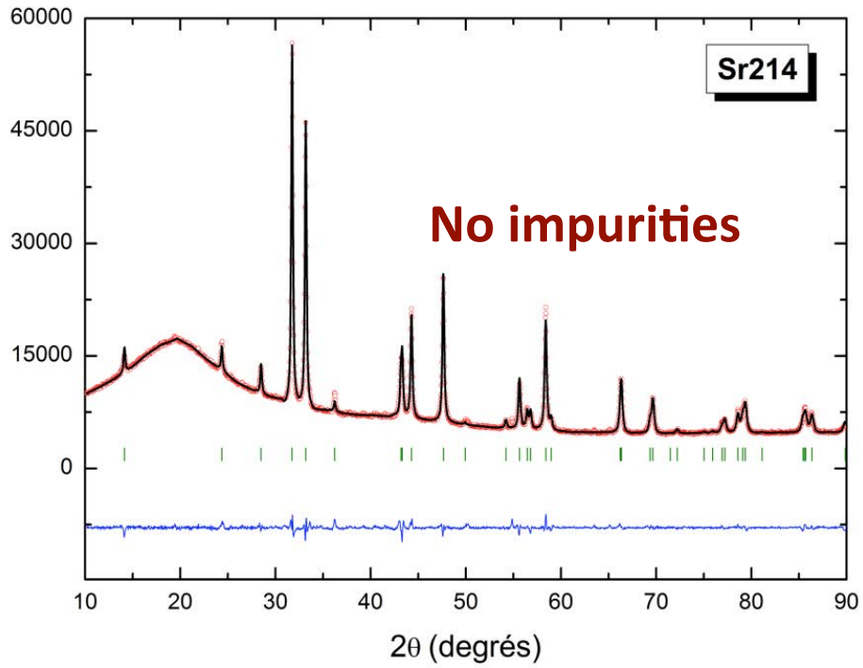

Sr_2CrO_4

Sr214
I4/mmm

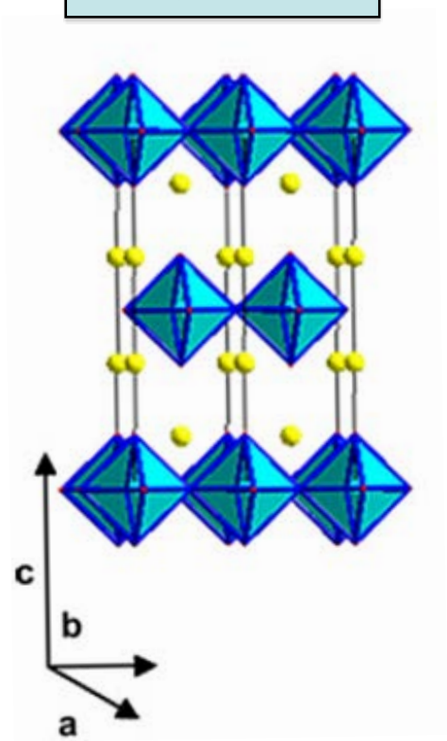

a ~ 3.81 Å

c ~ 12.52 Å

X-ray diffraction

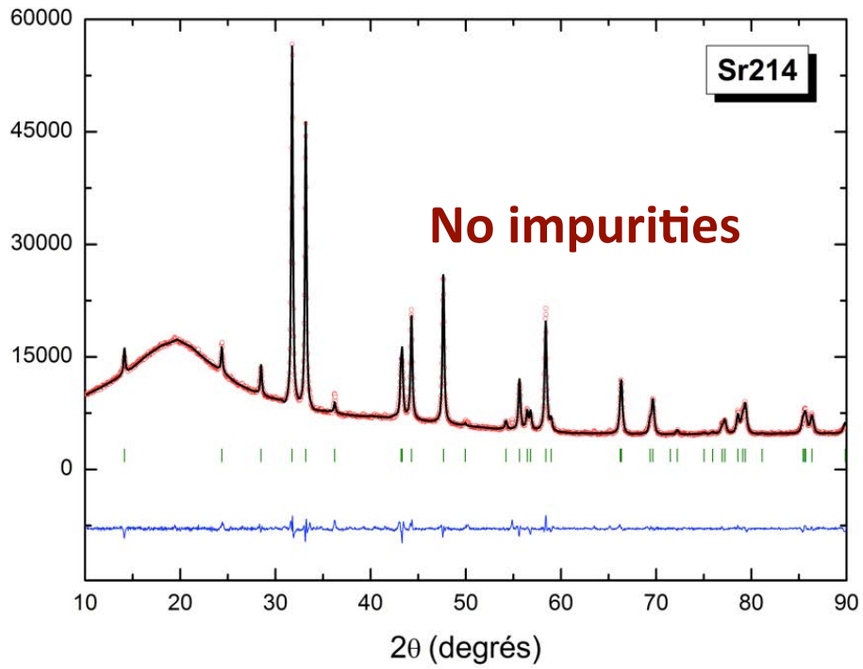

Transport measurement

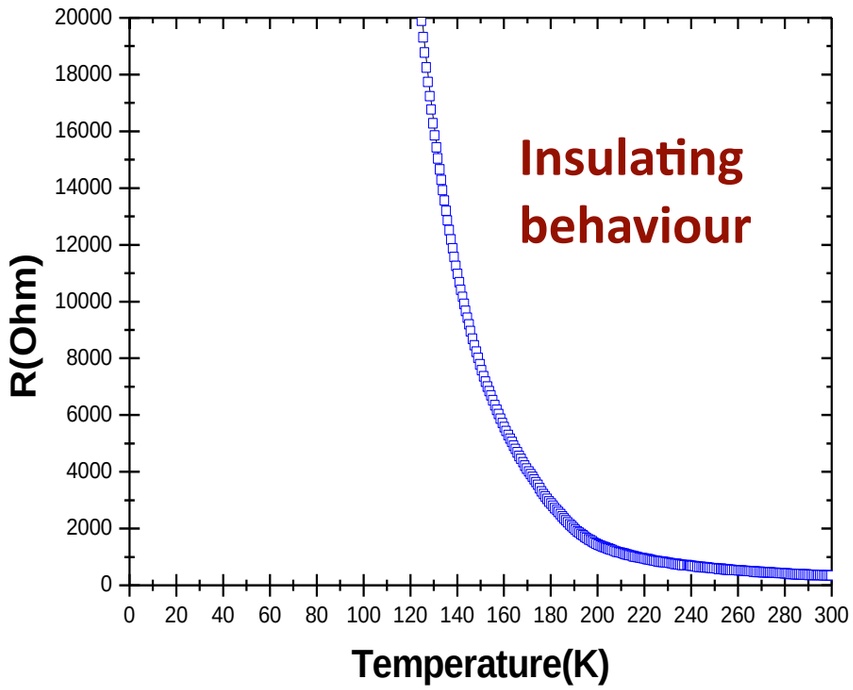

Calculations give metallic
(without magnetism & U)

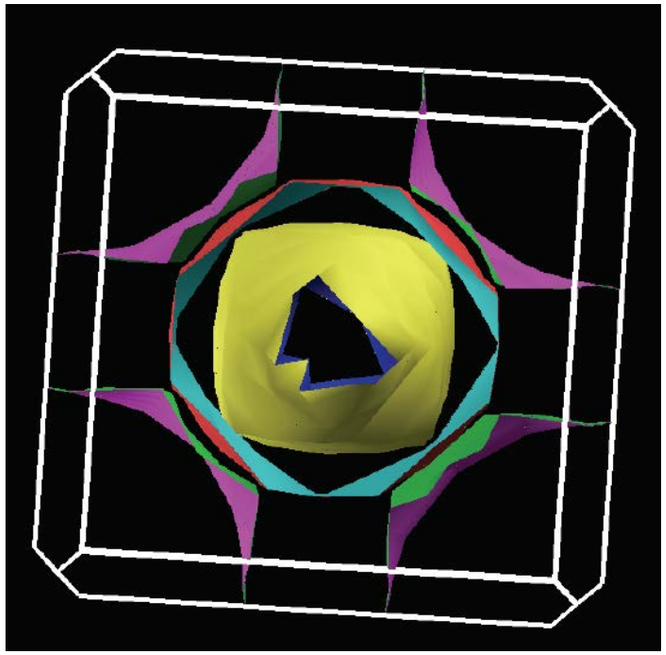

Sr_2CrO_4

Sr214
I4/mmm

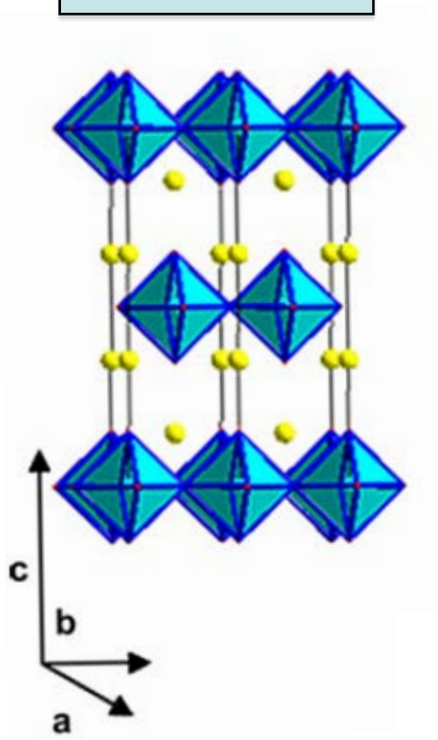

a ~ 3.81 Å

c ~ 12.52 Å

X-ray diffraction

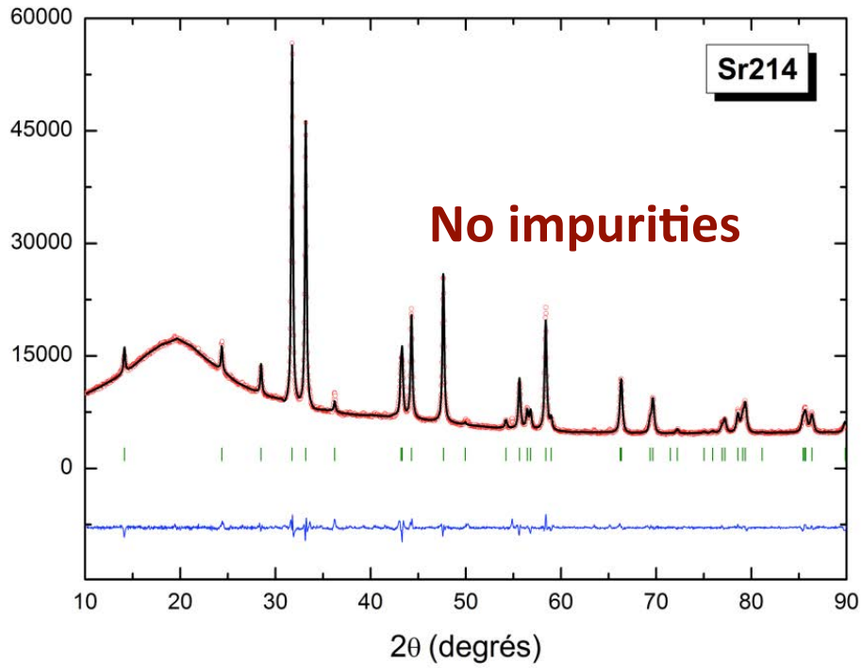

Transport measurement

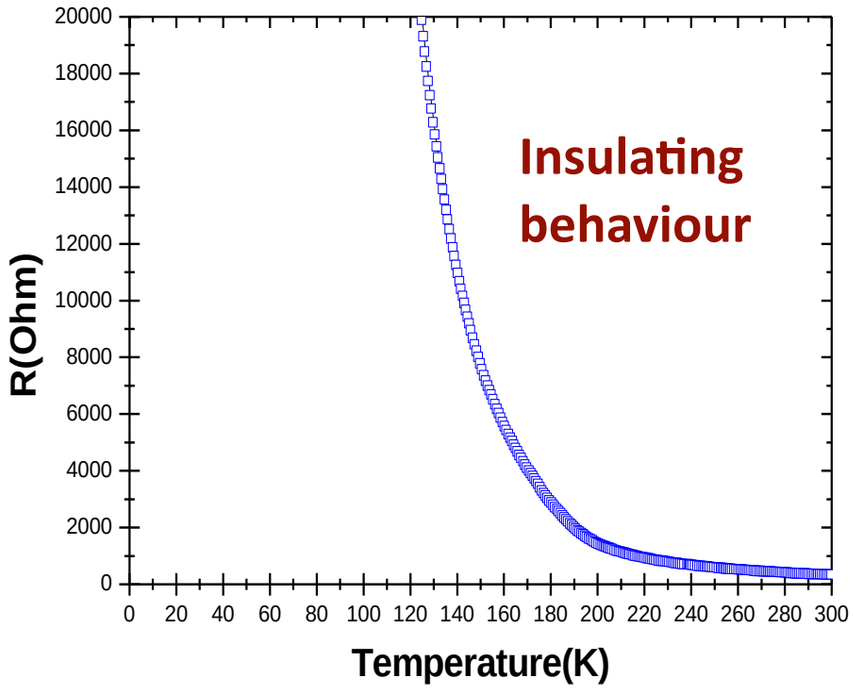

Magnetic measurement

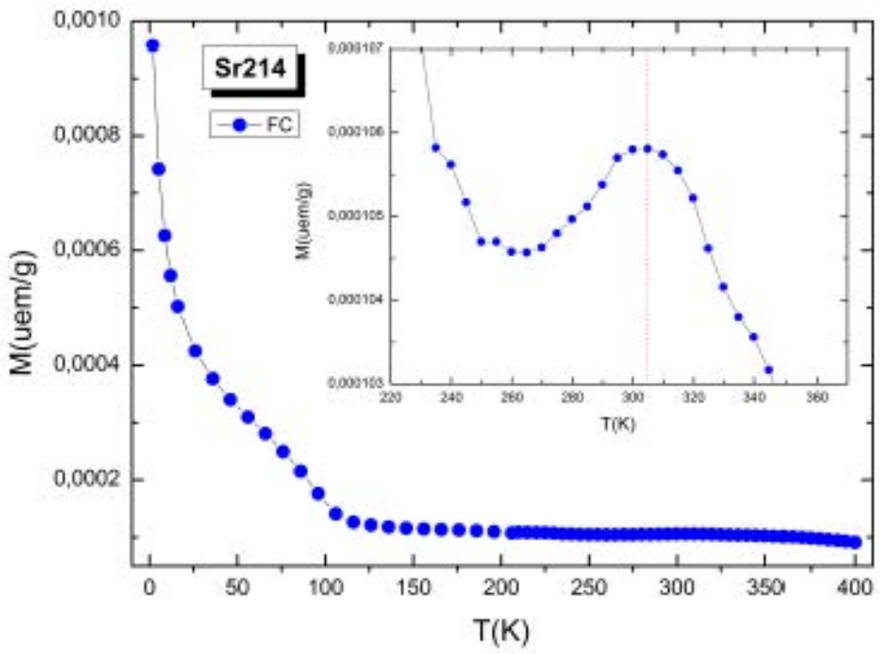

AFM

T_N = 305 K

Sr_2CrO_4

Neutron Powder diffraction

ILL, D1B & D2B instruments

Sr_2CrO_4

Neutron Powder diffraction

ILL, D1B & D2B instruments

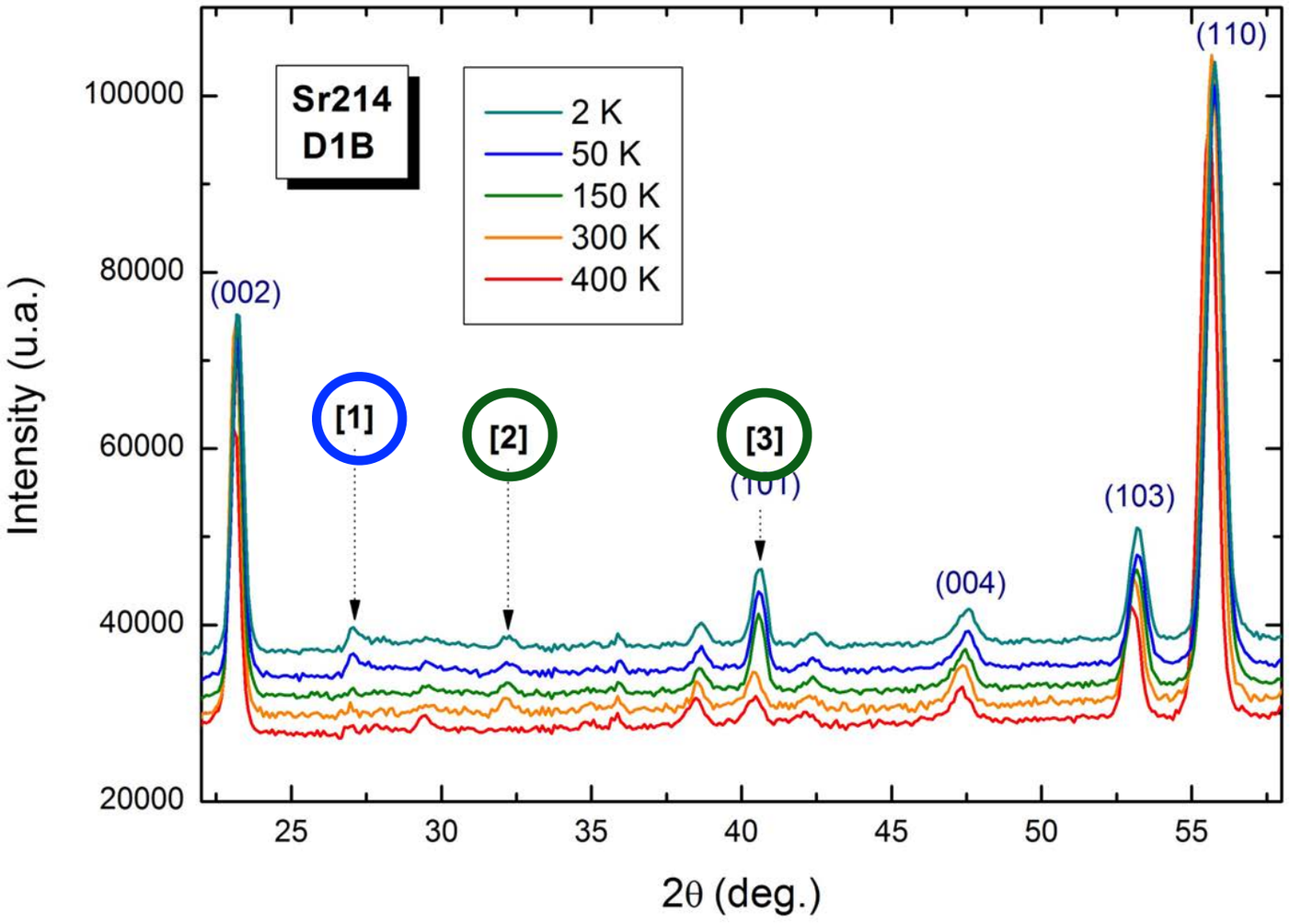

Magnetic peaks appearance

- **Number [2] and [3] : OK with T_N = 305 K**

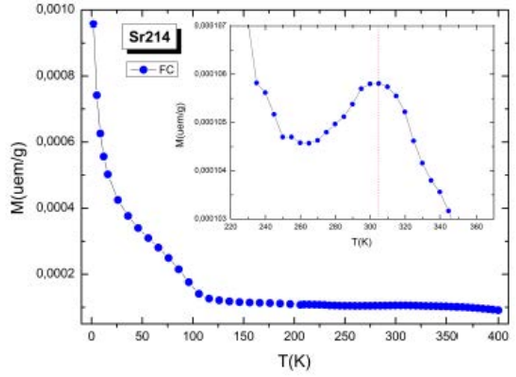

Sr_2CrO_4

Neutron Powder diffraction

ILL, D1B & D2B instruments

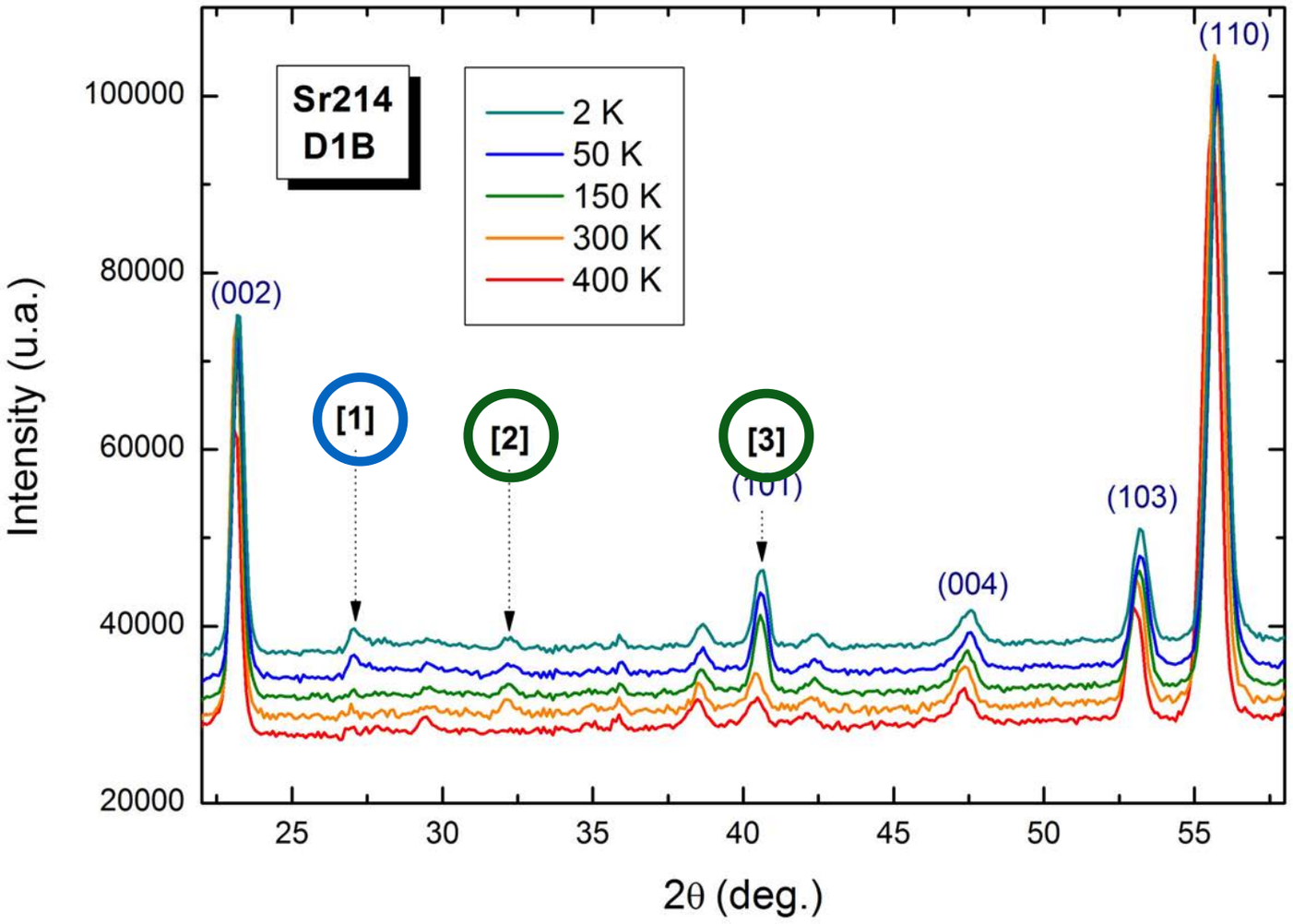

Magnetic peaks appearance

- **Number [2] and [3] : OK with T_N = 305 K**

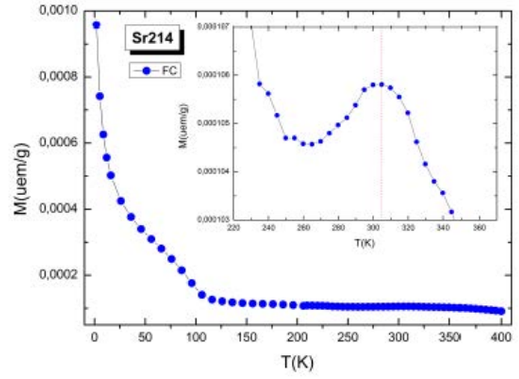

- **Number [1] : ?? Spin reorientation?**

Magnetic structure difficult to determine, work in progress..

Calculs give F <-> AF —> Helicoidal structure?

Sr_2CrO_4

Neutron Powder diffraction

ILL, D1B & D2B instruments

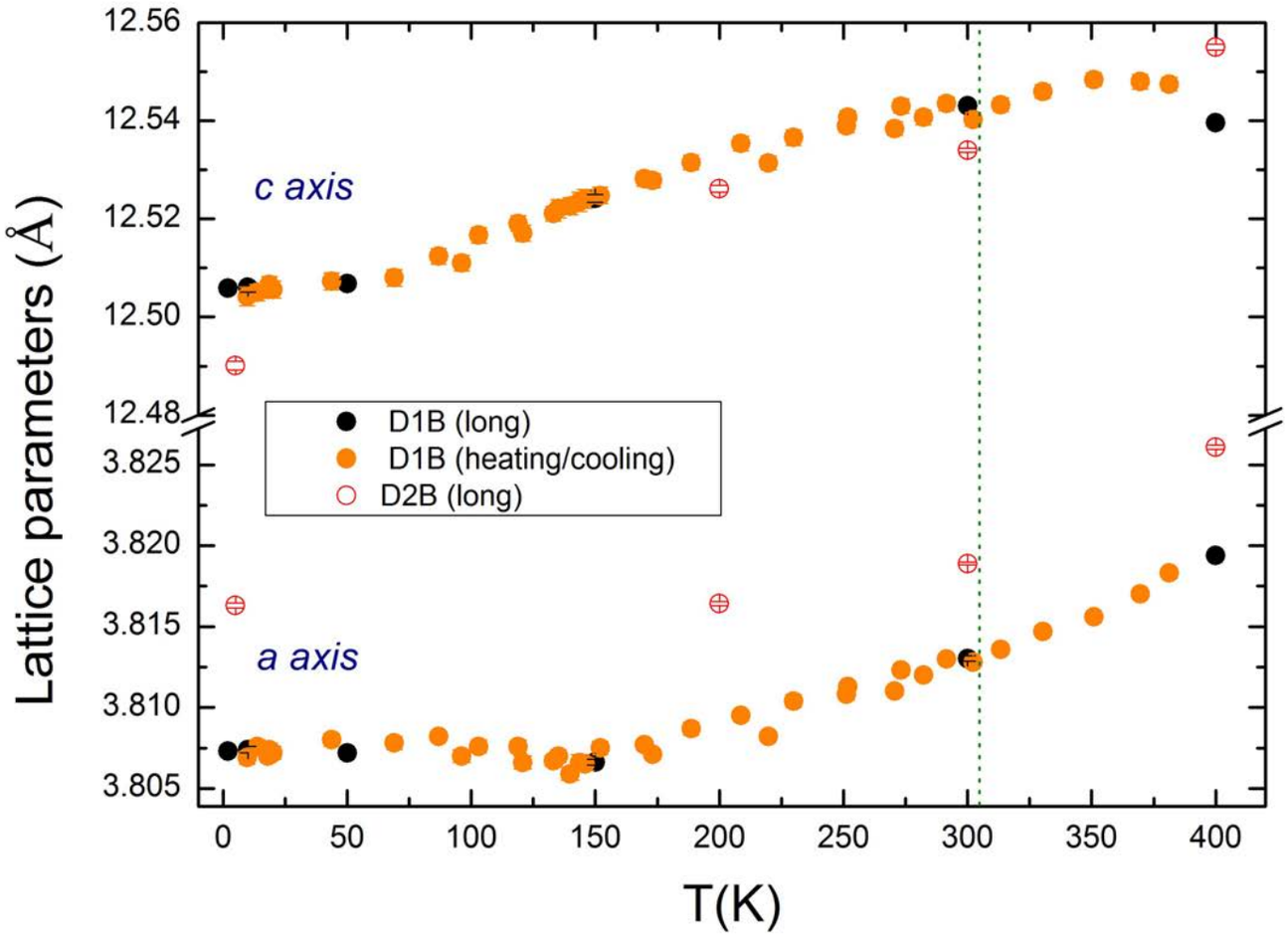

Sr_2CrO_4

Neutron Powder diffraction

ILL, D1B & D2B instruments

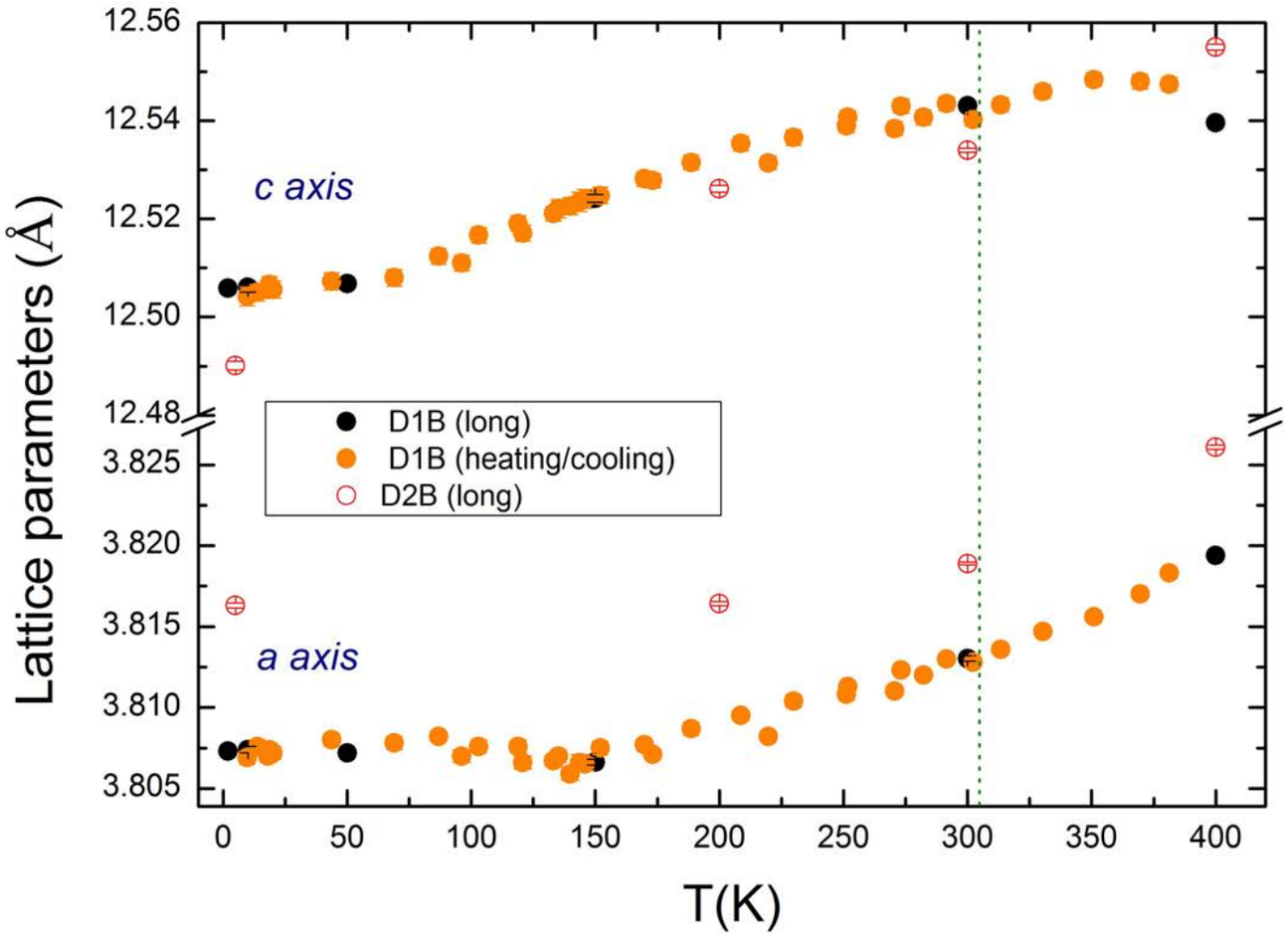

Sr327

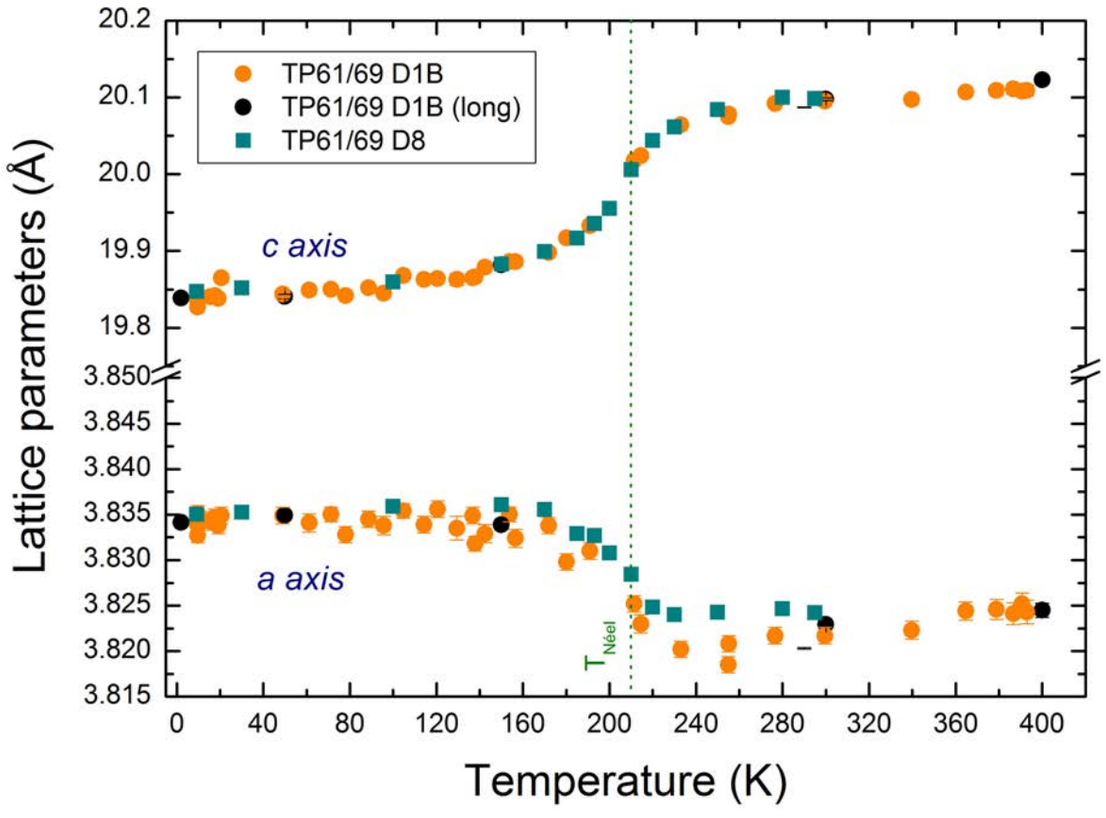

Sr_2CrO_4

Neutron Powder diffraction

ILL, D1B & D2B instruments

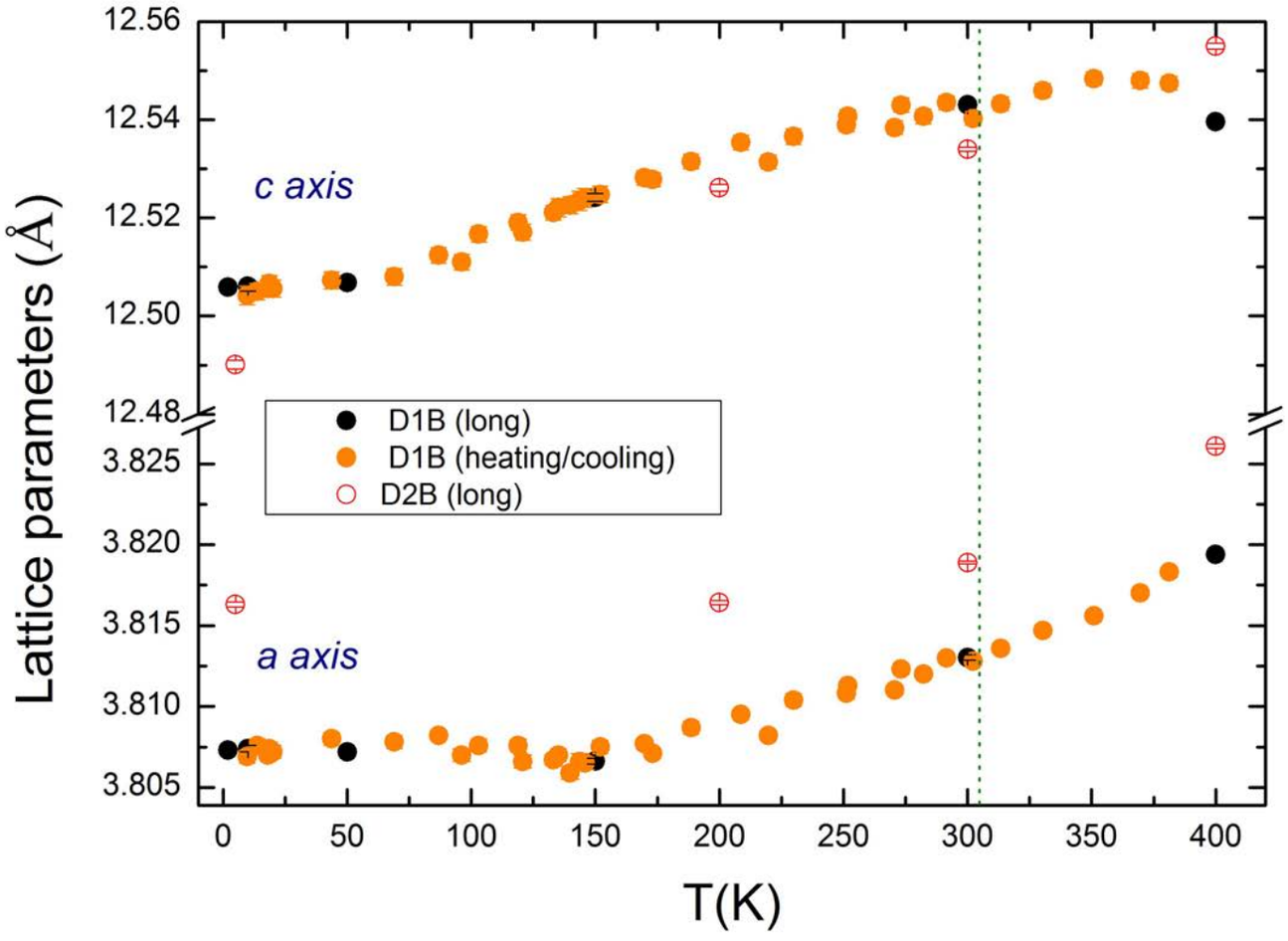

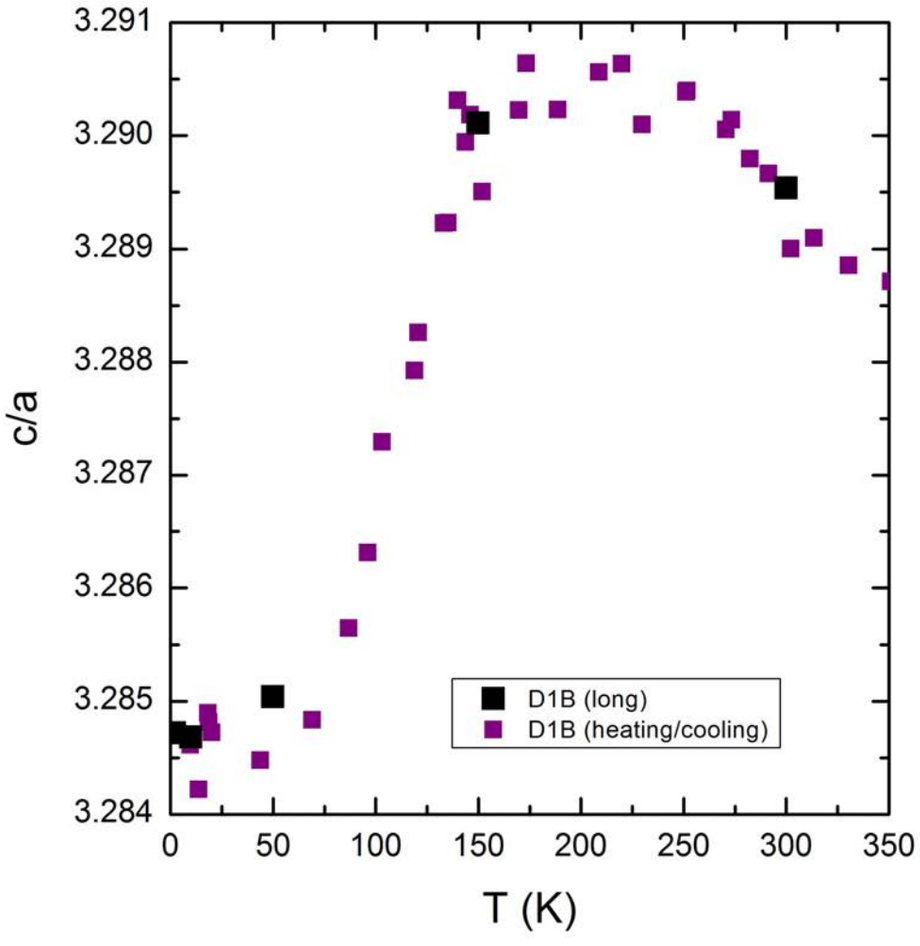

No anomaly at T_N=305K

Slight variation at 150K <—> Magnetic peak [1] ??

Sr_2CrO_4

Neutron Powder diffraction

ILL, D1B & D2B instruments

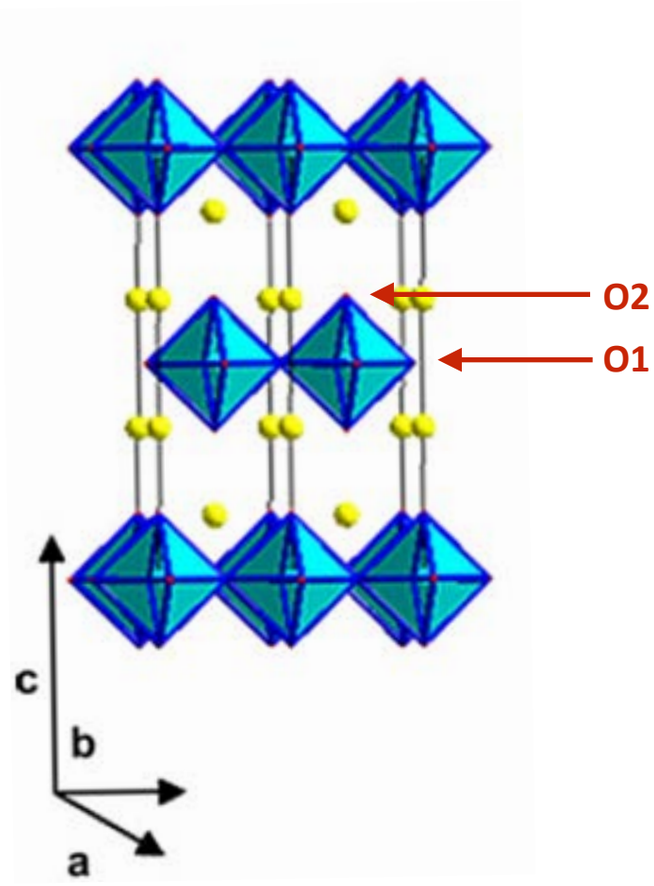

Sr_2CrO_4

Neutron Powder diffraction

ILL, D1B & D2B instruments

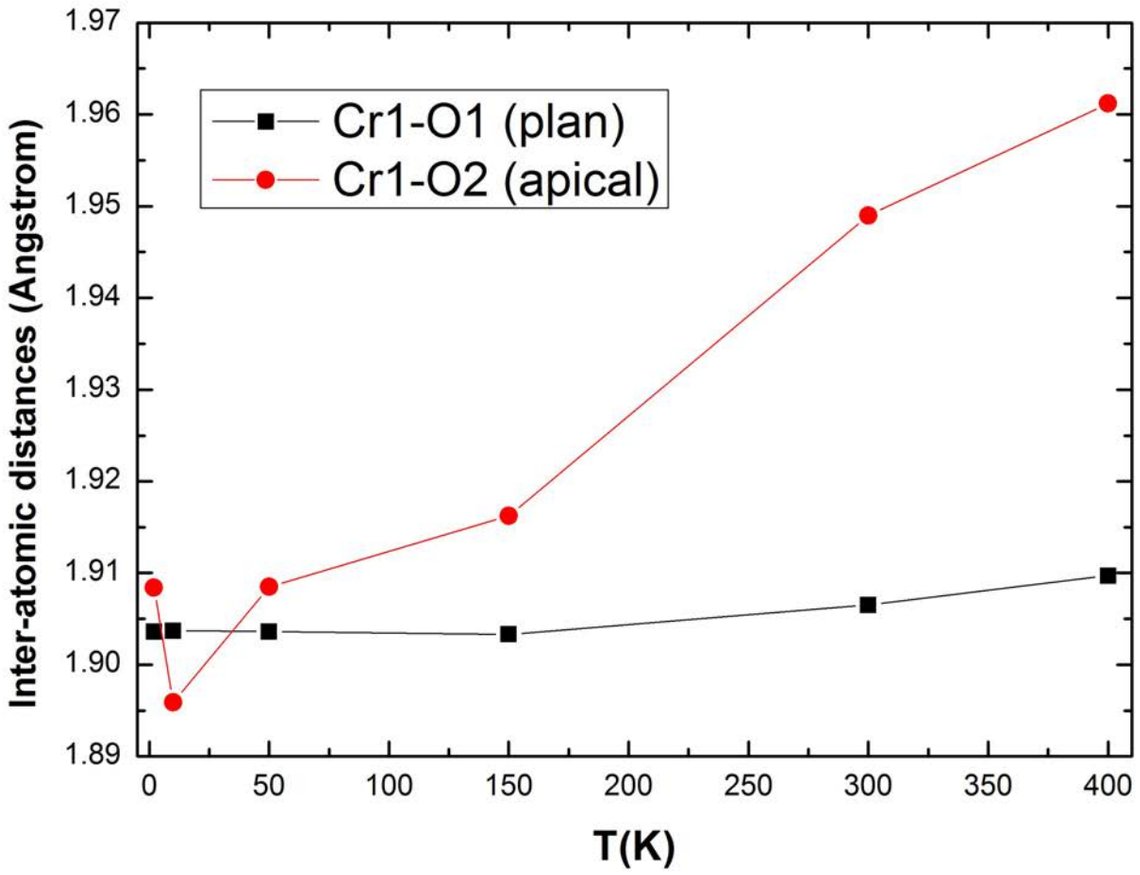

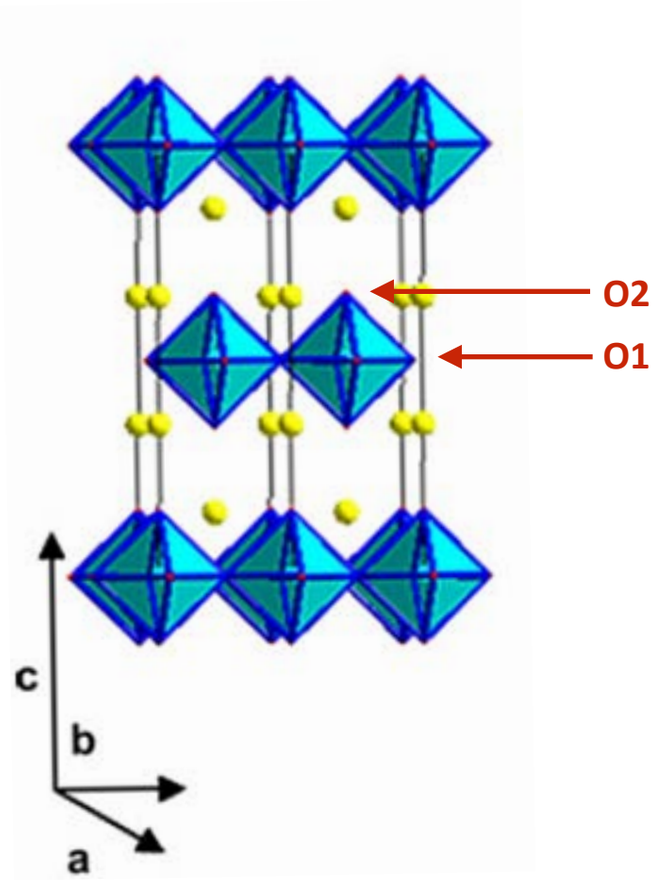

Sr_2CrO_4

Neutron Powder diffraction

ILL, D1B & D2B instruments

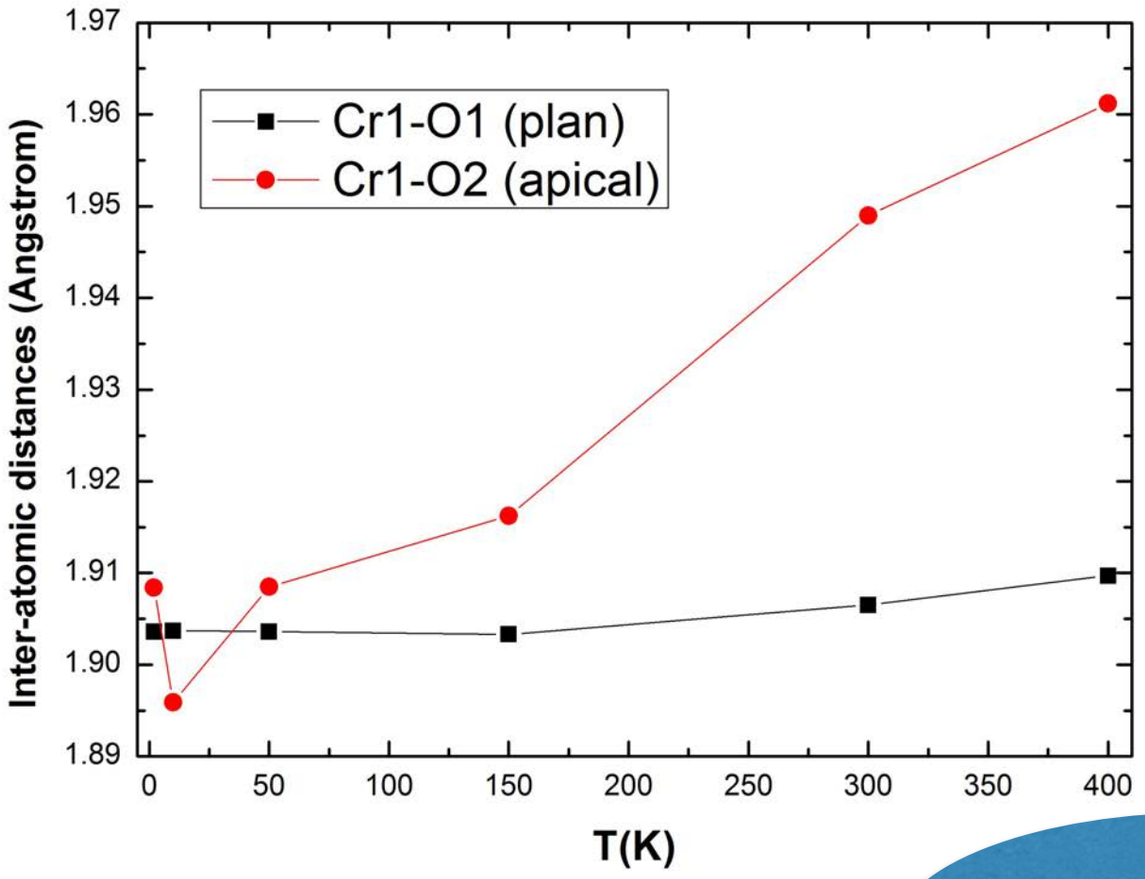

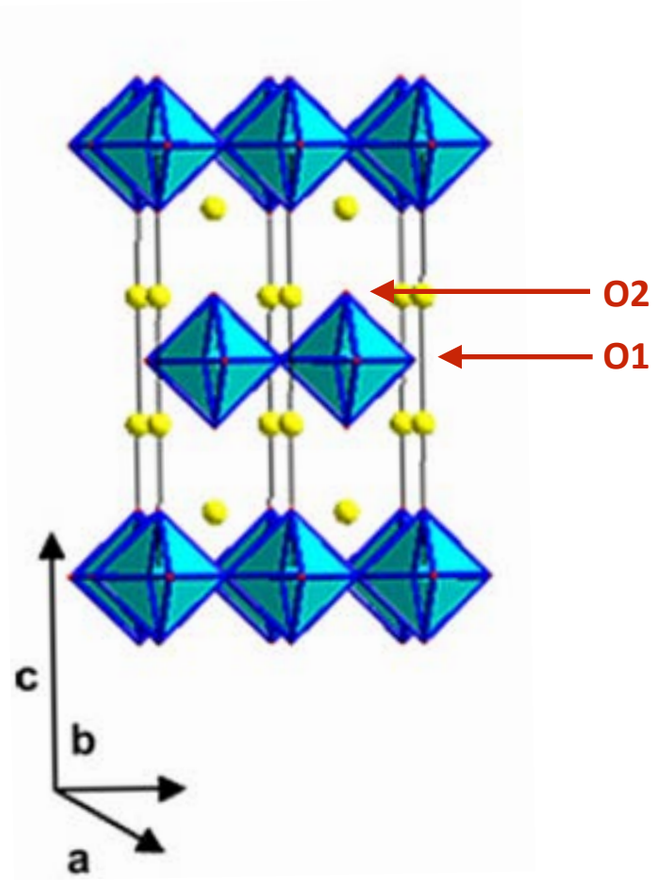

« Anti Jahn-Teller » effect

Low temperature

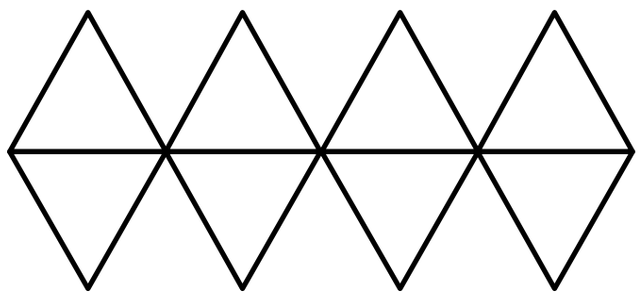

High temperature

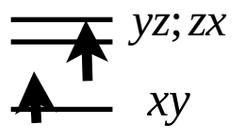

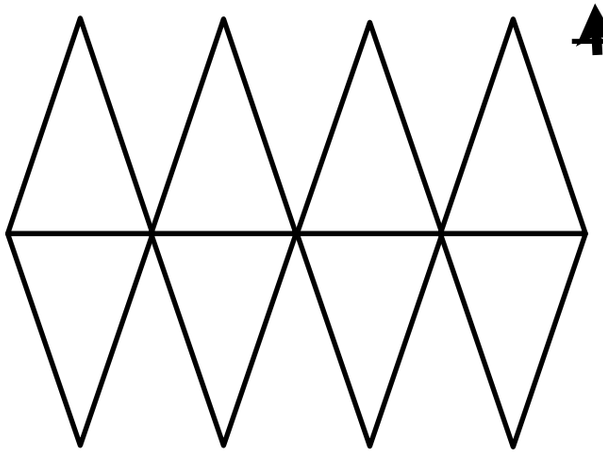

Sr_2CrO_4

Specific Heat

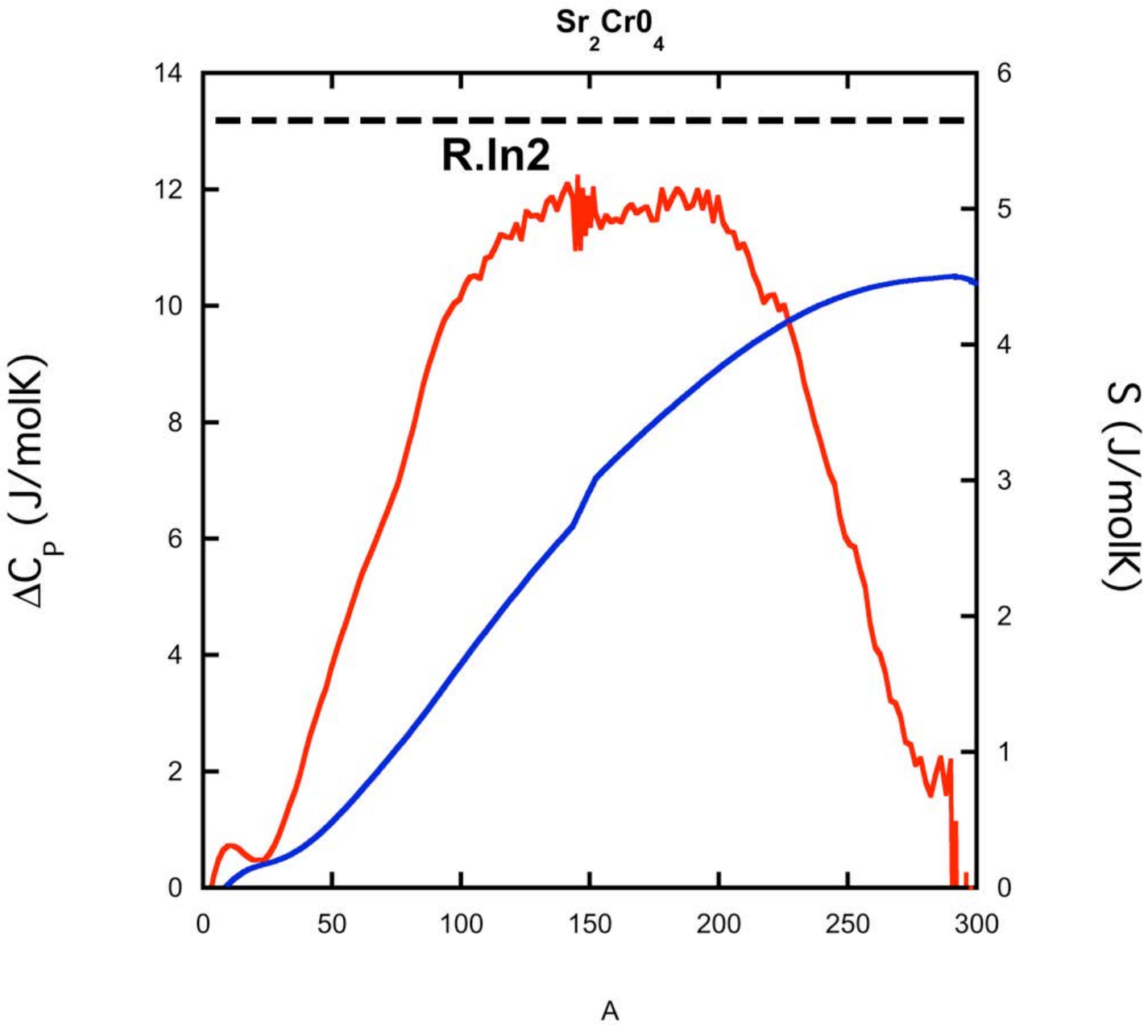

à refaire vendredi avec Gyorgy

New Ca-based phases

Graphs Sr327 transport /P

New Ca-based phases

$Ca_3Cr_2O_7$

Introduction : Perovskite $SrCrO_3$

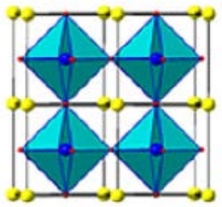

T>40K

cubic

paramagnetic

orbital degenerescence

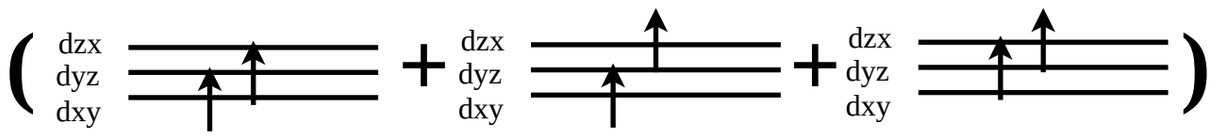

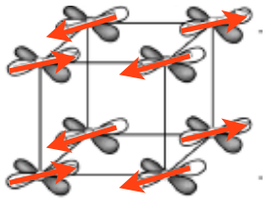

T<40K

tetragonal c/a=0.992

antiferromagnetic order

partial orbital order

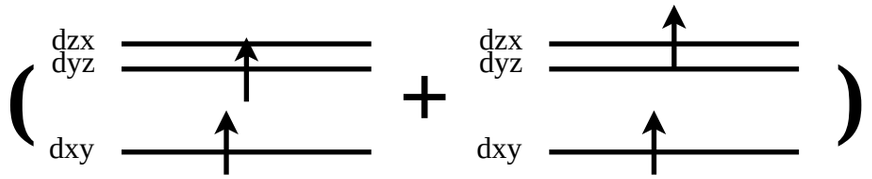

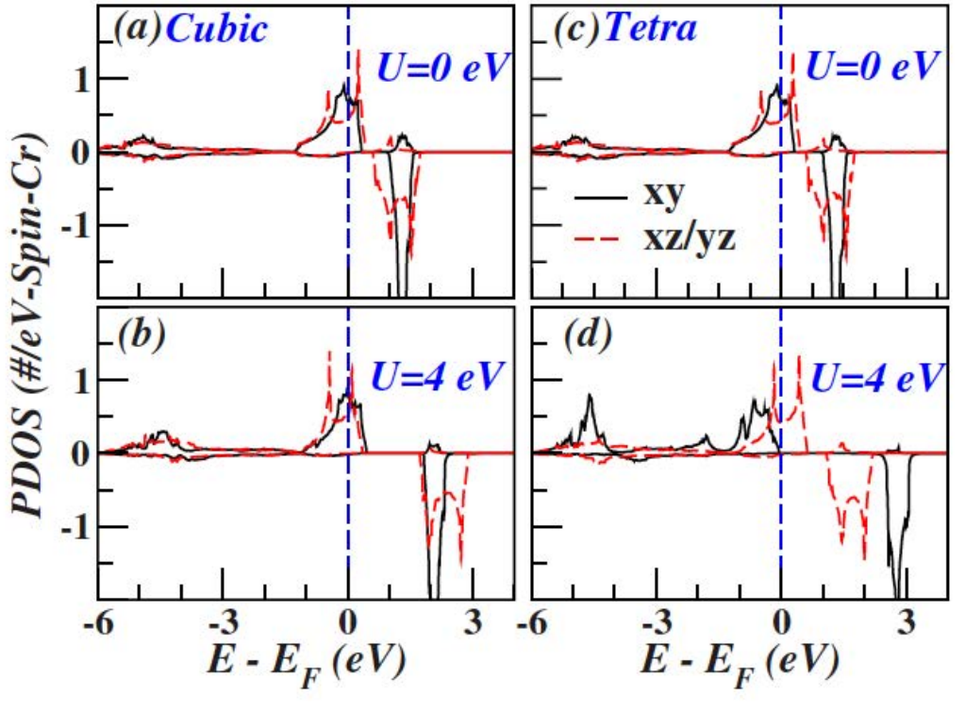

LDA+U calculations explain partial orbital ordering

FIG. 7. (Color online) U-dependent orbital-projected densities of states of Cr t_{2g} states for (a)–(b) the cubic and (c)–(d) the tetragonal phase, at U=0 and 4 eV in C-AFM order. At U=4 eV, an orbit-ordering transition in d_{xy} orbital occurs in the tetragonal phase.

Pickett *et al.*

PHYSICAL REVIEW B **80**, 125133 2009

Introduction : Perovskite $SrCrO_3$

LDA calculations give Metal

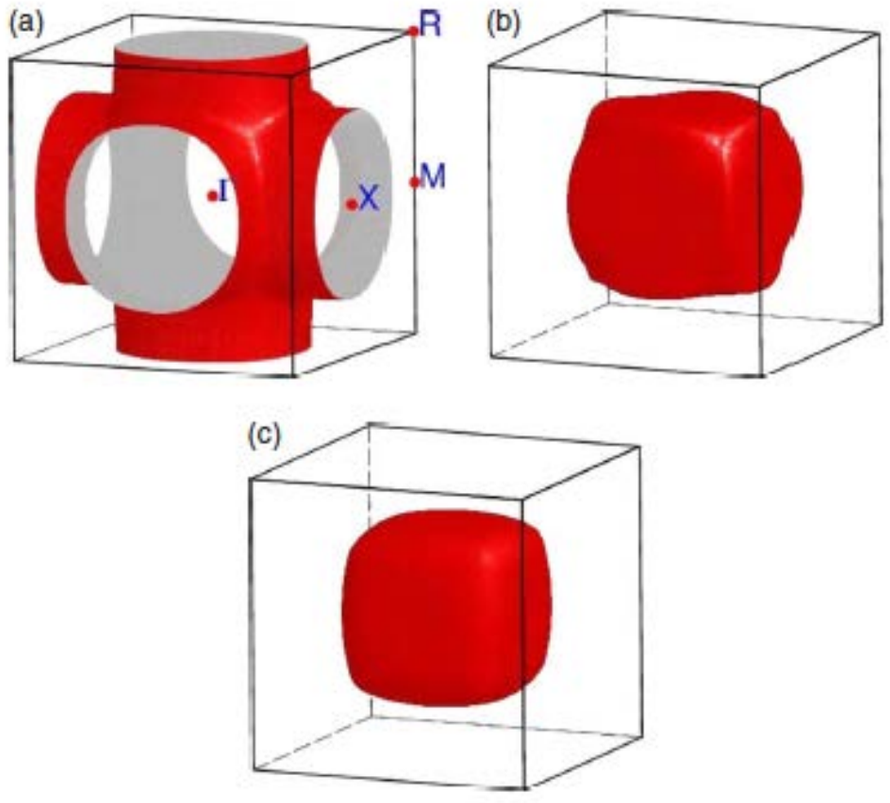

Pickett *et al.*

PHYSICAL REVIEW B **80**, 125133 2009

Proposed Metal-Insulator transition under pressure ?

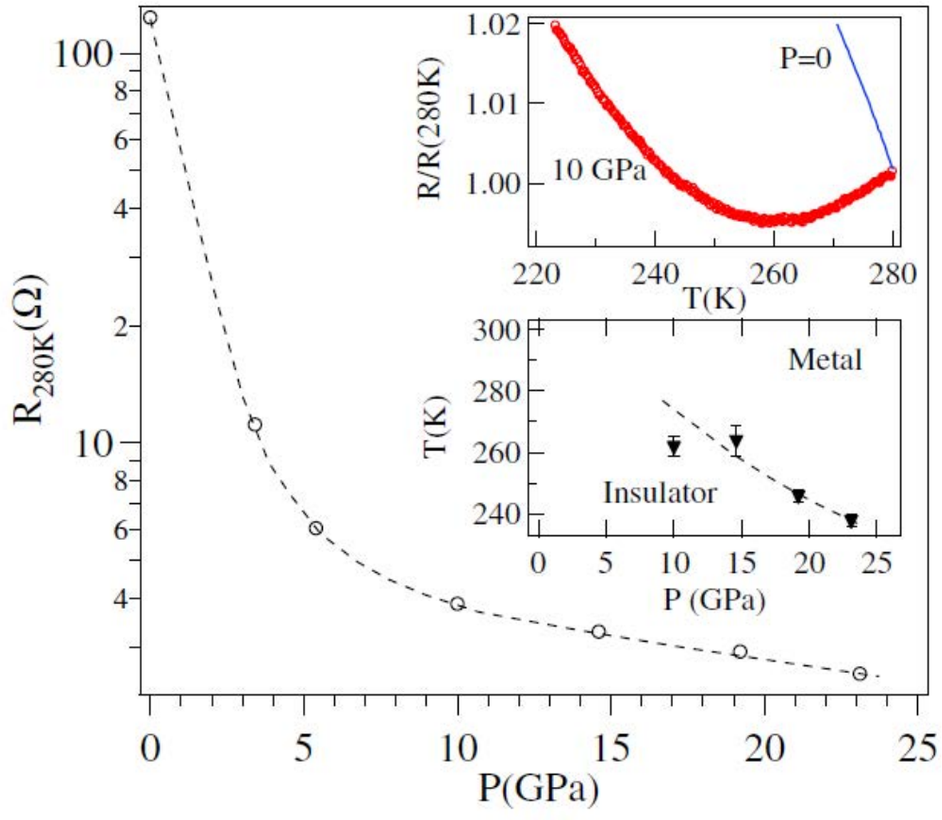

J.-S. Zhou, C.-Q. Jin, Y.-W. Long, L.X. Yang, and J. B. Goodenough, PRL ***96,*** *046408 (2006).*

Introduction : Perovskite $SrCrO_3$

4-wires transport measurement under pressure

Introduction : Perovskite $SrCrO_3$

4-wires transport measurement under pressure

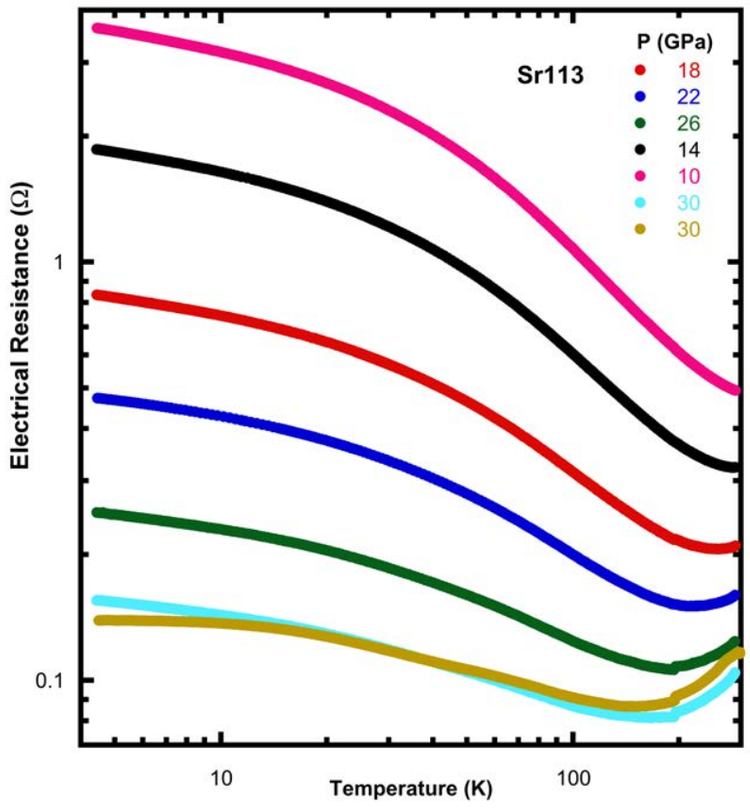

Our experiment :
Partial Metal-Insulator transition
between 14 and 18 GPa

Introduction : Perovskite $SrCrO_3$

4-wires transport measurement under pressure

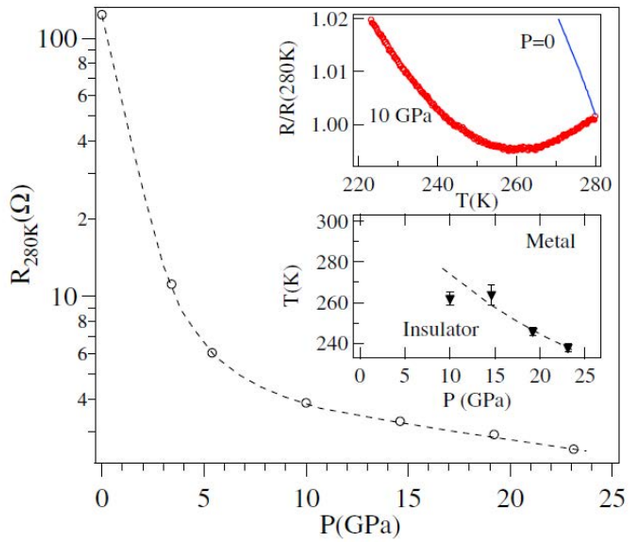

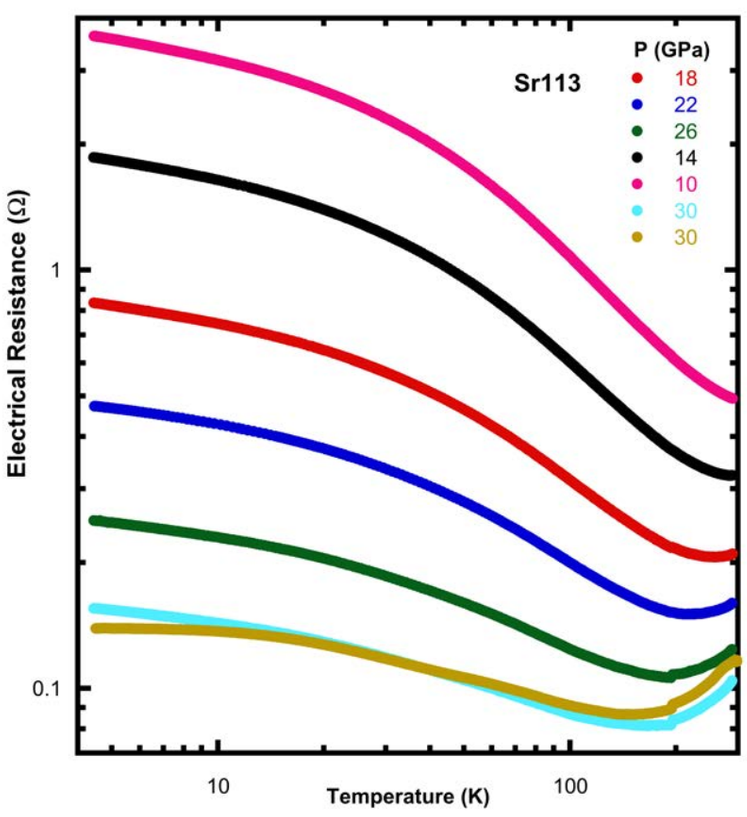

?

Our experiment :

Partial Metal-Insulator transition between 14 and 18 GPa

Introduction : Perovskite $SrCrO_3$

4-wires transport measurement under pressure

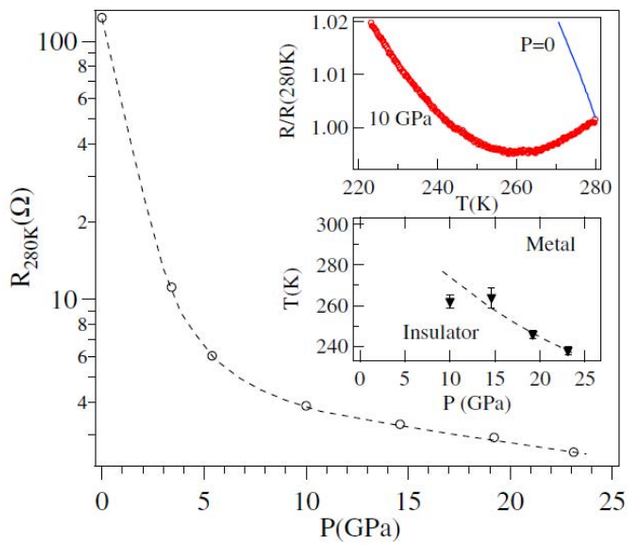

Estimated **Full Metal-Insulator** transition around **40 GPa**

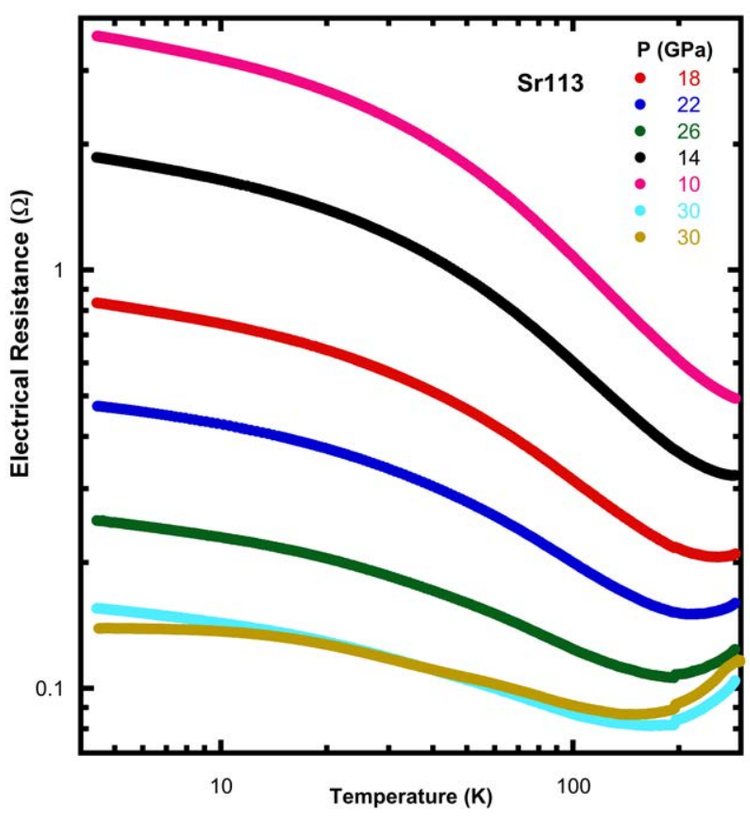

Our experiment :
Partial Metal-Insulator transition
between 14 and 18 GPa